

**THE CHARACTERIZATION OF BAX $\beta$ ,  
A SPLICE VARIANT OF THE PRO-APOPTOTIC BAX $\alpha$  PROTEIN**

By  
KATHLEEN POUND, B.Sc.

A Thesis  
Submitted to the School of Graduate Studies  
In Partial Fulfillment of the Requirements  
For the Degree  
Master of Science

McMaster University

© Copyright by Kathleen Pound, December 2001

MASTER OF SCIENCE (2001)  
(Biochemistry)

McMaster University  
Hamilton, Ontario

TITLE: The Characterization of Bax $\beta$ , a Splice Variant of the Pro-Apoptotic Bax $\alpha$   
Protein

AUTHOR: Kathleen Pound, B. Sc. (Queen's University)

SUPERVISOR: Professor D. W. Andrews

NUMBER OF PAGES: xii, 100

## ABSTRACT

$Bax\alpha$  is a pro-apoptotic member of the Bcl-2 protein family that regulates a key point in the control of apoptosis. The *bax* RNA undergoes a complex pattern of RNA splicing, with eight splice isoforms known to date. The next most abundant isoform to  $Bax\alpha$  is  $Bax\beta$ , which has a unique carboxyl-terminal sequence and consequently lacks the transmembrane domain of  $Bax\alpha$ . This study characterized  $Bax\beta$  as part of a larger project aimed at deducing the role of cellular localization in Bax protein function.

A transient transfection assay was designed to determine the cell death activity of a protein in adherent cells.  $Bax\beta$  induced cell death to a greater extent than  $Bax\alpha$  when transiently expressed in NIH 3T3 cells. The levels of  $Bax\beta$  expression were always low, regardless of the cell type or transfection method used. Additionally,  $Bax\beta$  adopted a conformation in which amino acids 13 to 19 are accessible to the monoclonal antibody 6A7. In  $Bax\alpha$  this epitope is only exposed in the membrane-bound activated conformation that is associated with accessibility of the BH3 domain of  $Bax\alpha$  that mediates protein-protein interactions among Bcl-2 family members. Although the mechanism remains elusive,  $Bax\beta$  was identified as a potent inducer of cell death.

*To my family*

## ACKNOWLEDGEMENTS

Thank you to Dr. David Andrews for giving me this opportunity to learn, and for his support and guidance throughout these studies. Thank you also to Dr. Brian Leber for his help, advice, and suggestions and to Dr. Justin Nodwell for his insight and ideas.

Thank you to Dr. L. Penn and E. Soucie of the Ontario Cancer Institute for all their help with reagents and cell lines; to Dr. L. Arsenault for writing the KS400 macros and everyone at the McMaster University Microscopy Unit for all their help; to Dr. B. Kay at the University of Wisconsin-Madison for the SH3 domain reagents; to Dr. Wang at the Lee Moffitt Cancer Center and Research Institute for the Bax $\beta$ -Bif-1 binding studies; to Dr. P. Whyte of the Department of Biochemistry at McMaster University for the NIH 3T3 cells; to Dr. G. Singh of the Department of Biology at McMaster University for the HT29 cells; and to Dr. R. Youle at the National Institutes of Health for antibodies.

Thank you to everyone in the Andrews lab for making this experience fun and full of laughter. I appreciate all of your unending help more than I could ever adequately express here. Thanks also to all of my friends who supported me during this experience and made this time in my life very special. Last but definitely not least, thank you to my family, for it is their love and support that made this happen.

## TABLE OF CONTENTS

|   |    |
|---|----|
| <b>1. Introduction</b>  | 1  |
| 1.1 Roles of oligomerization in Bax $\alpha$ function           | 3  |
| 1.2 Roles of membrane localization of Bax $\alpha$ in apoptosis | 6  |
| 1.3 Pore formation by Bax $\alpha$                              | 10 |
| 1.4 Isoforms of Bax   | 13 |
| <b>2. Materials and Methods</b>                                 | 19 |
| 2.1 General Materials   | 19 |
| 2.2 Plasmids  | 19 |
| 2.3 Antibodies  | 20 |
| 2.4 Protein Electrophoresis and Immunoblotting                  | 21 |
| 2.5 Transcription and Translation                               | 21 |
| 2.6 Tissue Cell Culture   | 22 |
| 2.7 NP-40 Cell Lysates  | 22 |
| 2.8 SDS Cell Lysates  | 23 |
| 2.9 Rat, Fetal and Mouse Tissue Lysates                         | 23 |
| 2.10 Tissue Lysate Immunoprecipitations                         | 24 |
| 2.11 6A7 Immunoprecipitations                                   | 25 |
| 2.12 Bax $\beta$ Immunoprecipitations                           | 26 |
| 2.13 Bax $\alpha$ Purification                                  | 26 |
| 2.14 Bax $\beta$ Antibody Purification                          | 26 |
| 2.15 Antibody Coupling  | 27 |

|  |           |
|--|-----------|
| 2.16 Pooled Cell Apoptosis Assay                           | 27        |
| 2.17 Transient Transfections                               | 27        |
| 2.18 Confocal Microscopy                                   | 28        |
| 2.19 <sup>35</sup> S Methionine Cell Labeling              | 28        |
| 2.20 GST-SH3 Domain Fusion Proteins                        | 29        |
| 2.21 ELISA Assay for Detecting SH3 Domain Interactions     | 29        |
| 2.22 Slot Blot Assay for Detecting SH3 Domain Interactions | 30        |
| 2.23 GST Immunoprecipitations                              | 31        |
| <b>3. Results</b>  | <b>32</b> |
| 3.1 Expression of Bax $\beta$                              | 32        |
| 3.2 Function of Bax $\beta$ in Apoptosis                   | 40        |
| 3.2.1 Rat-1 <i>myc</i> ERTM Pooled Cell Lines              | 41        |
| 3.2.2 Transient Transfection of NIH 3T3 cells              | 46        |
| 3.2.3 Conformation of the Bax $\beta$ Amino-Terminus       | 65        |
| 3.3 Significance of the Bax $\beta$ Carboxyl-Terminus      | 68        |
| <b>4. Discussion</b>                                       | <b>72</b> |
| <b>5. References</b>                                       | <b>77</b> |
| <b>6. Appendices</b>                                       | <b>86</b> |
| 6.1 Binding Among Bax Molecules                            | 86        |
| 6.2 PEST Sequence  | 88        |
| 6.3 Interactions with SH3 Domains                          | 93        |

## LIST OF FIGURES

|   |    |
|---|----|
| Figure 1: The structure of Bax $\alpha$ .   | 8  |
| Figure 2: Isoforms of Bax.  | 14 |
| Figure 3: The carboxyl-terminal sequences of Bax $\alpha$ and Bax $\beta$ .   | 15 |
| Figure 4: Epitopes recognized by the Bax antibodies.  | 34 |
| Figure 5: Bax protein expression in cell lines.   | 36 |
| Figure 6: Bax protein expression in rat and human tissues.  | 37 |
| Figure 7: Protein expression in Rat-1 <i>myc</i> ERTM pooled cell lines.  | 43 |
| Figure 8: Cleavage of the caspase substrate PARP in Rat-1 <i>myc</i><br>ERTM pooled cell lines treated with etoposide, serum<br>starvation, and Adriamycin.                                     | 45 |
| Figure 9: Protein expression in NIH 3T3 cells transiently transfected<br>with pBabe MN IRES GFP vector constructs.  | 50 |
| Figure 10: Protein expression in NIH 3T3 cells transiently transfected<br>with pBabe MN IRES GFP vector constructs 8, 18, and 40<br>hours post-transfection.                                    | 51 |
| Figure 11: The relative amount of GFP fluorescence per cell and the<br>relative transfection efficiencies of NIH 3T3 cells transiently<br>transfected with pBabe MN IRES GFP vector constructs. | 53 |

|  |    |
|--|----|
| Figure 12: Protein expression in NIH 3T3 cells transiently transfected with equal amounts of prcCMV vector construct and pEGFP-C1.   | 56 |
| Figure 13: NIH 3T3 cells transiently transfected with varying amounts of prcCMV vector construct and pEGFP-C1.   | 58 |
| Figure 14: The relative amount of EGFP fluorescence per cell and the relative transfection efficiencies of NIH 3T3 cells transiently transfected with varying amounts of prcCMV vector construct and pEGFP-C1. | 59 |
| Figure 15: Cleavage of the caspase substrate PARP in NIH 3T3 cells treated with Adriamycin, etoposide and staurosporine.   | 61 |
| Figure 16: NIH 3T3 cells transiently transfected with 3 $\mu$ g prcCMV constructs and 1 $\mu$ g pEGFP-C1 treated with 0 to 50 $\mu$ M Adriamycin for 24 hours.   | 63 |
| Figure 17: The relative amount of EGFP fluorescence per cell and the relative transfection efficiencies of transiently transfected NIH 3T3 cells treated with 0 to 50 $\mu$ M Adriamycin for 24 hours.         | 64 |
| Figure 18: Immunoprecipitations of Bax $\alpha$ , Bax $\beta$ , and Bax $\alpha$ - $\Delta$ S184 with the 6A7 and 2D2 antibodies at pH 7.5.  | 67 |
| Figure 19: Immunoprecipitations of Bax $\alpha$ , Bax $\beta$ , and Bax $\alpha$ - $\Delta$ S184 with the 6A7 and 2D2 antibodies at pH 6.9 and 8.1.  | 69 |

|   |    |
|---|----|
| Figure 20: Quantification of immunoprecipitations of Bax $\alpha$ , Bax $\beta$ , and Bax $\alpha$ - $\Delta$ S184 with the 6A7 and antibodies at pH 6.9 and 8.1.             | 70 |
| Figure 21: Co- immunoprecipitations of Bax $\beta$ and Bax $\alpha$ , and Bax $\beta$ and Bax $\alpha$ - $\Delta$ S184 with the $\alpha$ Bax $\beta$ antibody at pH 7.5.      | 87 |
| Figure 22: Schematic representation of PEST sequences.  | 89 |
| Figure 23: Pulse labeling of transfected NIH 3T3 cells and of Rat-1 <i>myc</i> ERTM pooled cell lines for Bax $\alpha$ , Bax $\beta$ , Bax $\alpha$ - $\Delta$ S184, and GFP. | 91 |
| Figure 24: Pulse labeling of MCF-7 cell, of Rat-1 <i>myc</i> ERTM parental cells, and of Rat-1 <i>myc</i> ERTM <i>bax</i> $\alpha$ pBabe MN IRES GFP cells for Bax $\alpha$ . | 92 |
| Figure 25: GST-SH3 domain fusion protein samples.   | 95 |
| Figure 26: Immunoprecipitations of <sup>35</sup> S methionine labeled Bax $\alpha$ and c-Src and Bax $\beta$ and c-Src.   | 99 |

## LIST OF ABBREVIATIONS

|                              |   |
|------------------------------|---|
| $\Delta\phi_m$               | Mitochondrial membrane potential                |
| AIF                          | Apoptosis inducing factor                       |
| ANT                          | Adenine nucleotide translocator                 |
| Bax $\alpha$ $\Delta$ C      | Bax $\alpha$ without its transmembrane domain   |
| Bax $\alpha$ - $\Delta$ S184 | Bax $\alpha$ with serine 184 deleted            |
| BH                           | Bcl-2 homology                                  |
| EGFP                         | Enhanced green fluorescent protein              |
| eIF-4G                       | Eukaryotic initiation factor 4G                 |
| ELISA                        | Enzyme-linked immunosorbent assay               |
| FACS                         | Fluorescence activated cell sorting             |
| GFP                          | Green fluorescent protein                       |
| IRES                         | Internal ribosome entry site                    |
| NMR                          | Nuclear magnetic resonance                      |
| NP-40                        | Nonidet P-40                                    |
| PARP                         | Poly (ADP-ribose) polymerase                    |
| <i>p</i> -NPP                | <i>p</i> -nitrophenol phosphate                 |
| PT                           | Permeability transition                         |
| PTP                          | Permeability transition pore                    |
| RT-PCR                       | Reverse transcriptase polymerase chain reaction |
| SDS                          | Sodium dodecyl sulfate                          |

|          |  |
|----------|--|
| SDS-PAGE | SDS polyacrylamide-gel electrophoresis |
| SH3      | Src homology 3                         |
| tBid     | Truncated Bid                          |
| TLB      | Tricene gel loading buffer             |
| VDAC     | Voltage dependent anion channel        |
| XIAP     | X-linked inhibitor of apoptosis        |

## 1. INTRODUCTION

Multicellular organisms eliminate redundant, damaged or infected cells by a characteristic program of cell suicide termed apoptosis, or programmed cell death (reviewed in Adams and Cory, 1998). The regulation of cell death is essential for normal development and the prevention of disease. Too little cell death can result in defects in development, propagation of a viral infection, or the emergence of cancer, while too much cell death can lead to autoimmune diseases, neurodegenerative disorders, and developmental problems (Adams and Cory, 1998).

The Bcl-2 protein family regulates a key point in the control of apoptosis. Its members include the anti-apoptotic proteins Bcl-2 (Lipford *et al.*, 1987), Bcl-X<sub>L</sub> (Boise *et al.*, 1993), Bcl $\omega$  (Gibson *et al.*, 1996), A1 (Lin *et al.*, 1993) and Mcl-1 (Kozopas *et al.*, 1993). Pro-apoptotic family member proteins include Bax (Oltvai *et al.*, 1993); Bid (Wang *et al.*, 1996); Bik (Boyd *et al.*, 1995); Bak (Chittenden *et al.*, 1995); Bad (Yang *et al.*, 1995) and Hrk (Inohara *et al.*, 1997). The Bcl-2 family proteins integrate diverse apoptotic stimuli, and they act at a common control point in many apoptotic pathways. If the apoptotic program within the cell continues past this point of control, the integrity of the mitochondrial membrane is compromised and mitochondrial proteins, such as cytochrome *c*, are released. Cytochrome *c* is an activator of Apaf-1 that in turn activates caspase-9 that goes

on to activate caspase-3. These caspases are cysteine-dependent aspartate-specific proteases that function as the executioners of apoptosis (Li *et al.*, 1997, Zou *et al.*, 1997). These enzymes cleave a wide variety of cellular proteins, and irreversibly commit the cell to die. As the Bcl-2 family proteins are at this key regulatory point of apoptosis, understanding the function of the Bcl-2 family of proteins is very important to the development of therapies for disorders involving inappropriate cell death.

The homologies within the Bcl-2 protein family are found in four regions of the Bcl-2 protein sequence, termed the Bcl-2 homology (BH) 1, BH2, BH3, and BH4 domains (Gross *et al.*, 1999). Most of the anti-apoptotic proteins contain at least the BH1 and BH2 domains, and the most similar to Bcl-2 contain all four BH domains (reviewed in Adams and Cory, 1998). The pro-apoptotic proteins can be divided into two sub-families based on sequence similarity to Bcl-2.

Representatives of the first subfamily that contain the BH1, BH2, and BH3 domains include Bax $\alpha$ , and Bak. The other pro-apoptotic family, consisting of proteins like Bid and Bad, contain only the BH3 domain (reviewed in Adams and Cory, 1998). The many family members are regulated by a wide variety of mechanisms, which enables appropriate responses to diverse apoptotic stimuli of differing intensities.

The Bax $\alpha$  protein is a member of the pro-apoptotic group of Bcl-2 proteins that have BH1, BH2, and BH3 domains. Bax $\alpha$  is required for normal development of certain cell types, most notably lymphoid cells and male germ cells (Knudson

*et al.*, 1995). The ability of *bax* knockout mice to survive into adulthood without gross abnormalities in cell proliferation is indicative of the redundancy that exists in the control of the apoptotic pathway. However, when *bak*, another pro-apoptotic Bcl-2 family member, is also knocked out fewer than 10% of the mice survived and they had multiple developmental defects (Lindsten *et al.*, 2000).

Three main models regarding the mechanism of Bax $\alpha$  function have been proposed. Bax $\alpha$  could interact with anti-apoptotic Bcl-2 family members abrogating their function, it could regulate the functions of mitochondrial proteins during apoptosis, or Bax $\alpha$  could act independently as a pore forming protein and provide a channel for the release of apoptosis activating factors such as cytochrome *c*.

### **1.1 Roles of oligomerization in Bax $\alpha$ function**

The earliest studies of Bax $\alpha$  showed that it can form homodimers and that overexpressed anti-apoptotic Bcl-2 can compete for Bax $\alpha$  through heterodimerization (Oltvai *et al.*, 1993). The BH3 region of Bax $\alpha$ , an amphipathic  $\alpha$ -helix encompassing amino acids 54 to 77, was shown to be essential for the binding of Bax $\alpha$  with other Bcl-2 family members, both pro- and anti-apoptotic, and for Bax $\alpha$  death agonist activity (Zha *et al.*, 1996a, Wang *et al.*, 1998, Simonian *et al.*, 1996a, Simonian *et al.*, 1996b, Sedlak *et al.*, 1995). The importance of the BH3 domain in inducing cell death is highlighted by its

presence in all of the pro-apoptotic Bcl-2 family proteins (Zha *et al.*, 1996a, Wang *et al.*, 1998).

However, Bax $\alpha$  dimerization data needs to be examined with caution. The Bax $\alpha$  molecule displays varying conformational states in different detergents (Hsu and Youle, 1998, Suzuki *et al.*, 2000). Non-ionic detergents, such as Triton X-100 and Nonidet P-40 (NP-40) induced a conformational change that caused exposure of a normally buried amino-terminal epitope recognized by the monoclonal antibody 6A7, concomitant with Bax $\alpha$  homo- and hetero-oligomerization (Hsu and Youle, 1998). Many of the immunoprecipitations and cell lysates used in studies of Bax $\alpha$  protein interactions involved the use of Triton X-100 or NP-40 detergents. In contrast, CHAPS, a zwitterionic detergent, did not induce exposure of the 6A7 epitope nor Bax $\alpha$  homo- or hetero-oligomerization (Hsu and Youle, 1998). Additionally, crosslinking studies found no significant Bax $\alpha$ -Bcl-X<sub>L</sub>, Bax $\alpha$ -Bcl-2, or Bax $\alpha$ -Bax $\alpha$  oligomer formation upon induction of apoptosis by staurosporine in HL-60 promyelocytic leukemia cells (Hsu and Youle, 1998). Thus, the BH3 domain of Bax $\alpha$  may be inaccessible for oligomerization under some physiological conditions (Hsu and Youle, 1998).

There is increasing evidence that homo-oligomerization of Bax $\alpha$  once it has localized to the mitochondrial membrane is very important for its apoptotic function. Monomeric Bax $\alpha$  in the cytosol of FL5.12 cells translocated to the mitochondria upon induction of apoptosis where it could be crosslinked as a dimer and this was inhibited by Bcl-2 (Gross *et al.*, 1998). Enforced dimerization

of Bax $\alpha$  molecules also resulted in the induction of apoptosis (Gross *et al.*, 1998). In HeLa cells large Bax oligomers have been found following the induction of apoptosis by treatment with staurosporine or UV irradiation. No other proteins were present in the oligomerized complexes, and this process was inhibited by Bcl-2 (Antonsson *et al.*, 2001). In cultured kidney proximal tubule cells the formation of homo-oligomers by Bax $\alpha$  can be prevented by the anti-apoptotic protein Bcl-2, the protective effects of which did not require Bcl-2 – Bax associations (Mikhailov *et al.*, 2001). Thus, while interactions among Bax $\alpha$  molecules at the mitochondria in apoptotic cells are important for function, binding between pro- and anti-apoptotic family members might be less important than originally thought.

Interactions among pro-apoptotic Bcl-2 family members, including Bax $\alpha$ , have been demonstrated to be important for the acceleration of apoptosis. Bax oligomerization and integration into the outer mitochondrial membrane occurs following binding to tBid, the truncated form of the pro-apoptotic protein Bid and member of the BH3 domain only pro-apoptotic family (Eskes *et al.*, 2000, Ruffolo *et al.*, 2000, Wei *et al.*, 2001). In addition, Bax $\alpha$  and Bak have been found to group in large clusters at the mitochondria during cell death, although whether they actually form hetero-oligomers in these clusters is not known (Nechushtan *et al.*, 2001). Hence interactions among pro-apoptotic Bcl-2 family members are physiologically relevant and important in the apoptotic process.

## 1.2 Roles of membrane localization of Bax $\alpha$ in apoptosis

Bax $\alpha$  has a carboxyl-terminal transmembrane domain that controls its membrane targeting. In healthy cells, Bax $\alpha$  is present predominantly in the cytoplasm and induction of apoptosis results in movement of Bax $\alpha$  to the mitochondria early in the apoptotic process (Hsu *et al.*, 1997, Wolter *et al.*, 1997, Gross *et al.*, 1998). Deleting the carboxyl-terminal transmembrane domain from a GFP-Bax $\alpha$  fusion inhibited the protein's death promoting activity in Cos-7 monkey kidney epithelial cells (Wolter *et al.*, 1997). Studies done in the yeast *Saccharomyces cerevisiae* showed that deletion of the Bax $\alpha$  transmembrane domain entirely abrogated its death-inducing function (Zha *et al.*, 1996b). As yeast have no endogenous Bax $\alpha$  (or other Bcl-2 family proteins), only the truncated protein was present. Other experiments in mammalian cells have shown that removal of the Bax $\alpha$  carboxyl-terminus has no effect on its role in promoting cell death (Hsu *et al.*, 1997, Zha *et al.*, 1996b). However, it is conceivable that the truncated Bax $\alpha$  proteins are interacting through oligomerization with endogenous Bax $\alpha$ , and are achieving mitochondrial membrane localization in this manner. In which case, the interaction of Bax $\alpha$  with the mitochondria, facilitated by the carboxyl-terminal transmembrane domain, is essential for its pro-apoptotic activity.

The nuclear magnetic resonance (NMR) solution structure of full length Bax $\alpha$  isolated in the absence of detergent showed that Bax $\alpha$  is composed of nine

$\alpha$ -helices (Figure 1) (Suzuki *et al.*, 2000). The hydrophobic pocket, which contains the second  $\alpha$ -helix that encompasses the BH3 domain and mediates protein-protein interactions, is occupied by the ninth  $\alpha$ -helix of Bax $\alpha$ , which encompasses the carboxyl-terminal transmembrane domain (Suzuki *et al.*, 2000). Thus the core pocket of the Bax $\alpha$  protein is only available to bind to other proteins after the carboxyl-terminal helix has moved out of this pocket. It is suggested that this helix exits the hydrophobic pocket when it integrates into the mitochondrial membrane (Suzuki *et al.*, 2000). Such a mechanism is consistent with biochemical data that indicate a requirement of membrane localization for apoptotic function.

Mutagenesis studies of Bax $\alpha$  expressed in Cos-7 cells and L929 murine fibrosarcoma cells, found that serine 184 in the carboxyl-terminal transmembrane region is the most important amino acid residue regulating sub-cellular localization (Nechushtan *et al.*, 1999). Changing the serine 184 residue to a charged hydrophilic amino acid resulted in a block in the mitochondrial binding of Bax $\alpha$  and a corresponding elimination of its apoptotic activity. In contrast, substitution of serine 184 with a hydrophilic amino acid or deletion of serine 184 resulted in an increase in mitochondrial membrane binding with an increase in apoptotic activity (Nechushtan *et al.*, 1999). The serine 184 amino acid forms a hydrogen bond with aspartate 98 that is located in the hydrophobic pocket of the Bax $\alpha$  molecule (Suzuki *et al.*, 2000). The deletion of serine 184 or substituting this amino acid with a hydrophobic one abolishes this hydrogen-bonding activity,



**Figure 1:** The structure of Bax $\alpha$ .

A ribbon representation of an averaged minimized NMR structure for Bax $\alpha$  is shown (PDB 1F16). The backbone is in blue, with the BH3 domain in cyan and the carboxyl-terminal transmembrane helix in purple. The 6A7 antibody epitope is in red.

promoting the dissociation of the carboxyl-terminal  $\alpha$ -helix of the protein from the hydrophobic pocket, increasing the membrane accessibility of the carboxyl  $\alpha$  helix, which results in an increased apoptotic activity. Additionally, mutations in a peptide of the transmembrane  $\alpha$ -helix changed the conformation of the peptide, as determined by infrared spectroscopy, and altered the position of the peptide when inserted into membranes, as indicated by the efficiency with which encapsulated carboxyfluorescein was released from liposomes by these peptides. (Martinez-Senac *et al.*, 2001).

In addition to the membrane localization of Bax $\alpha$ , the protein undergoes a conformational change at its amino-terminus during apoptosis that results in its activation. This amino-terminal conformational change is recognized by the 6A7 monoclonal antibody (Figure 1). Deletion of the Bax $\alpha$  carboxyl-terminal transmembrane domain resulted in 6A7 binding, and deletion of the amino-terminus of Bax $\alpha$  resulted in spontaneous insertion of the molecule into the mitochondrial membrane where it exerted cytotoxic effects (Nechushtan *et al.*, 1999, Goping *et al.*, 1998). These pieces of evidence suggest a relationship between membrane localization and the conformational change. Soucie *et al.* (2001) have reported that the translocation of Bax $\alpha$  occurs prior to the change in conformation that exposes the 6A7 epitope, and that the activation of Bax $\alpha$  indicated by 6A7 reactivity does not occur in the absence of the cellular oncogene Myc. This conformational change has also been shown by Khaled *et al.* (1999) to be pH dependent, with exposure of amino-terminal epitopes and the

carboxyl-terminal transmembrane domain occurring at pH 7.8 or higher, however other researchers have not detected any pH dependent changes in the Bax $\alpha$  structure (Suzuki *et al.*, 2000). Thus two steps must take place for Bax $\alpha$  to exert its pro-apoptotic effect: Bax $\alpha$  monomers must translocate from the cytoplasm to the outer mitochondrial membrane, where they then undergo a conformational change detectable at the amino-terminus that renders them active.

### **1.3 Pore formation by Bax $\alpha$**

The Bax $\alpha$  structure has strong similarities with those of the anti-apoptotic protein Bcl-X<sub>L</sub> and the pro-apoptotic protein Bid (Muchmore *et al.*, 1996, Chou *et al.*, 1999). Although the primary sequences of these proteins are quite different, their structural similarities suggest that the functional models proposed for these different molecules may be applicable to each other. The structures resolved for Bcl-X<sub>L</sub>, Bid, and Bax $\alpha$  all showed striking similarities with the pore-forming domains of certain bacterial toxins, such as diphtheria toxin and colicin (Muchmore *et al.*, 1996, Chou *et al.*, 1999, Suzuki *et al.*, 2000). The central  $\alpha$ 5 and  $\alpha$ 6 helices of the Bcl-X<sub>L</sub> molecule were shown to be very important for this pore structure (Muchmore *et al.*, 1996). Accordingly, the  $\alpha$ 5 and  $\alpha$ 6 helices of Bax $\alpha$  may also be involved in pore formation. However, the NMR structure of Bax $\alpha$  does not provide information on the conformation after insertion into the mitochondrial membrane. While there is evidence that Bax $\alpha$  can form a pore in

membranes, this would probably require it to undergo a large conformational change.

Bax $\alpha$  $\Delta$ C (Bax $\alpha$  with no transmembrane domain) forms pH- and voltage-dependent ion-conducting channels in planar lipid bilayers and it can trigger the release of carboxyfluorescein molecules from liposomes. This latter action was blocked by Bcl-2 at physiological pH (Antonsson *et al.*, 1997). Bax $\alpha$  $\Delta$ C also inserts into potassium chloride loaded-vesicles with a broad pH range of activity, from pH 4 to pH 7, where it caused a rapid release of ions (Schlesinger *et al.*, 1997). Bax $\alpha$ , with and without its hydrophobic transmembrane domain, decreases the lifetime of planar phospholipid bilayers in a voltage- and concentration-dependent manner (Basanez *et al.*, 1999). Because most experiments were done with carboxyl-terminal deletion mutants of Bax $\alpha$  and use artificial membrane systems, the physiological relevance of these results remains uncertain.

Mitochondria have been found to have a central role in the apoptotic process. Permeability transition (PT) is an important step during cell death. It involves the disruption of the mitochondrial membrane potential ( $\Delta\psi_m$ ), and the release of many proteins from the intramembrane space which include the nuclease-activator apoptosis inducing factor (AIF) and the caspase activators Smac/DIABLO and cytochrome c (reviewed in Zamzami and Kroemer, 2001). PT is thought to result from the opening of a large pore located at contact sites of the inner and outer membranes (reviewed in Zamzami and Kroemer, 2001). This

permeability transition pore (PTP) is posited to be formed by a group of proteins that include hexokinase, creatine kinase, the voltage-dependent anion channel (VDAC), the adenine nucleotide translocator (ANT), the peripheral benzodiazepine receptor, and cyclophilin D (Gross et al., 1999).

An important role ascribed to Bax $\alpha$  in apoptosis is the release of cytochrome *c* from mitochondria through an unidentified mechanism which may or may not involve the PTP (Eskes et al., 1998, Rosse et al., 1998). It is possible that pores formed by oligomers of Bax $\alpha$  could release this molecule from mitochondria. Oligomers of Bax $\alpha$  $\Delta$ C form channels in pure liposomes and release cytochrome *c* from isolated mitochondria (Saito *et al.*, 2000, Antonsson *et al.*, 2000). A major limitation of these studies is again the absence of the transmembrane domain of Bax $\alpha$ , which would be expected to have significant effects on the conformation of the molecule and its interactions with membranes. Interestingly, Shimizu *et al.* (2000) found using planar lipid bilayers that full length Bax $\alpha$  formed ion channels, however these channels could not release cytochrome *c*. The addition of VDAC to Bax $\alpha$  in the lipid bilayers did result in the formation of a channel through which cytochrome *c* could pass (Shimizu *et al.*, 2000). Bax $\alpha$  interacts directly with VDAC and ANT (Narita *et al.*, 1998, Marzo *et al.*, 1998). While these studies provide clues as to the role of Bax $\alpha$  in the release of apoptotic molecules, like cytochrome *c*, from mitochondria, no specific mechanism for the function of Bax $\alpha$  has as of yet been defined.

## 1.4 Isoforms of Bax

The *bax* gene is composed of six exons and undergoes a complex pattern of alternative RNA splicing (Oltvai *et al.*, 1993). Of the seven identified splice isoforms, the RNA encoding Bax $\alpha$  is the most widely distributed and well characterized. Bax $\alpha$  is encoded by six exons, resulting in a 1.0 kb RNA transcript that is translated into a 21 kDa protein (Oltvai *et al.*, 1993). All three BH domains and the carboxyl-terminal transmembrane domain are in Bax $\alpha$  (Figure 2) (Oltvai *et al.*, 1993).

Bax $\beta$  is encoded by the next most abundant transcript, a 1.5 kb RNA created by the retention of intron 5 (Oltvai *et al.*, 1993). Northern blot analysis suggests Bax $\beta$  transcript is not a result of aberrant splicing as RNA of this isoform is more abundant than that for Bax $\alpha$  in mouse brain, duodenum, and liver (Oltvai *et al.*, 1993). Additionally, the sequence of the exon4/intron5 splice junction is evolutionarily conserved in both human and mouse *bax* (Oltvai *et al.*, 1993). The 630 bp intron 5 encodes 60 amino acids before a stop codon is encountered, resulting in a 24 kDa protein (Oltvai *et al.*, 1993). Although Bax $\beta$  contains the BH1, BH2, and BH3 domains, it has a unique carboxyl-terminus replacing the hydrophobic transmembrane domain of Bax $\alpha$  (Oltvai *et al.*, 1993) (Figure 2). Interestingly, we have identified proline-rich regions in this new carboxyl-terminal tail that resemble Src homology 3 (SH3) domain binding sites (Figure 3). SH3 domains are protein modules of 50 to 70 amino acids that mediate protein-protein interactions by binding short, proline-rich regions in

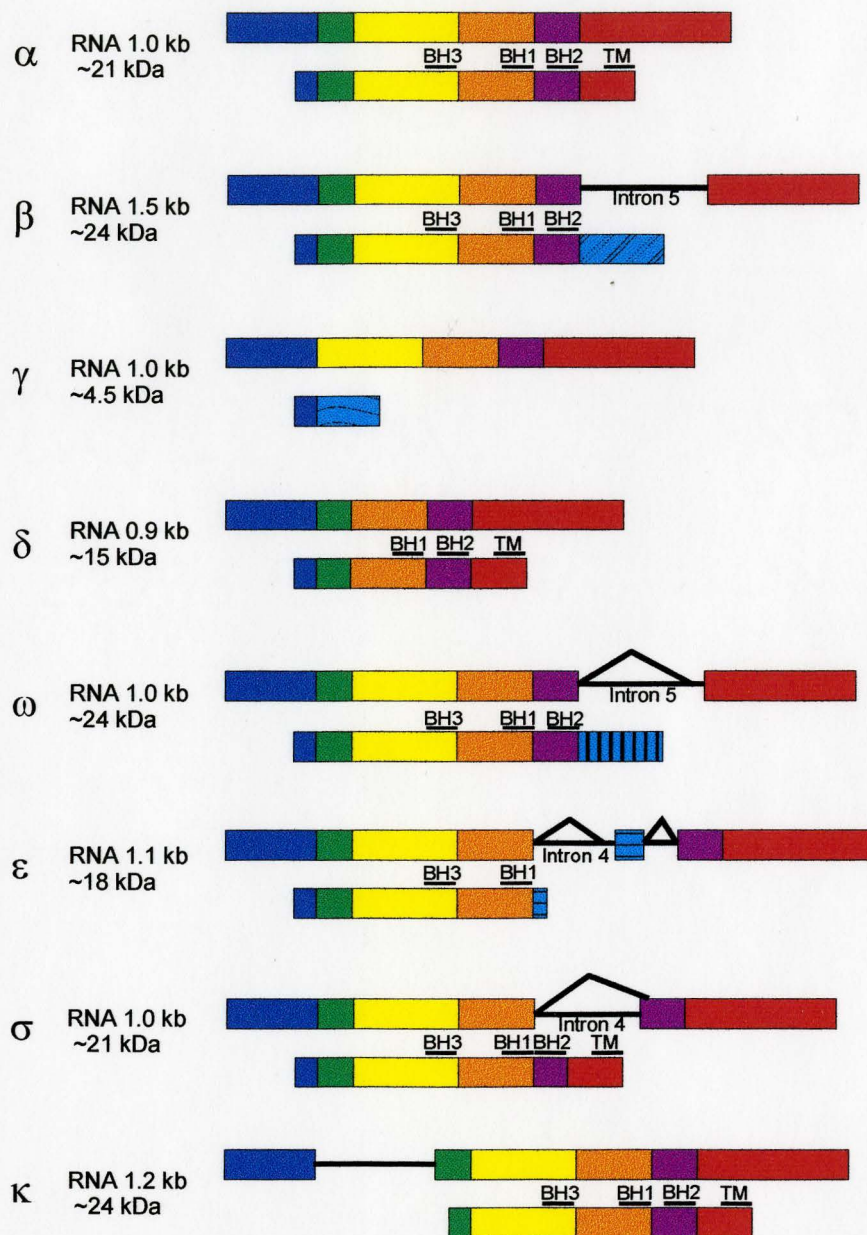


**Figure 2:** Isoforms of Bax.

Schematics of the mRNA and protein forms of the eight Bax isoforms are shown, with their approximate sizes given in kb and kDa, respectively. The different exons are denoted by different colours, and the corresponding region of the protein is the same colour. Introns are shown as black lines. Lines above the protein schematics indicate the BH regions and transmembrane domain.

**Bax $\alpha$**

Exon 5|Exon 6

**DFLRERLLGWIQDQGGW**DGLLSYFGTPTWQ

**TVTIFVAGVLTASLTIW**KKMG

**Bax $\beta$**

Exon 5|Intron 5

**DFLRERLLGWIQDQGGW**VRLL**KPPHPH**HRAL

***TTAPAPPSLPPATPL***GPWAFWSASQWCPLPIF

RSSDVVYNAFSLRV

**Figure 3:** The carboxyl-terminal sequences of Bax $\alpha$  and Bax $\beta$ .

Amino acid sequences of the carboxyl-terminal sequences of Bax $\alpha$  and Bax $\beta$  are shown, with the exon5/exon6 boundary in Bax $\alpha$  and the exon5/intron5 boundary in Bax $\beta$  marked with a vertical line. The sequences common to both proteins are highlighted in blue. The Bax $\alpha$  transmembrane sequence is highlighted in purple. The putative SH3 domain ligand sequences in Bax $\beta$  are highlighted in yellow, and the putative PEST sequence is in italicized bold type.

ligand proteins (cited in Sparks *et al.*, 1996). Thus Bax $\beta$  may be targeted to SH3-containing proteins rather than to membranes. Alternatively, this sequence may mediate rapid protein turnover, as it also resembles a PEST sequence (Rogers *et al.*, 1986).

A third splice variant, Bax $\gamma$ , also lacks a transmembrane domain, as it is missing exon 2 that results in a frameshift mutation leading to the synthesis of a 4.5 kDa protein (Figure 2) (Oltvai *et al.*, 1993). Bax $\delta$  lacks exon 3, and consequently the BH3 domain, but it retains the BH1, BH2, and transmembrane domains (Apte *et al.*, 1995). Bax $\omega$  is created through alternative splicing at exon 5 with a new splice acceptor site 49 bp 5' to the Bax $\alpha$  acceptor site on exon 6. This new 49 bp insertion results in a translational frameshift to encode a predicted a 24 kDa protein that, like Bax $\beta$ , contains the BH1, BH2, and BH3 domains, but no transmembrane sequence (Figure 2) (Zhou *et al.*, 1998). Bax $\epsilon$  is generated by the addition of 97 bp to the mRNA by the alternative splicing of a new exon located between exons 4 and 5. Because of a shift in the reading frame that stops translation, the predicted size of the Bax $\epsilon$  protein is 18 kDa. The Bax $\epsilon$  coding sequence does not include the BH2 or transmembrane domains (Figure 2) (Shi *et al.*, 1999). Bax $\sigma$  has the BH1, BH2, BH3, and transmembrane domains of Bax $\alpha$ , however it is missing amino acids 159 to 171 of the Bax $\alpha$  protein (Figure 2) (Schmitt *et al.*, 2000). Bax $\kappa$  has a 446 bp insert between exons 1 and 2 which causes a translational frameshift resulting in a shortened protein

that retains the BH1, BH2, BH3 and transmembrane domains, but is missing 19 amino acids at its amino-terminus (Figure 2) (Jin *et al.*, 2001). While these splice variants have been identified by their encoding RNAs, little is known of their protein expression or function.

Complete deletion of the transmembrane domain of Bax $\alpha$  is problematic as it causes unregulated insertion into membranes (Schlesinger *et al.*, 1997, Antonsson *et al.*, 1997). It also induces changes to the characteristics of amino-terminal conformational change, membrane localization, and apoptotic function of this protein (Nechushtan *et al.*, 1999, Goping *et al.*, 1998). Furthermore, the Bax protein truncated immediately amino-terminal to the putative transmembrane domain is not found in cells. Bax $\beta$  exhibits an alternative carboxyl-terminal sequence in lieu of the transmembrane domain. Consequently, it could potentially be a good control for studies involving the interaction of Bax $\alpha$  with membranes. As such, Bax $\beta$  is an interesting protein to analyze both for its potential roles in the apoptotic pathway and for use in functional comparisons with Bax $\alpha$ .

In this project Bax $\beta$  was characterized as part of a larger project aimed at deducing the role of cellular localization in Bax protein function. My studies focused on searching for the expression of the Bax $\beta$  protein in tissues, assaying the function of Bax $\beta$  in apoptosis, and investigating the significance of the unique Bax $\beta$  carboxyl-terminus. Bax $\beta$  exhibited a strong cell death inducing phenotype when expressed by transient transfection of cDNA into NIH 3T3 cells.

Additionally these and other cell types were intolerant of high levels of Bax $\beta$  expression, which supports the finding that Bax $\beta$  has deleterious effects on cell survival. *In vitro* studies showed that the 6A7 epitope exposure associated with Bax $\alpha$  activation constitutively occurs with Bax $\beta$ . While this suggests that the BH3 domain of Bax $\beta$  might be available for protein-protein interactions, no interactions between Bax $\alpha$  and Bax $\beta$  were found *in vitro*.

## **2. MATERIALS AND METHODS**

### **2.1 General Materials**

The chemical reagents used were from Sigma Chemicals or Gibco-BRL. Reagents used for molecular manipulations were from New England Biolabs or MBI Fermentas. NEN-Mandel supplied the <sup>35</sup>S methionine. The *Escherichia coli* strains used were DH5 $\alpha$  and JM109 cells from New England Biolabs, and SURE and BL21 cells from Stratagene.

### **2.2 Plasmids**

Protocols for DNA digestion, mapping by restriction endonucleases, and the isolation and purification of DNA were performed as detailed in the laboratory manual of Dr. David W. Andrews (McMaster University). The Bax $\alpha$  (p750), Bax $\beta$  (p1200), Bax $\alpha\Delta$ S184 (p1398), c-Src (p152), and Pre-prolactin (p39) clones used for *in vitro* translation contain the gene of interest downstream of an SP6 promoter and the *Xenopus*  $\beta$ -globin 5' untranslated region. The pBabe MN IRES GFP vector (p1248) was received from Dr. Linda Penn of the Ontario Cancer Institute. Catherine Hollerbach cloned Bcl-2, and Bcl-X<sub>L</sub> into the pBabe MN IRES GFP vector in the laboratory of Dr. David Andrews (p1264 and p1268 respectively). I cloned the Bax $\alpha$ , Bax $\beta$ , and Bax $\alpha\Delta$ S184 proteins into the pBabe MN IRES GFP multiple cloning site region (p1461, p1462, and p1463). I also

cloned the Bax $\alpha$  and Bax $\beta$  proteins into prcCMV (Invitrogen) (p655) in the multiple cloning site (p1535 and p1536). The pEGFP-C1 vector (p1452) was obtained from Clontech laboratories. The GST-SH3 domain fusion clones for the c-Abl, Grb2, Cortactin, PLC $\gamma$ , P9, P7, p53BP2, and c-Src proteins were obtained from Dr. Brian K. Kay of the University of Wisconsin-Madison (Yamabhai and Kay, 1997) (p1345 to p1353). The fusion proteins are downstream of an IPTG-inducible TAC promoter. The Src ligand –BAP construct is also from Dr. Brian K. Kay, and is downstream of an IPTG-inducible TAC promoter (Yamabhai and Kay, 1997) (p1356).

### **2.3 Antibodies**

The antibodies used in these experiments include: Max 5, a rabbit polyclonal antibody raised to a region in the Bax amino-terminus (Zhu *et al.*, 1996), the human-specific monoclonal antibody 2D2 (Hsu *et al.*, 1997), a monoclonal antibody called 1D1 specific for rat Bax and 5B7 that is specific for mouse Bax (Hsu and Youle, 1998), the monoclonal antibody 6A7 which recognizes amino acids 13 to 19 in the N-terminus of Bax only after the conformational change associated with apoptosis occurs (Hsu and Youle, 1997), and 2C8, a monoclonal antibody to human and rat Bax (Hsu and Youle, 1998). A sheep polyclonal antibody specific for a peptide in the Bax $\beta$  tail was made with the Ex Alpha Biological company, as was a sheep polyclonal antibody to Bcl-2. A rabbit polyclonal antibody specific for Bcl-X<sub>L</sub> was made in the laboratory of Dr.

David W. Andrews. Mouse  $\alpha$ PARP was obtained from BioMol and mouse  $\alpha$ actin was obtained from ICN. The c-Src monoclonal antibody is from Cambridge Research Pharmaceuticals. The  $\alpha$ GST antibody is a rabbit polyclonal to the entire GST protein made by the laboratory of Dr. David W. Andrews (McMaster University). The  $\alpha$ GFP antibody is a rabbit polyclonal antibody from Clontech.

#### **2.4 Protein Electrophoresis and Immunoblotting**

Protein samples were quantified using the BCA assay (Pierce), or the Bradford assay (Bio-Rad). They were separated on 15% SDS-PAGE gels according to the laboratory manual of Dr. David W. Andrews (McMaster University). Immunoblotting was done using nitrocellulose membranes for all blots, except PVDF membrane for PARP, and a Hoefer transfer apparatus. The conditions for Western blotting were as those in the laboratory manual of Dr. David W. Andrews (McMaster University).

#### **2.5 Transcription and Translation**

Transcription and translation were performed in a rabbit reticulocyte lysate system following the method of Dr. David W. Andrews (McMaster University) or using an S30-lysate system according to the protocol of Mr. Jonathan S. Millman as detailed in the laboratory manual of Dr. David W. Andrews (McMaster University). Quantification of the translation products was done using

phosphorimaging, as described by Dr. David W. Andrews (McMaster University) in the laboratory manual.

## **2.6 Tissue Cell Culture**

MCF-7, Rat-1 *myc* ERTM, MDCK, Vero, and HT29 cells were grown in  $\alpha$ minimal essential medium ( $\alpha$ MEM) supplemented with 10% fetal bovine serum (FBS, Sigma), penicillin and streptomycin (Gibco-BRL). RL-7 cells were grown in RPMI media (Gibco-BRL) supplemented with 10% fetal bovine serum (FBS, Sigma), penicillin and streptomycin (Gibco-BRL). NIH 3T3 cells were grown in Dulbecco's Modified Eagle Medium (DMEM) supplemented with 10% calf serum (Sigma), penicillin and streptomycin (Gibco-BRL).

## **2.7 NP-40 Cell Lysates**

Confluent tissue culture cells were removed from a 10 cm culture dish or from 4 wells of a 12-well plate in the case of transfections using a rubber policeman, pooled if necessary, and pelleted in a clinical centrifuge for 3 minutes at 4°C. The supernatant was discarded, and the cell pellet washed 3 times in 1 ml of phosphate buffered saline (PBS) [137 mM NaCl, 2.7 mM KCl, 4.3 mM Na<sub>2</sub>PHO<sub>4</sub>, 1.4 mM KH<sub>2</sub>PO<sub>4</sub>]. The pellet was resuspended in 50 to 100  $\mu$ l of NP-40 lysis buffer [50 mM Tris-HCl, pH 7.5, 150 mM NaCl, 1% NP-40] supplemented with 1mM PMSF and 1X PIN [200X stock: 20  $\mu$ g/ml chymostatin, 20  $\mu$ g/ml antipain, 20  $\mu$ g/ml leupeptin, 20  $\mu$ g/ml pepstatin, 40  $\mu$ g/ml aprotinin] depending

on the size of the cell pellet. This was incubated on ice for 15 minutes, and then centrifuged at maximum speed at 4°C for 10 minutes. The supernatant was transferred to a new tube, flash frozen in liquid nitrogen, and stored at -80°C until use.

## **2.8 SDS Cell Lysates**

Confluent tissue culture cells were removed from a 10 cm culture dish or from 4 wells of a 12-well plate in the case of transfections using a rubber policeman, pooled if necessary, and pelleted in a clinical centrifuge for 3 minutes at 4°C. The supernatant was discarded, and the cell pellet washed once in 1 ml of PBS. The cell pellet was resuspended in 200 µl of 100°C SDS-lysate buffer [10 mM Tris-HCl pH 7.5, 10 mM NaCl, 1% SDS] and was passed through a 25 gauge syringe 6 to 8 times until lysed. The lysate was flash frozen in liquid nitrogen, and stored at -80°C until use.

## **2.9 Rat, Fetal and Mouse Tissue Lysates**

The rat and mouse tissues were harvested and placed into 10 ml of Buffer A [0.5M triethanolamine, 0.5 M potassium acetate, 0.05 M magnesium acetate, 0.01 M EDTA, 1.8% glacial acetic acid, 0.25 M sucrose (added fresh)]. The mouse tissue lysates were made from pooled samples from four mice. The fetal tissues were frozen in liquid nitrogen immediately following harvesting and stored at -80°C until use. The tissues were then placed into a tube of fresh Buffer A

containing 1 mM PMSF, 1X PIN, and DTT to 1 mM. The tissue was cut into 3 mm cubes and run through a Polytron homogenizer for approximately 5 seconds at speed 90. The samples were centrifuged at 800 g for 20 minutes, and the resulting supernatant was centrifuged at 100 000 g for 1 hour at 4°C. The supernatants were flash frozen in liquid nitrogen, and stored at -80°C until use.

## **2.10 Tissue Lysate Immunoprecipitations**

For the immunoprecipitations of the rat, mouse and fetal tissue cell lysates, 100 µg of each lysate was diluted in 1 ml of 1X TXSWB [1% Triton X-100, 100 mM Tris-HCl, pH 8.0, 100 mM NaCl, 10 mM EDTA] supplemented with 1 mM PMSF and 1X PIN. 5µl of Protein G beads (either Protein G Sepharose 4 Fast Flow or Gammabind Protein G, both from Pharmacia) were added, and the immunoprecipitations were incubated at 4°C with rotating, for 2 hours. The beads were pelleted, and the supernatants incubated with 1 µl of each antibody: 1D1 ascites fluid, 2C8 ascites fluid, and Baxβ for the rat tissues, and also 2D2 ascites fluid for the fetal tissues. These were incubated 2 hours with rotating at 4°C. 5 µl of Protein G beads were added and the samples were incubated overnight with rotating at 4°C. The beads were pelleted and washed 3 times with 1 ml of 1X TXSWB, and 2 times with 0.5 ml of 0.1 M Tris-HCl, pH 8.0, 0.1 M NaCl. The samples were resuspended in 20 µl of tricene gel loading buffer (TLB) [2% SDS, 0.05 M Tris-HCl, pH 8.0, 1 mM EDTA, 0.05% bromophenol blue, 10%

glycerol, 0.25 M DTT] heated at 100°C for 10 minutes, and stored at -20°C.

Analysis was by Western blotting after SDS-PAGE.

The immunoprecipitations performed with the Affi-Gel 10-coupled Bax $\beta$ , and 6A7 antibodies used 100  $\mu$ g of tissue lysate in 1 ml of 1X TXSWB. 10  $\mu$ l of the Affi-Gel 10 coupled-antibodies were added to each immunoprecipitation and they were incubated overnight with rotating at 4°C. The washes were carried out as described above, and the samples were resuspended in 20  $\mu$ l of TLB.

### **2.11 6A7 Immunoprecipitations**

For the immunoprecipitations, 10  $\mu$ l of <sup>35</sup>S methionine labeled protein was pre-cleared for one hour at 4°C in 0.5 ml of the appropriate buffer with 5  $\mu$ l of Protein G beads, which had been washed in the corresponding buffer. The buffers used were either 10 mM Hepes pH 6.9 or 8.1, with 150 mM NaCl, 0.2% Triton X-100 or CHAPS, with PIN and PMSF or 1X TXSWB. The beads were pelleted, and the supernatant incubated with 5  $\mu$ l of the 6A7 or 2D2 antibody ascites fluid overnight at 4°C. 5  $\mu$ l of Protein G beads were added to the immunoprecipitation reaction and incubated for 2 hours at 4°C. The beads were washed three times in 500  $\mu$ l of the corresponding buffer followed by two washes with 0.1 M Tris and 0.1 M NaCl. The samples were resuspended in 20  $\mu$ l of TLB.

## **2.12 Bax $\beta$ Immunoprecipitations**

The  $\alpha$ Bax $\beta$  antibody immunoprecipitations were performed like the 6A7 immunoprecipitations but using 1X TXSWB with PIN and PMSF with 2  $\mu$ l of antibody and 5  $\mu$ l of Protein G sepharose beads.

## **2.13 Bax $\alpha$ Purification**

Recombinant Bax $\alpha$  was purified by Mr. Matthew G. Annis using the IMPACT protein purification system (New England Biolabs). The cells were lysed in buffer [20 mM Tris-HCl pH 8.0, 50 mM NaCl, 0.1 mM EDTA] by French Press. The lysate was loaded onto the column and then the column was flushed with the above buffer supplemented with 20% glycerol and 0.2% CHAPS. The cleavage step was done with 50 mM DTT in the glycerol/CHAPS buffer overnight at room temperature. All washing and elution steps were done with the glycerol/CHAPS buffer.

## **2.14 Bax $\beta$ Antibody Purification**

The sheep polyclonal  $\alpha$ Bax $\beta$  antibody was purified using a DEAE Affi-Gel Blue antibody purification column from Bio-Rad. 5 ml of serum was dialyzed for a minimum of 6 hours in 20 mM Tris-HCl pH 7.2. The serum was then centrifuged at 100 000 g for 30 minutes at 4°C. The supernatant was loaded onto a 20 ml DEAE Affi-Gel Blue column equilibrated with 20 mM Tris-HCl pH 7.2. The column was washed with 50ml of buffer containing 20 mM Tris-HCl pH

7.2 and 25 mM NaCl, and eluted with 50:50 ml gradient of 20 mM Tris-HCl pH 8.0 with 25 mM to 100 mM NaCl. A final elution of 50 ml of 100 mM NaCl was done. Fractions of 5 ml were collected during the elution steps.

### **2.15 Antibody Coupling**

Affinity purified  $\alpha$ Bax $\beta$ , 2D2, 6A7, and Sheep $\alpha$ Bax antibodies were coupled to Affi-Gel 10 agarose, as outlined in the Bio-Rad protocol.

### **2.16 Pooled Cell Apoptosis Assay**

The requisite cell lines were grown in 6 cm dishes until 80% confluent. At this time, they were treated with 6  $\mu$ M etoposide, 0.03% FBS, or 10  $\mu$ M Adriamycin, all with 100 nM of 4-hydroxytamoxifen, for the desired length of time. At the end of the incubation, they were lysed using the SDS method and the PARP and actin proteins were analyzed by Western blotting.

### **2.17 Transient Transfections**

Transient transfections were done using the MBI Fermentas ExGen 500 reagent according to the manufacturer's protocol with the following modifications: coverslip-lined 12-well plates were used with 1 ml of the appropriate regular media, 4  $\mu$ g of DNA, and 19.74  $\mu$ l of ExGen 500 (9 equivalents) were used. A 10 minute spin at approximately 200 g at room temperature was done immediately after addition of the ExGen 500-DNA complexes to the cells. The media was

changed, without washing the cells, after a 1 hour incubation. The transfected cells were incubated for 18 hours prior to visualization. SDS lysates were also made 18 hours post-transfection, unless otherwise indicated.

## **2.18 Confocal Microscopy**

The slides of transiently transfected cells were washed twice with PBS, and fixed with 4% paraformaldehyde in PBS for 30 minutes at room temperature. They were then washed once with PBS and incubated with 1  $\mu$ M SYTO 63 for 10 minutes at 37°C. The slides were washed twice with PBS, dried, and mounted onto coverslips as detailed in the laboratory manual of Dr. David Andrews. They were visualized using the Zeiss 510 confocal microscope at the McMaster University Microscopy Facility. Green fluorescent protein was observed using an argon 488 laser and the FITC filter set. SYTO 63 was visualized using a HeNe 633 laser and a 637 nm filter.

## **2.19 <sup>35</sup>S Methionine Cell Labeling**

<sup>35</sup>S methionine cell labeling was performed following the method of the laboratory manual of Dr. David W. Andrews (McMaster University). The Bax proteins were immunoprecipitated with 2D2 and Max5 antibodies, while GFP proteins were immunoprecipitated with  $\alpha$ GFP antibody.

## **2.20 GST-SH3 Domain Fusion Proteins**

GST-SH3 domain fusions of the SH3 domains of c-Abl, both Grb2N SH3 domains, Cortactin, PLC $\gamma$ , P9, P7, p53BP2, and Src were received from Dr. Brian K. Kay at the University of Wisconsin-Madison. They were induced in DH5 $\alpha$  cells, lysed by French press and purified following the methods of Dr. Kay, outlined in Sparks *et al.* (1995). GST-SH3 domain fusion proteins were purified using Glutathione Sepharose 4B columns (Pharmacia) following the protocol in the laboratory manual of Dr. David Andrews (McMaster University).

## **2.21 ELISA Assay for Detecting SH3 Domain Interactions**

These experiments were done following the methods of Yamabhai and Kay, 1997. 1 to 10  $\mu$ g of each GST-SH3 fusion proteins were added to each well of a high binding microtitre plate (Costar). The total volume was increased to 150  $\mu$ l with PBS, and the wells were sealed with Scotch tape. The plate was incubated for 1 to 3 hours at room temperature, or at 4°C overnight. 150  $\mu$ l of 1.0 % (w/v) bovine serum albumin (BSA) in PBS was added to each microtitre well. The wells were sealed and the plate was incubated for 1 to 3 hours at room temperature, or at 4°C overnight. The solution was discarded by rapidly inverting the plate, and blotting residual liquid on a mat of paper towels. The wells were washed 3 times with Tris-buffered saline (TBS) [25 mM Tris-HCl, pH 7.5, 145 mM NaCl, 3 mM KCl] containing 0.1% Tween-20. Expression of the Src-ligand-BAP fusion protein was induced in *E. coli* cells by the addition of 1 mM IPTG when the

cells had grown to an optical density of 0.5 at 600 nm, followed by incubation overnight at 37°C. The cells were pelleted and the supernatant was flash frozen in liquid nitrogen, and stored at -20°C. 100 µl of the Src-ligand-BAP containing supernatant was added to each well, and the plate was incubated at room temperature for 2 hours. The wells were washed 3 times with TBS-0.1% Tween 20. The bound alkaline phosphate fusion proteins were detected by the addition of 8 mM *p*-nitrophenol phosphate (pNPP) as directed in the Gibco-BRL/Life Technologies protocol.

## **2.22 Slot Blot Assay for Detecting SH3 Domain Interactions**

0.001 to 0.5 mg of each of the GST-SH3 domain fusion proteins (c-Abl, p53BP2, and c-Src SH3 domains) were diluted in PBS and slot blotted onto a nitrocellulose membrane following the directions of the Minifold II Slot Blot System (Schleicher and Schuell). Once blotted, the membrane was blocked in Blocking Buffer [140 mM NaCl, 10 mM KPO<sub>4</sub>, pH 7.4, 0.02% sodium azide, 0.5% skim milk] for 30 minutes to 2 hours at room temperature, or at 4°C overnight. <sup>35</sup>S methionine labeled Bax $\alpha$ , Bax $\beta$ , Src-ligand-BAP, and Pre-prolactin were made *in vitro*, and these reactions were salt exchanged over G25 Sephadex to remove unincorporated <sup>35</sup>S methionine. The slot blots were washed three times with Wash Buffer [100mM NaCl, 10mM KPO<sub>4</sub>, 0.1% Triton X-100], probed with the translated proteins diluted in wash buffer for two hours at room temperature, washed three more times with wash buffer and dried on the bench overnight.

The membranes were then exposed to film and developed. Attempted optimizations of the washing conditions included using 0.25% to 1% Triton X-100, and 1% Triton X-100 with 0.1% SDS, as well as changing the NaCl concentrations from 25 mM to 1 M.

### **2.23 GST Immunoprecipitations**

The  $\alpha$ GST antibody immunoprecipitations from the GST-SH3 domain lysates were done using 10  $\mu$ g of cell lysate diluted in 0.5 ml of PBS or 0.5 ml of TBS-T [25 nM Tris-HCl pH 7.5, 145 mM NaCl, 3 mM KCl, 0.1% Tween-20]. This was bound to 2  $\mu$ l of  $\alpha$ GST antibody and 5  $\mu$ l of Protein A agarose beads (Pharmacia) or 5  $\mu$ l of Glutathione Sepharose 4B (Pharmacia) for 2 hours with rotating at 4°C. 0.5 ml of TBS-T was added to the PBS binding samples prior to this step. The  $^{35}$ S methionine labeled Bax $\alpha$ , Bax $\beta$ , and Src-ligand-BAP proteins were pre-cleared with 5  $\mu$ l of Protein A agarose beads or Glutathione Sepharose 4B for 1 hour with rotating at 4°C. The beads were pelleted and the supernatant was incubated with the GST-SH3 domain protein-beads overnight with rotating at 4°C. Three washes of 500  $\mu$ l of the TBS-T buffer were done followed by two washes with 0.1 M Tris and 0.1 M NaCl. The samples were resuspended in 20  $\mu$ l of TLB.

### 3. RESULTS

#### 3.1 Expression of Bax $\beta$

When the *bax $\alpha$*  cDNA was discovered, the *bax $\beta$*  cDNA was also found. Northern blots were performed on the interleukin-3 – dependent murine cell line, FL5.12, and on RL-7 cells, a human follicular lymphoma B-cell line that bears a t(14:18) translocation (Oltvai *et al.*, 1993). FL5.12 cells had only *bax $\alpha$*  mRNA. However, RL-7 cells expressed both the 1.0 kb *bax $\alpha$*  transcript and the 1.5 kb *bax $\beta$*  transcript (Oltvai *et al.*, 1993). This 1.5 kb transcript encoded *bax $\beta$* , as shown by a Northern blot with a probe specific to the unspliced intron 5 present only in *bax $\beta$*  (Oltvai *et al.*, 1993). Low amounts of a 24 kDa protein that co-immunoprecipitated with Bcl-2 was found in RL-7 cells, however this 24 kDa protein was never conclusively identified as Bax $\beta$  (Oltvai *et al.*, 1993). *bax $\beta$*  mRNA has been found in many mouse tissues using the reverse transcriptase polymerase chain reaction (RT-PCR). It is co-expressed with *bax $\alpha$*  in lung, stomach, kidney, thymus, lymph node, bone marrow, pancreas, and spleen. *bax $\beta$*  mRNA was very abundant in brain, with almost no *bax $\alpha$*  mRNA detected (Oltvai *et al.*, 1993). Ribonuclease protection assays have also detected *bax $\beta$*  mRNA in human brain, liver, heart, lung and kidney (Zhou *et al.*, 1998). Immunohistochemical studies of Bax expression in mouse tissues using an antibody to the amino-terminus detected a 24 kDa protein at high levels in

pancreas, epididymis and at lower levels in small intestine (Krajewski *et al.*, 1994). This protein could be Bax $\beta$ , Bax $\omega$ , or Bax $\kappa$  as they are all 24 kDa in size and identical to Bax $\alpha$  at the amino-terminus. However, the protein distributions differ markedly from the mRNA levels determined by Oltvai *et al.* (1993). Therefore, I examined both tissue and cell lines for expression of Bax $\beta$ .

Numerous antibodies that bind the common amino-terminus of Bax were used in these studies: a rabbit polyclonal antiserum (Max5), a human-specific monoclonal antibody (2D2) (Hsu *et al.*, 1997), and monoclonal antibodies 1D1 and 5B7 that are specific for rat and mouse Bax respectively (Hsu and Youle, 1998) (of note, 1D1 was made using a peptide (CGSGDHLGGGGPTSS) that does not exactly match amino acids 3 to 16 of rat Bax), a monoclonal antibody (6A7) which recognizes amino acids 13 to 19 in the N-terminus of Bax only after the conformational change associated with apoptosis occurs (Hsu and Youle, 1997), and 2C8, a monoclonal antibody to amino acids 43 to 62 (Hsu and Youle, 1998). These antibody epitopes have been mapped to the Bax $\alpha$  sequence, as shown in Figure 4A. In addition, a sheep antiserum was raised against the specific carboxyl-terminus of Bax $\beta$  to definitively identify this Bax isoform (Figure 4B). This antibody immunoprecipitates native Bax $\beta$  protein, but it does not recognize denatured Bax $\beta$  on Western blots (data not shown).

A variety of cell lines were screened for expression of Bax $\beta$ . RL-7 cells and the MCF-7 human breast carcinoma cell line were lysed using the non-ionic NP-40 detergent. Immunoprecipitations with the 2D2 antibody followed by

**A)**

|                                     |          |  |                   |           |  |  |  |  |  |
|-------------------------------------|----------|--|-------------------|-----------|--|--|--|--|--|
|                                     |          | <u><math>\alpha</math> mouse Bax 5B7</u>     |                   |           |  |  |  |  |  |
|                                     |          | <u><math>\alpha</math> rat Bax 1D1</u>       |                   |           |  |  |  |  |  |
|                                     |          | <u><math>\alpha</math> universal Bax 6A7</u> |                   |           |  |  |  |  |  |
|                                     |          | <u><math>\alpha</math> human Bax 2D2</u>     |                   |           |  |  |  |  |  |
|                                     |          | <u><math>\alpha</math> human Bax Max5</u>    |                   |           |  |  |  |  |  |
| <b>human Bax<math>\alpha</math></b> | <b>1</b> | MDGSG EQPRG GGPTS SEQIM                      | KTGAL LLQGF IQDRA | <b>30</b> |  |  |  |  |  |
| <b>human Bax<math>\beta</math></b>  | <b>1</b> | MDGSG EQPRG GGPTS SEQIM                      | KTGAL LLQGF IQDRA | <b>30</b> |  |  |  |  |  |
| <b>mouse Bax<math>\alpha</math></b> | <b>1</b> | MDGSG EQLGS GGPTS SEQIM                      | KTGAF LLQGF IQDRA | <b>30</b> |  |  |  |  |  |
| <b>rat Bax<math>\alpha</math></b>   | <b>1</b> | MDGSG EQLGG GGPTS SEQIM                      | KTGAF LLQGF IQDRA | <b>30</b> |  |  |  |  |  |

**B)**

|                                    |            |  |  |  |  |  |            |
|------------------------------------|------------|--|--|--|--|--|------------|
|                                    |            |  |  |  |  | <u><math>\alpha</math> Bax<math>\beta</math></u> |            |
| <b>human Bax<math>\beta</math></b> | <b>159</b> | VRLLK PPHPH HRALT TAPAP PSLPP ATPLG PWAFFW |  |  |  |  | <b>193</b> |
|                                    | <b>194</b> | SRSQW CPLPI FRSSD WYNA FSLRV               |  |  |  |  | <b>218</b> |

**Figure 4:** Epitopes recognized by the Bax antibodies.

- A) The amino-terminal sequences for human, mouse, and rat Bax $\alpha$  and human Bax $\beta$  are shown. The black lines above the sequences denote the epitopes recognized by the specified antibodies. Omitted from this figure for clarity is the  $\alpha$  universal Bax 2C8 that recognizes amino acids 43 to 62.
- B) The carboxyl-terminal sequence of human Bax $\beta$  is shown, with the epitope recognized by the  $\alpha$ Bax $\beta$  antibody denoted by the black line above the sequence.

Western blotting with the Max5 antibody showed the presence of Bax $\alpha$  but were inconclusive for Bax $\beta$  in MCF-7 cells (Figure 5A). Control immunoprecipitations performed in the absence of cell lysate (data not shown) demonstrated bands of similar size to Bax $\beta$  on the Western blots. These correspond to the light chain of the antibody used for immunoprecipitation and would have obscured signal from Bax $\beta$  if it was of low abundance. Western blots were also done using 10  $\mu$ g of protein from NP-40 lysates of Madin Darby canine kidney (MDCK) cells, Vero cells (a monkey kidney epithelial cell line) and HT29 human colon adenocarcinoma cells (and the photodynamic therapy-induced resistant subclone HT29-A11 cell line) using the polyclonal Max5 antibody (Figure 5B,C). Bax $\beta$  was not detected in any of these cell lines.

Rat tissue homogenates were made, without detergent, of brain, lung, heart, stomach, spleen, and pancreas, and immunoblotted with the rat-specific 1D1 antibody. Bax $\alpha$  was the major protein detected on these Western blots (Figure 6A), even in the brain, where levels of *bax $\beta$*  mRNA are very high compared to *bax $\alpha$*  in other tissues and in which there is no detectable *bax $\alpha$*  mRNA (Oltvai *et al.*, 1993). Other cross-reacting bands are present on the gels, but all above 25.8 kDa in size, and consequently are not likely to represent Bax $\beta$ .

Immunoprecipitations were done to amplify the Bax $\beta$  signal, using the 2C8, 6A7, or  $\alpha$ Bax $\beta$  antibody followed by Western blotting with the 1D1 antibody (data not shown). Unfortunately, a strong cross-reacting band of approximately

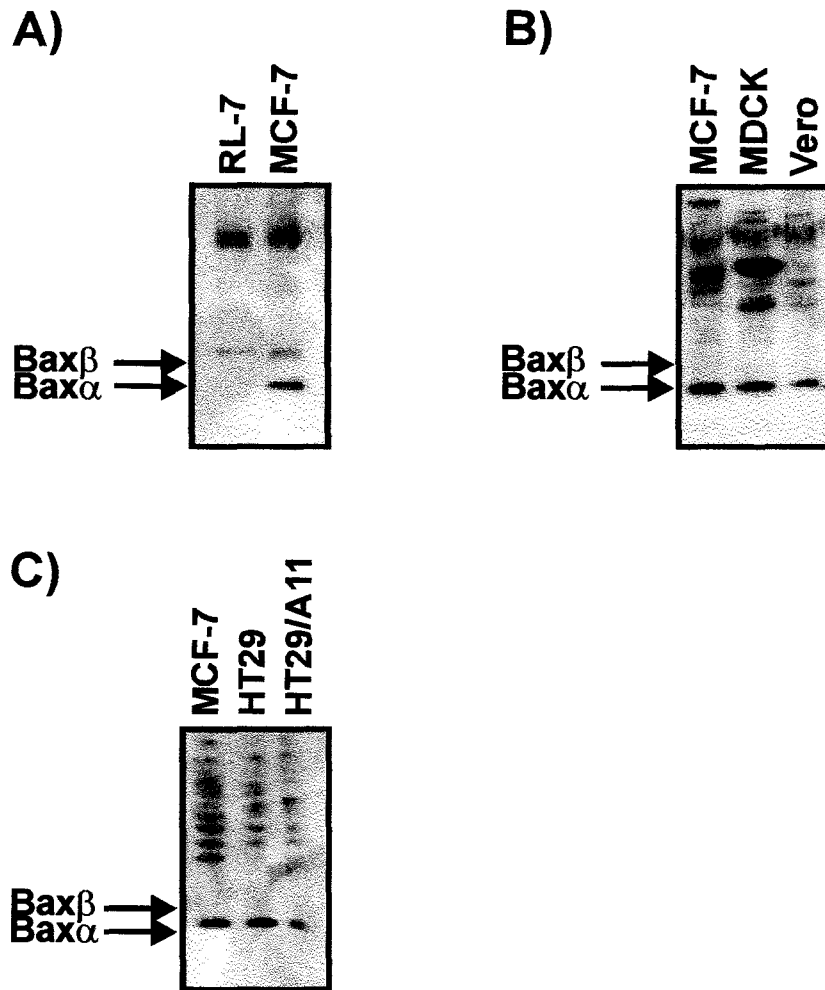


**Figure 5:** Bax protein expression in cell lines.

- A) Immunoprecipitates with the 2D2 antibody of 10  $\mu$ g of NP-40 lysates from RL-7 and MCF-7 cells were immunoblotted with the Max5 antibody. The expected positions of Bax $\alpha$  and Bax $\beta$  migration are indicated (arrows).
- B) Immunoblots of 10  $\mu$ g of NP-40 lysates from MCF-7, MDCK, and Vero cells were done with the Max5 antibody. The expected positions of Bax $\alpha$  and Bax $\beta$  migration are indicated (arrows).
- C) Immunoblots of 10  $\mu$ g of NP-40 lysates from MCF-7, HT29, and HT29/A11 cells were done with the Max5 antibody. The expected positions of Bax $\alpha$  and Bax $\beta$  migration are indicated (arrows).

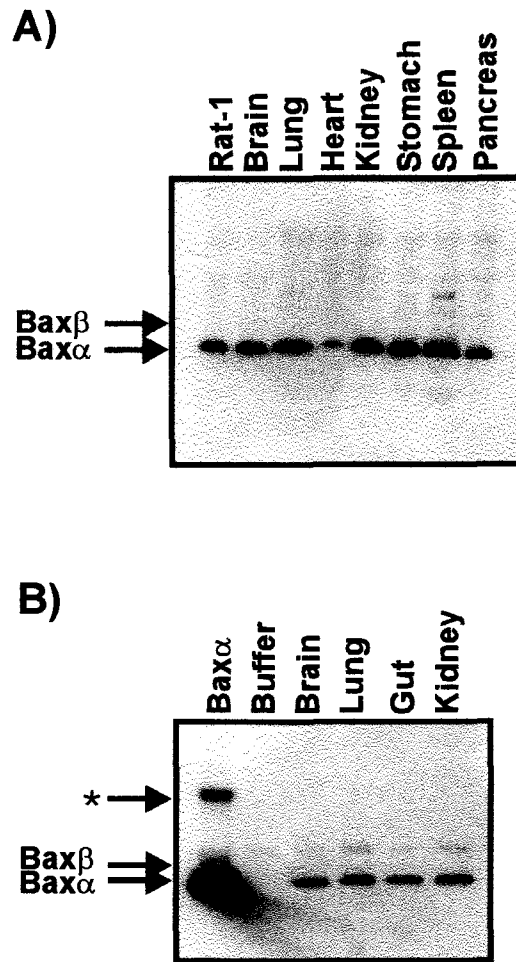


**Figure 6:** Bax protein expression in rat and human tissues.

- A) Immunoblots of 50  $\mu$ g of various rat tissue homogenates were done with the 1D1 antibody. Rat-1 fibroblast NP-40 cell lysate was used as a control. The positions of Bax $\alpha$  and Bax $\beta$  migration are indicated (arrows).
- B) Immunoprecipitates with the 2D2 antibody of 50  $\mu$ g of various human fetal tissue homogenates were immunoblotted with the Max5 antibody. Recombinant Bax $\alpha$  was used as a control. The positions of Bax $\alpha$  and Bax $\beta$  migration are indicated (arrows). The \* denotes a cross-reacting band found in the recombinant Bax $\alpha$  protein sample.

28 kDa obscured any Bax $\beta$  signal potentially present. This 28 kDa band is light chain protein from the immunoprecipitating antibody, as it was present in samples without tissue lysate. Furthermore, this problem was not due to Protein G detaching from the sepharose beads used for immunoprecipitation, as the bands persisted using antibodies coupled to Affigel-10 (data not shown).

Tissue homogenates of human fetal brain, lung, kidney and gut tissues were immunoblotted with either Max5 polyclonal antibody or 2D2 monoclonal antibody. Bax $\alpha$ , but no Bax $\beta$  was observed (Figure 6B). The problem with light chain cross-reactivity discussed above was also present with Western blotting using these human tissues. Therefore, our methods do not allow us to detect Bax $\beta$  in rat or human tissues.

To confirm the presence of Bax $\beta$  protein in mouse tissue (Krajewski *et al.*, 1994) brain, lung, heart, kidney, stomach, spleen, duodenum and colon were homogenized. Immunoblots of 10  $\mu$ g of the tissues using the cross-species 2C8 monoclonal antibody failed to detect Bax $\alpha$  or Bax $\beta$  (data not shown). 50  $\mu$ g of these tissue samples were also probed with the 5B7 and 2C8 antibodies, used at a dilution of 1:20 of culture fluid as reported by Hsu and Youle to detect Bax in purified thymocytes (1998) (data not shown). However, the secondary  $\alpha$ mouse antibody used for the Western blots reacted very strongly with the light chain protein in infiltrating lymphocytes present in the mouse tissue homogenates used here. Pre-treatment of the tissue lysates to remove the immunoglobulin proteins from the homogenates or the use of a primary antibody for mouse Bax produced

by an animal other than a mouse would enable protein expression in the mouse tissues to be determined. As these approaches were not tried, the presence of Bax isoforms in mouse tissues was not resolved in this study.

In all of the cell and tissue lysates tested with a variety of antibodies to the Bax protein, the Bax $\beta$  isoform was not detected. It is possible that Bax $\beta$  was not expressed in the cells and tissues tested, that it was very short-lived, that it was present at levels below the detection capabilities of the assay, or that it was not being efficiently released from the cells during the lysis procedure.

It is improbable that Bax $\beta$  is not expressed, as the amount of *bax $\beta$*  mRNA is very high in some tissues, most notably brain (Oltvai *et al.*, 1993). However, recent studies examining mRNA levels and protein abundance reveal a low correlation between these values (Gygi *et al.*, 1999, Ideker *et al.* 2001), with up to 30-fold differences in protein level for the same amount of transcript in *Saccharomyces cerevisiae* (Gygi *et al.*, 1999). Clearly translational and post-translational regulation are critical determinants of protein levels in eukaryotic cells. Thus, Bax $\beta$  levels may be translationally-regulated, with very high mRNA levels but little to no protein expressed. However, this extreme difference is rarely seen, as proteins with very high mRNA are usually expressed at detectable levels. It is possible that regulated splicing of *bax $\beta$*  mRNA as a translationally “inert” species functions as a means of avoiding the production of excess amounts of the toxic Bax $\alpha$  isoform in certain circumstances.

Alternatively, *bax $\beta$*  mRNA might be translated *in vivo*, but the resulting protein has such a short half-life that the protein was not detected using the methods described. This possibility is explored in other experiments (Section 3.3.1). A further possibility is that Bax $\beta$  is expressed in cell types that were not tested here or under different cellular conditions, or that Bax $\beta$  was not effectively extracted from the cells using the NP-40 detergent or during the homogenizing of the tissues. However, Bax $\alpha$ , a partly membrane bound protein, was efficiently extracted; Bax $\beta$  lacks an insertion sequence and is therefore not likely to be an integral membrane protein. Therefore, while a wide variety of tissues and cell lines were probed for expression of Bax, only Bax $\alpha$  was found using the available techniques.

### **3.2 Function of Bax $\beta$ in Apoptosis**

It is difficult to predict the function of Bax $\beta$ . It could behave in a pro-apoptotic manner due to similarity with Bax $\alpha$ . Alternatively, if the carboxyl-terminus of the Bax $\alpha$  protein is important for function, the Bax $\beta$  isoform may be neutral, or even oppose the function of Bax $\alpha$ .

The function of Bax $\beta$  in apoptosis was examined with four different assays: 1) transfected cell pools were treated with apoptosis-inducing agents, 2) a transient transfection assay was designed to look at the effect of Bax $\beta$  in various conditions, 3) the amino-terminal conformation of the Bax $\beta$  protein was

examined using the 6A7 antibody that recognizes the active conformation of Bax $\alpha$ , and 4) the potential for hetero-oligomerizations between the different Bax isoforms was investigated by co-immunoprecipitation.

### 3.2.1 Rat-1 *myc* ERTM Pooled Cell Lines

Creating stable cell lines expressing pro-apoptotic proteins has significant disadvantages, as stable transfectants will either express low levels of the proteins or have developed resistance to their pro-apoptotic function. Therefore, there are few stable cell lines overexpressing Bax proteins, and we were unable to generate any. The creation of inducible cell lines was also attempted without success, as the surviving clones did not express the protein after induction, conceivably due to leaky expression of the Bax proteins. Therefore pooled cell lines which have undergone minimal passages when expressing the Bax proteins were used to examine the function of Bax $\beta$  in apoptosis.

Rat-1 fibroblasts in which the *c-myc* oncogene is fused to a tamoxifen-inducible estrogen receptor (Rat-1 *myc* ERTM) were used for these experiments. Myc changes to an active conformation upon exposure to 4-hydroxytamoxifen. The pBabe MN IRES GFP vector was used to transfer the *bax* $\alpha$ , *bax* $\beta$ , or the Bax $\alpha$  mutant of increased pro-apoptotic activity (*bax* $\alpha$ - $\Delta$ S184) genes, along with the green fluorescent protein (GFP) reporter gene, into the cells. This was done through retroviral infections by Erinn Soucie in the laboratory of Dr. Linda Penn at the Ontario Cancer Institute. The target gene was cloned into the vector followed

by an internal ribosome entry site (IRES) and the *gfp* gene, and the constructs were verified by sequencing (data not shown). Thus a single mRNA encoded both the protein being tested and GFP. The two coding regions were translated separately, but expression of GFP was evidence for transcription of the target gene. Unlike GFP fusion proteins, this system avoids potential interferences with protein function caused by a large GFP moiety fused to either the amino- or carboxyl-terminus of the protein. Green cells, indicative of successful infection with the vector, were pooled by fluorescence activated cell sorting (FACS). This sorted population contained cells expressing different levels of GFP.

Expression of the Bax proteins was verified by Western blots of 20  $\mu$ g of NP-40 lysates with Max5 antibody to detect exogenous human Bax but not the endogenous rat Bax. Infection with *bax $\alpha$*  resulted in high levels of protein (Figure 7A). Cells infected with *bax $\alpha$ - $\Delta$ S184*, a more apoptotic form of Bax, had barely detectable levels of protein. This cell line also had a very low number of GFP-positive cells that survived infection (0.5% compared to 75% for *bax $\alpha$* ).

Therefore, significant expression of *Bax $\alpha$ - $\Delta$ S184* was probably counter-selected, and we did not characterize this line further. Cells were efficiently infected with *bax $\beta$*  (74.7%), but with very low levels of protein expression (Figure 7A). While these cells did not die like the *Bax $\alpha$ - $\Delta$ S184* cells, they did not overexpress *Bax $\beta$* .

A second infection was performed to allow selection of only the 25% of cells expressing the highest levels of GFP. The *Bax $\alpha$*  cell line again exhibited elevated levels of *Bax $\alpha$*  expression (Figure 7B). *Bax $\beta$*  expression was higher

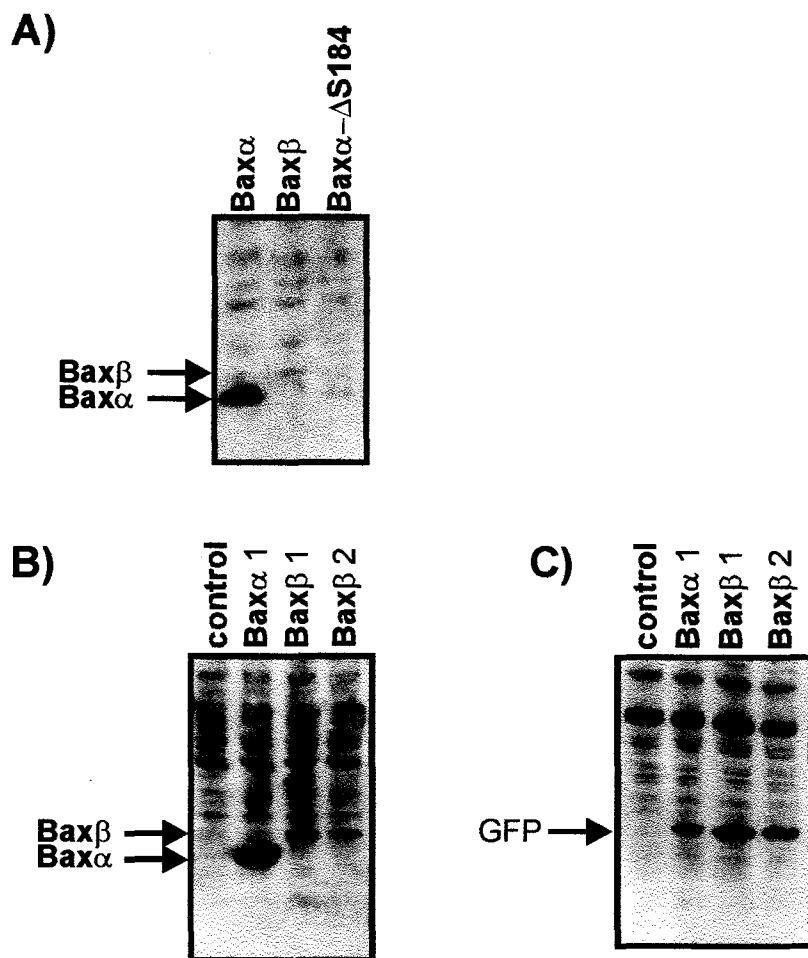


**Figure 7:** Protein expression in Rat-1 *myc* ERTM pooled cell lines.

- A) Immunoblots of 20  $\mu$ g of NP-40 lysates of the first set of Rat-1 *myc* ERTM pooled cell lines were done with the Max5 antibody. The positions of Bax $\alpha$  and Bax $\beta$  migration are indicated (arrows).
- B) Immunoblots of 20  $\mu$ g of NP-40 lysates of the second set of Rat-1 *myc* ERTM pooled cell lines that were sorted for the top 25% of GFP-expressing cells (Bax $\alpha$ 1 and Bax $\beta$ 1) and sorted for GFP fluorescence equal to Bax $\alpha$ 1 (Bax $\beta$ 2) were done with the Max5 antibody. The positions of Bax $\alpha$  and Bax $\beta$  migration are indicated (arrows).
- C) Immunoblots of 20  $\mu$ g of NP-40 lysates of the second set of Rat-1 *myc* ERTM pooled cell lines that were sorted for the top 25% of GFP-expressing cells (Bax $\alpha$ 1 and Bax $\beta$ 1) and sorted for GFP fluorescence equal to Bax $\alpha$ 1 (Bax $\beta$ 2) were done with the  $\alpha$ GFP antibody. The position of GFP migration is indicated (arrow).

than in the previous pooled cell population, but still low compared to Bax $\alpha$ . This pool of Bax $\beta$  cells was re-sorted for levels of GFP similar to the Bax $\alpha$  pool. However, with this secondary selection the levels of both Bax $\beta$  and GFP decreased (Figure 7C). As Bax $\beta$  expression levels paralleled GFP levels, the mRNA was transcribed. This suggests that the Rat-1 fibroblast cells will not tolerate Bax $\beta$  protein overexpression, the *bax $\beta$*  mRNA is an inefficient template for translation, or the Bax $\beta$  protein is subject to high turnover rates.

The Bax $\alpha$  and the Bax $\beta$  pooled cell lines with the highest levels of Bax protein expression (Bax $\alpha$ 1 and Bax $\beta$ 1) were used for further studies. The parental cell line, Rat-1 *myc* ERTM, was used as a control. The cells were treated with various inducers of apoptosis for up to 12 hours: 6  $\mu$ M of etoposide, serum starvation, or 10  $\mu$ M of Adriamycin. In all cases, Myc function was enabled by treatment with 100 nM of 4-hydroxytamoxifen to potentiate apoptosis. Cell death was assessed by cleavage of poly (ADP-ribose) polymerase (PARP).

All stimuli resulted in PARP cleavage first detectable at six hours, and by nine hours just under half of the PARP was cleaved in the parental cell line (Figure 8). Overexpression of Bax $\alpha$  enhanced the effect of etoposide and Adriamycin as PARP cleavage occurred approximately three hours earlier (Figure 8). This effect was not seen with serum starvation. Thus Bax $\alpha$  is not a critical component in the apoptotic pathway induced by serum starvation in fibroblasts, consistent with the model proposed by Annis *et al.* (2001).

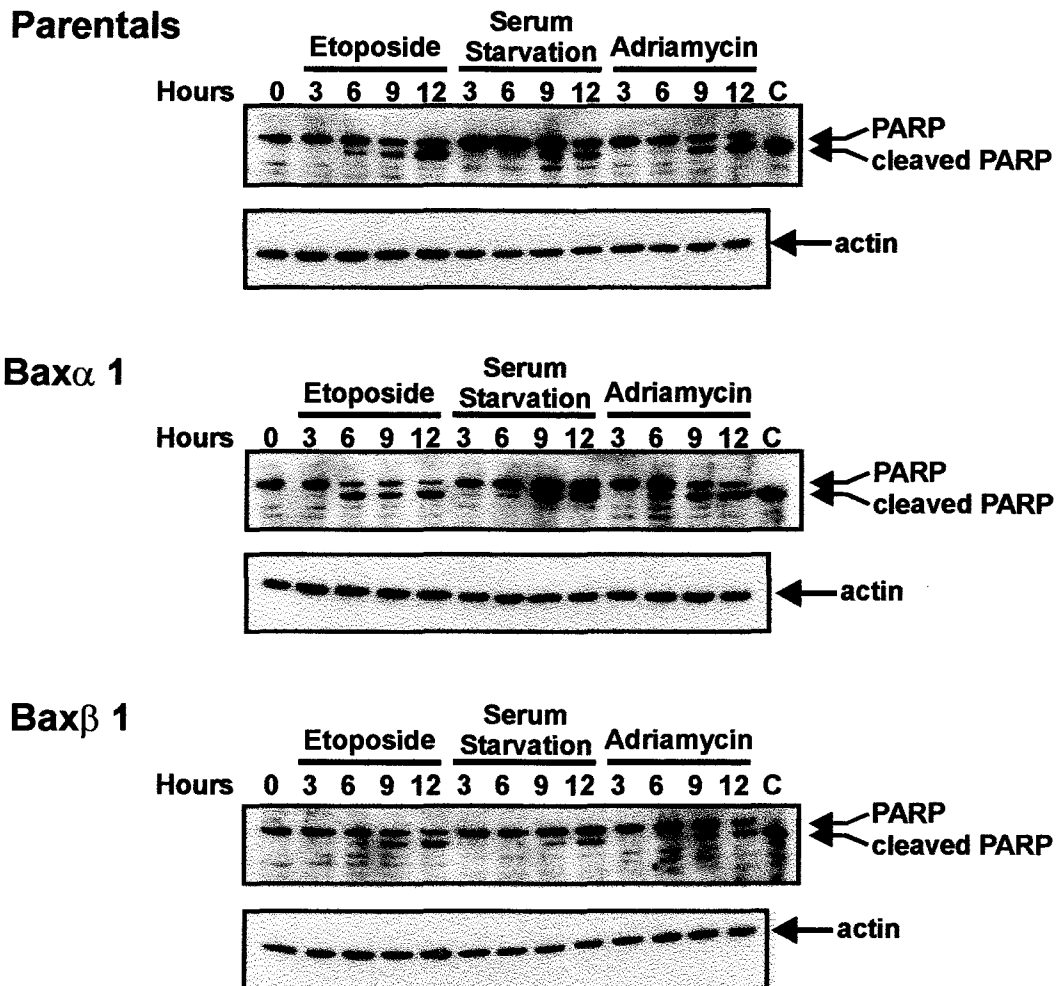


**Figure 8:** Cleavage of the caspase substrate PARP in Rat-1 *myc* ERTM pooled cell lines treated with etoposide, serum starvation, and Adriamycin.

Immunoblots of 5  $\mu$ g of protein from SDS lysates of the parental cell line, Rat-1 *myc* ERTM, and the pooled cell lines Rat-1 *myc* ERTM Bax $\alpha$ 1 and Rat-1 *myc* ERTM Bax $\beta$ 1 were done with  $\alpha$ PARP antibody. These cell lines express the highest levels of Bax proteins, and were treated with 100 nM tamoxifen to induce Myc function. They were further treated with 6  $\mu$ M etoposide, or serum starvation, or 10  $\mu$ M Adriamycin for 0 to 12 hours. The migration positions of full length and cleaved PARP proteins are indicated (arrows). Actin was run as a control demonstrating that equal amounts of protein were loaded in each lane. The control (C) is NP-40 lysate from MCF-7 breast cancer cell line treated with 10  $\mu$ M Adriamycin for 24 hours, a condition known to result in cleavage of PARP.

In contrast to cells expressing Bax $\alpha$ , the Bax $\beta$  expressing cells did not differ from the parental cell line in susceptibility to induce apoptosis (Figure 8). This may be due to the low levels of Bax $\beta$  expressed compared to Bax $\alpha$ , if the “potency” of these two isoforms is roughly equivalent. Alternatively, the creation of the pooled cell lines requires cell passage that may have resulted in tolerance to Bax $\beta$  if its effect is more potent than that of Bax $\alpha$ . Finally, Bax $\beta$  may have no effect on apoptosis. Unfortunately, these experiments do not allow us to distinguish among these possibilities.

### **3.2.2 Transient Transfection of NIH 3T3 cells**

To circumvent these problems, many investigations have examined the effect of pro-apoptotic proteins using transient transfections. Cell viability is measured by the level of expression of a reporter gene in the population of transfected cells (Wolter *et al.*, 1997, Inohara *et al.*, 1997, Jurgensmeier *et al.*, 1998). The reporter gene used in my studies was GFP. (Other investigators have also used luciferase.) Using GFP has several advantages: living cells can be examined with minimal toxicity, expression can be detected without exogenous substrate, and the fluorescent signal is strong (Welsh and Kay, 1997, Wood, 1995). NIH 3T3 mouse embryonic fibroblast cells were chosen as they are easily transfectable, have a relatively normal morphology, and a large cytoplasmic area amenable to immunofluorescence and confocal microscopy. A variety of transfection reagents were assayed, and the ExGen 500 reagent (MBI

Fermentas) exhibited low toxicity and gave maximal transfection efficiencies of up to 50%.

The cells were grown on glass coverslips, and after transfection fixed with paraformaldehyde and stained with SYTO 63 (Molecular Probes), a cell-permeant stain that binds nucleic acids. In fixed cells the dye binds extra-nuclear nucleic acids predominantly at the mitochondria. SYTO 63 absorbs light at 657 nm and an emission maximum of 673 nm (Molecular Probes). In contrast, GFP has an excitation maximum of 488 nm and an emission maximum of 507 nm (Clontech). As the excitation and emission peaks do not significantly overlap, SYTO 63 and GFP were used concurrently. Distinct signals for both were detected using the Zeiss 510 confocal microscope. By examining the adherent cells, any effects of removing the cells from the growth surface are avoided.

Images were taken on the Zeiss 510 confocal microscope using a pinhole setting for thick sections of 20  $\mu\text{m}$ , permitting capture of total fluorescence from the entire cell. Additionally, the brightness and contrast settings were set such that the dimmest cells were visible in the image and kept as part of the data set. Even though these settings resulted in some cells being at or above the maximum detectable GFP fluorescence, all of the transfected cells were included to obtain an accurate numerator to measure the degree of cell death. Ten images of 20X magnification were taken from random locations on each slide, with one slide per transfection.

The confocal images were subsequently converted to TIFF images for quantification using macros written for the Zeiss KS 400 data analysis program. One macro (Red-Green 2) calculated the pixel intensities of all of the green cells and the red pixel intensities of only the transfected (*i.e.* green) cells. The green and corresponding red pixel intensities from each image were then plotted on a scattergram of red intensity versus green intensity for at least eight images and a least-squares line of best fit was calculated. The slope of this line reflects the relative GFP fluorescence per cell of the transfected cells in the population, independent of the number of cells. These slopes were plotted as a histogram.

A second macro (Red-Green 3) calculated all of the green pixel intensities and all of the red pixel intensities for each image. The red and green pixel intensities for each image were added. These total red and total green values for at least eight images were plotted on a scattergram of red intensity versus green intensity. A least-squares line of best fit for all of the images from each slide was calculated. The slope of this line reflected the relative transfection efficiency, *i.e.* the percentage of cells that were green. These slopes were plotted as a histogram.

The first set of transfections used the pBabe MN IRES GFP constructs with the NIH 3T3 cells. Co-transfection with a similar plasmid encoding Bax $\alpha$ - $\Delta$ S184 was used to trigger apoptosis, and in its absence the pBabe MN IRES GFP parental vector was used to keep the amount of *gfp* cDNA, and consequently the amount of GFP production, constant. This maximized the

transfection efficiency and enabled comparisons among the transfections, in the presence and absence of Bax $\alpha$ - $\Delta$ S184.

Cell lysates were made 18 hours after transfection and immunoblotted for the Bcl-2 family proteins and GFP. Antibodies specific for the human Bcl-2 family proteins were used to detect transfected rather than endogenous proteins. Bcl-2, Bcl-X<sub>L</sub>, and Bax $\alpha$  were easily detected (Figure 9A). Expression of GFP was confirmed by immunoblotting and confocal microscopy (Figure 9B and data not shown). Bax $\alpha$ - $\Delta$ S184 was expressed at very low levels; these cells expressed no detectable GFP, consistent with the low number of green cells seen by confocal microscopy (Figure 9 and data not shown). Similar to Bax $\alpha$ - $\Delta$ S814, Bax $\beta$  was also expressed at low levels (Figure 9A). However GFP expression of *bax $\beta$*  transfected cells was comparable to cells transfected with *bax $\alpha$* , as determined by Western blotting and confocal microscopy (Figure 9B and data not shown). Therefore Bcl-2, Bcl-X<sub>L</sub>, and Bax $\alpha$  were well expressed from the pBabe MN IRES GFP construct in NIH 3T3 cells, whereas Bax $\alpha$ - $\Delta$ S814 and Bax $\beta$  were expressed at low levels.

The expression of Bax $\alpha$ , Bax $\beta$ , and Bax $\alpha$ - $\Delta$ S184 increased from 8 to 40 hours after transfection (Figure 10). However, Bax $\beta$  protein levels remained much lower than Bax $\alpha$ . The expression of GFP was not detectable until 18 hours post-transfection, and increased by 40 hours (Figure 10). This correlated with an increase in GFP fluorescence seen by confocal microscopy. A cross-reacting

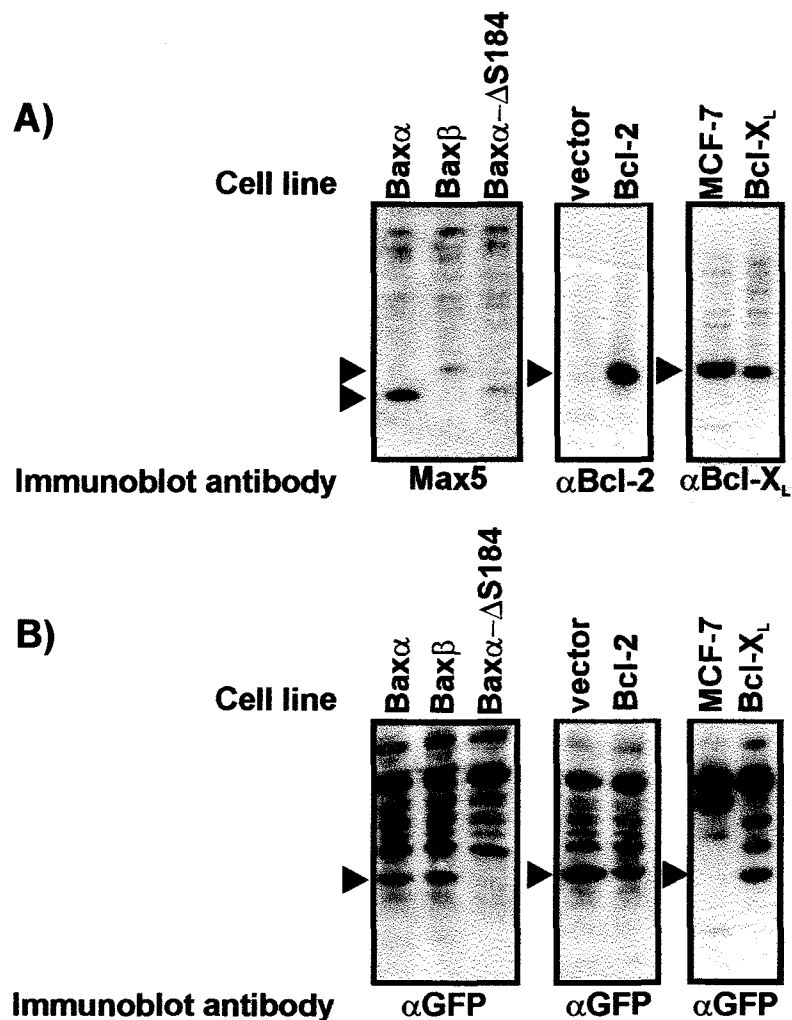


**Figure 9:** Protein expression in NIH 3T3 cells transiently transfected with pBabe MN IRES GFP vector constructs.

- A) Immunoblots of 20  $\mu$ g of NP-40 lysates from NIH 3T3 cells transiently transfected with the pBabe MN IRES GFP vector, *bax $\alpha$* , *bax $\beta$* , *bax $\alpha$ - $\Delta$ S184*, *bcl-2*, or *bcl-X<sub>L</sub>* in the pBabe MN IRES GFP vector, or MCF-7 cell lysate that stably expresses exogenous *Bcl-X<sub>L</sub>* were done with the indicated antibody. The positions of *Bax $\alpha$* , *Bax $\beta$* , *Bcl-2*, and *Bcl-X<sub>L</sub>* migration are indicated (arrows).
- B) Immunoblots of 20  $\mu$ g of NP-40 lysates from NIH 3T3 cells transiently transfected with the pBabe MN IRES GFP vector, *bax $\alpha$* , *bax $\beta$* , *bax $\alpha$ - $\Delta$ S184*, *bcl-2*, or *bcl-X<sub>L</sub>* in the pBabe MN IRES GFP vector, or MCF-7 cell lysate that stably expresses exogenous *Bcl-X<sub>L</sub>* were done with the  $\alpha$ GFP antibody. The position of GFP migration is indicated (arrow).

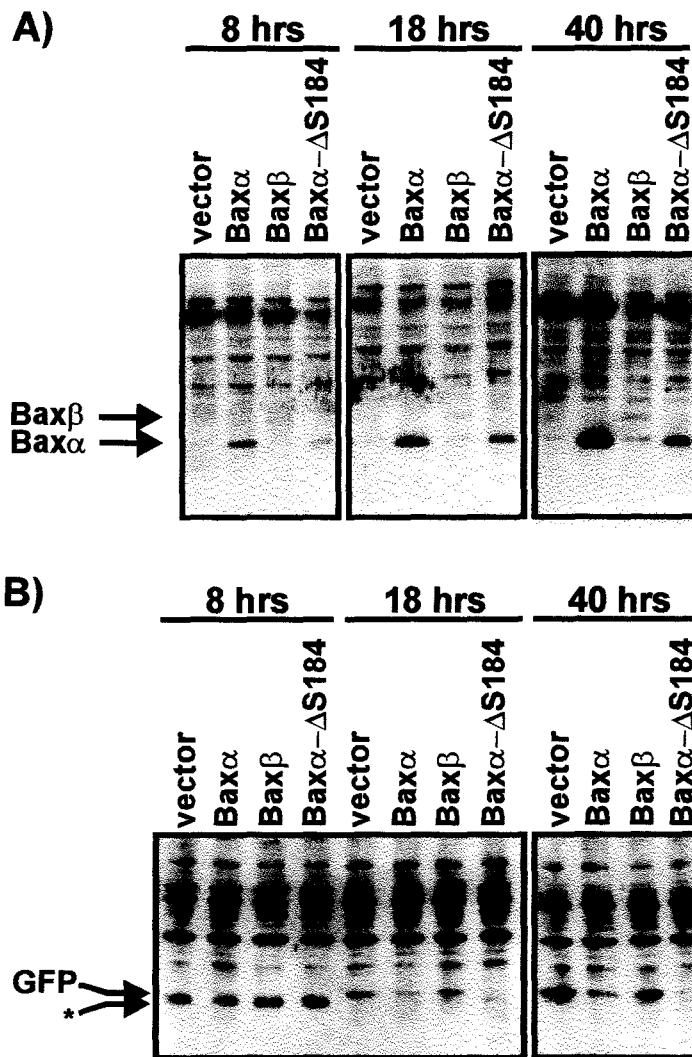


**Figure 10:** Protein expression in NIH 3T3 cells transiently transfected with pBabe MN IRES GFP vector constructs 8, 18, and 40 hours post-transfection.

A) Immunoblots of 20  $\mu$ g of NP-40 lysates from NIH 3T3 cells 8, 18, and 40 hours post-transfection with *bax $\alpha$* , *bax $\beta$* , and *bax $\alpha$ - $\Delta$ S184* in the pBabe MN IRES GFP vector were done with the Max5 antibody. The positions of Bax $\alpha$  and Bax $\beta$  migration are indicated (arrows).

B) Immunoblots of 20  $\mu$ g of NP-40 lysates from NIH 3T3 cells 8, 18, and 40 hours post-transfection with *bax $\alpha$* , *bax $\beta$* , and *bax $\alpha$ - $\Delta$ S184* in the pBabe MN IRES GFP vector were done with the  $\alpha$ GFP antibody. The position of GFP migration is indicated (arrow). The \* denotes a cross-reacting band, smaller in size than GFP.

band a bit smaller than GFP was present in the 8 hour lysates. This protein was verified as not being GFP by confocal microscopy, as no green cells were detected at this time (data not shown). Measurements of GFP intensity and transfection efficiency were done 18 hours post-transfection, for at 40 hours the cells were very crowded and were impossible to visualize individually (data not shown).

The  $Bax\alpha$ - $\Delta S184$  cells likely underwent cell death and lifted off the coverslip prior to the fixing of the samples for microscopy and cell lysate production, which is consistent with the extremely low levels of GFP. The  $Bax\beta$  transfected cells did not die however, as GFP-positive cells remained in these samples. It is very unlikely that  $Bax\beta$  was not produced due to problems in transcription from the vector. It was cloned into the pBabe MN IRES GFP vector in the same manner as  $Bax\alpha$ , which was effectively transcribed and translated, indicating no problems in the common 5' untranslated region of the gene. This cloning was also verified through sequencing (data not shown). Therefore, the reduced levels of  $Bax\beta$  were likely due to either low levels of  $Bax\beta$  production or degradation of  $Bax\beta$  in the cell.

An examination of the amount of green fluorescence per cell and the transfection efficiency revealed no significant differences among the various transfections (Figure 11). Co-transfection with  $bax\alpha$ - $\Delta S184$  compared to vector was associated with a decrease in GFP fluorescence per cell and transfection

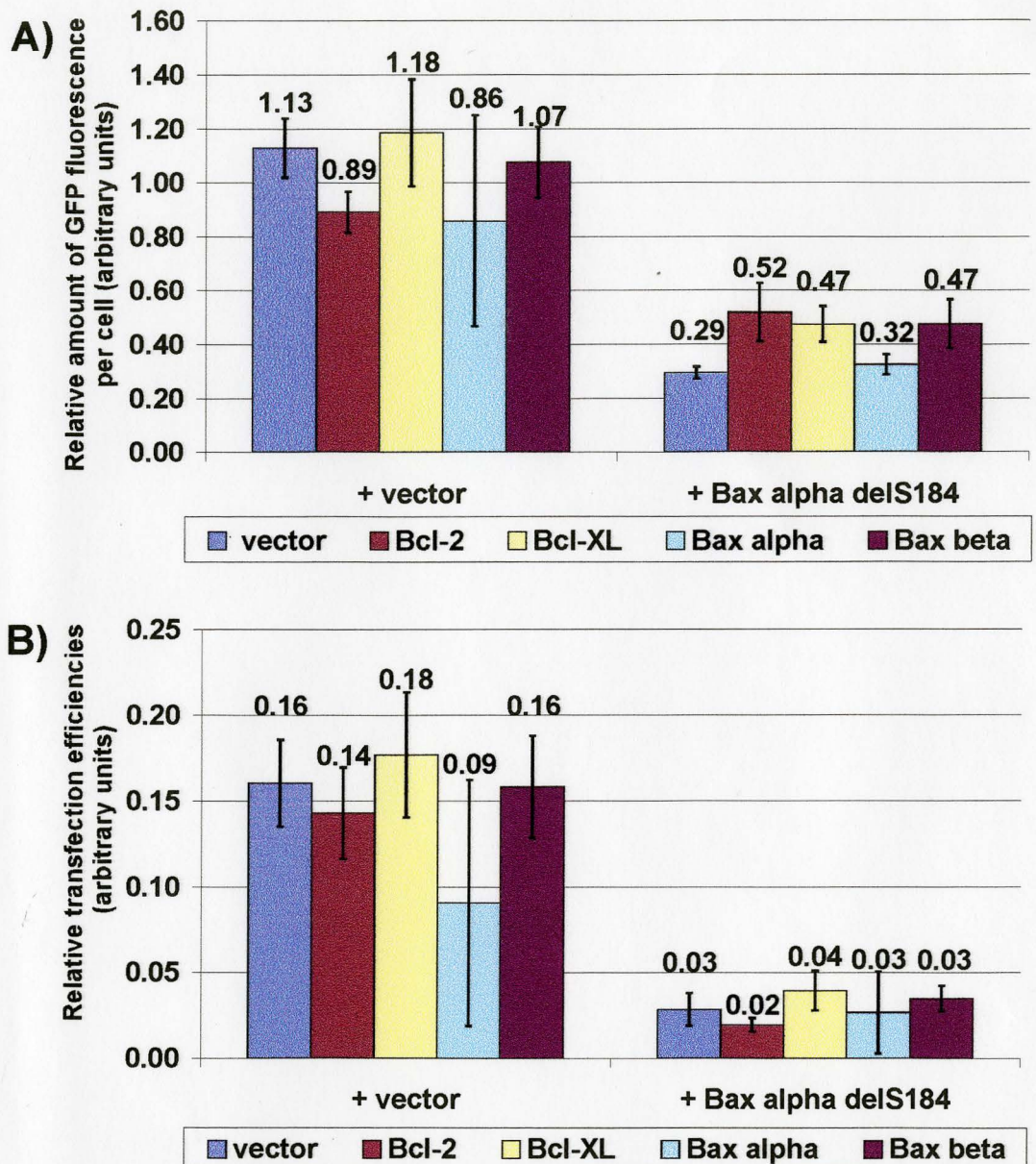


**Figure 11:** The relative amount of GFP fluorescence per cell (A) and the relative transfection efficiencies (B) of NIH 3T3 cells transiently transfected with pBabe MN IRES GFP vector constructs.

2  $\mu$ g of parent vector or vectors encoding a Bcl-2 family member were co-transfected into NIH 3T3 cells with either 2  $\mu$ g of parent pBabe MN IRES GFP vector or 2  $\mu$ g of *bax $\alpha$ - $\Delta$ S814* pBabe MM IRES GFP vector. The relative amount of GFP fluorescence per cell and the relative transfection efficiency for each sample were calculated. Seven samples were analyzed for the vector, Bcl-2, and Bax $\beta$ , six samples for Bcl-X $_L$ , and two samples for Bax $\alpha$ . The error expressed is the standard error of the mean for each sample, with the range of values shown for Bax $\alpha$ .

efficiencies for all constructs. Thus this assay did not allow us to detect functional differences among Bcl-2 family members.

A literature search revealed a possible explanation for this unexpected result. Data was published while these studies were underway regarding the regulation of translation during apoptosis. While many cellular stresses, including apoptosis, inhibit cap-dependent translation, the cap-independent translation mechanism mediated by IRES elements continues to function (Holcik *et al.*, 2000a). The eukaryotic initiation factor 4G (eIF-4G) required for assembly of the ribosome-mRNA complex in translation is cleaved by caspase-3 during apoptosis, abolishing its function (Clemens *et al.*, 2000). The IRES sequence enables the association of the ribosome and mRNA in the absence of eIF-4G with a different assembly of initiation factors. The exact details of this process are unknown. IRES elements have been found in the 5' untranslated regions of genes which encode growth factors and oncogenes (Holcik *et al.*, 2000a), including the anti-apoptotic X-linked inhibitor of apoptosis (XIAP) and pro-apoptotic Apaf-1. Both proteins are translated during apoptosis (Holcik *et al.*, 2000b, Coldwell *et al.*, 2000). By regulating proteins involved in the control of cell death at the level of translation, the cell can rapidly respond to changes in cellular stresses.

Consequently, GFP fluorescence would not reflect apoptosis as it would continue to be translated in this vector. This may explain why no effects of Bcl-2 family members were observed with the transient transfections when co-

transfected with vector (Figure 11). However, more pronounced pro-apoptotic effects such as those caused by Bax $\alpha$ - $\Delta$ S184 were detected with this system.

Therefore the assay system was modified: Bcl-2 family members were cloned into the prcCMV vector, such that they were transcribed from a cmv promoter and underwent cap-dependent translation. These constructs were co-transfected with pEGFP-C1, a vector that expresses an enhanced green fluorescent protein (EGFP), also from a cmv promoter. While the two genes were on separate plasmids, this approach enabled both the Bcl-2 family genes and the *egfp* gene to be transcribed and translated in the same manner in healthy and apoptotic cells.

NIH 3T3 cells were co-transfected with 2  $\mu$ g each of a Bcl-2 family gene prcCMV construct and of pEGFP-C1. Expression of the different proteins from these constructs were similar to the pBabe MN IRES GFP constructs. Once again, only low levels of Bax $\beta$  were expressed (Figure 12). The vector, *bcl-2*, and *bcl-X<sub>L</sub>* transfections showed good GFP expression, while the *bax $\alpha$* -transfected cells expressed lower GFP, and the GFP levels were further reduced in the *bax $\beta$*  transfections (Figure 12B). All of these constructs were verified by sequencing, and the *bax $\alpha$*  and the *bax $\beta$*  genes were cloned in the same manner, resulting in the same 5' regions of these genes (data not shown). Thus the low level of Bax $\beta$  expression was observed in two cell types, with two different vectors and different methods of transfection.

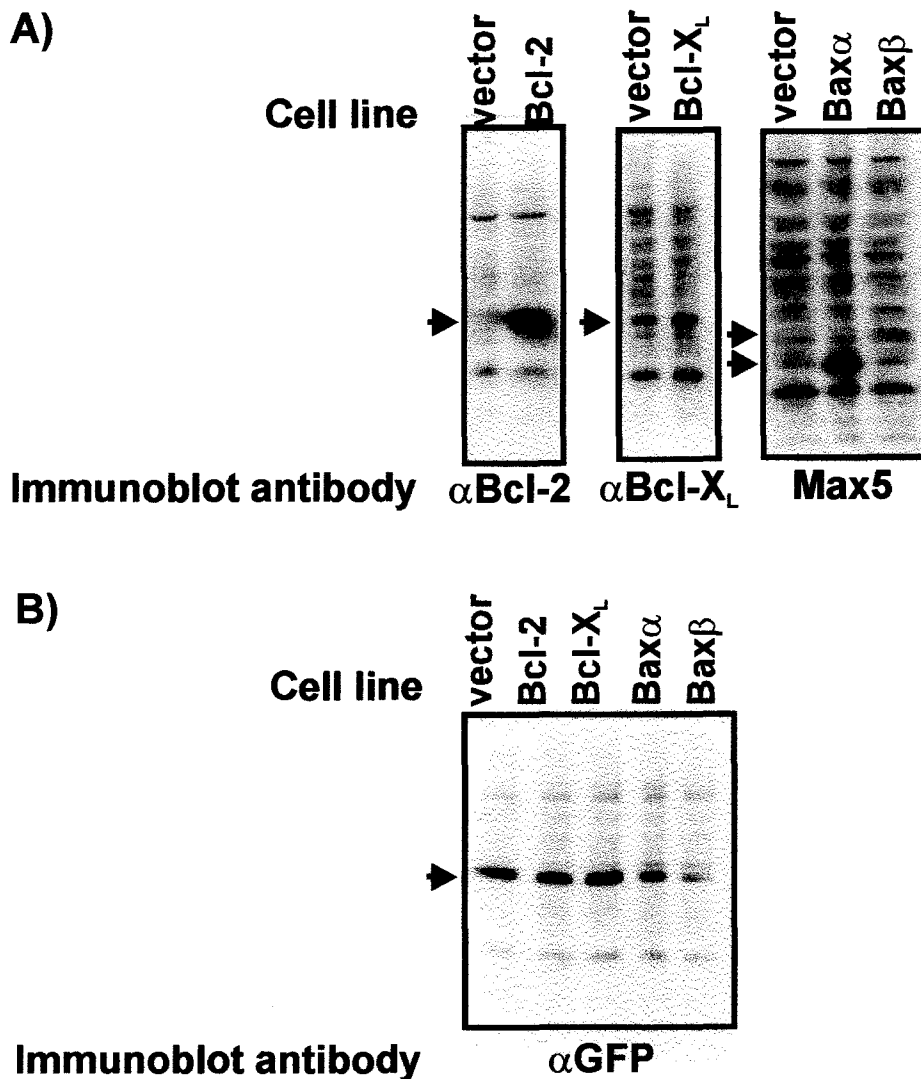


**Figure 12:** Protein expression in NIH 3T3 cells transiently transfected with equal amounts of prcCMV vector construct and pEGFP-C1.

- A) Immunoblots of 20  $\mu$ g of NP-40 lysates from NIH 3T3 cells transiently co-transfected with the prcCMV vector, *bcl-2*, *bcl-X<sub>L</sub>*, *bax $\alpha$* , or *bax $\beta$*  in prcCMV and pEGFP-C1 were done with the indicated antibody. The position of Bcl-2, Bcl-XL, Bax $\alpha$ , and Bax $\beta$  migrations are indicated (arrows).
- B) Immunoblots of 20  $\mu$ g of NP-40 lysates from NIH 3T3 cells transiently co-transfected with the prcCMV vector, *bcl-2*, *bcl-X<sub>L</sub>*, *bax $\alpha$* , or *bax $\beta$*  in prcCMV and pEGFP-C1 were done with the  $\alpha$ GFP antibody. The position of GFP migration is indicated (arrow).

Cells were co-transfected with varying amounts of the Bcl-2 family prcCMV constructs and pEGFP-C1, to keep the total amount of DNA at 4  $\mu\text{g}$ . No changes in EGFP fluorescence per cell were seen in any of the transfections, except for the Bax $\beta$  samples in which it was decreased (Figures 13, 14A). This lower EGFP fluorescence per cell suggests Bax $\beta$  toxicity. Some of the EGFP signals were above the detection limit of the image. Exclusion of these from the data set did not significantly change the result (data not shown), therefore all green fluorescence values were used in the analyses.

EGFP expression was not toxic in a dose dependent manner, as variation in expression levels was seen in the vector transfected cells (Figures 13, 14B). This is consistent with other studies in NIH 3T3 cells where GFP toxicity was only observed after 48 hours (Liu *et al.*, 1999).

The transfection efficiencies of the different constructs are shown in Figure 14B. The effects of the Bcl-2 family proteins were not seen upon co-transfection of 2  $\mu\text{g}$  of the prcCMV construct with of 2  $\mu\text{g}$  of pEGFP-C1. However, when the amount of EGFP plasmid was decreased with a corresponding increase in the Bcl-2 family member plasmid, the amount of Bcl-2 family member expressed was high enough to produce detectable effects. Bcl-2 demonstrated a toxic phenotype of a lowered transfection efficiency (Figures 13, 14B). This effect has been seen in other studies where transient expression of Bcl-2 at high levels induces apoptosis in a variety of cell types (Wang *et al.*, 2001, Shinoura *et al.*, 1999, Uhlmann *et al.*, 1998). Transfection of constructs containing only the Bcl-2

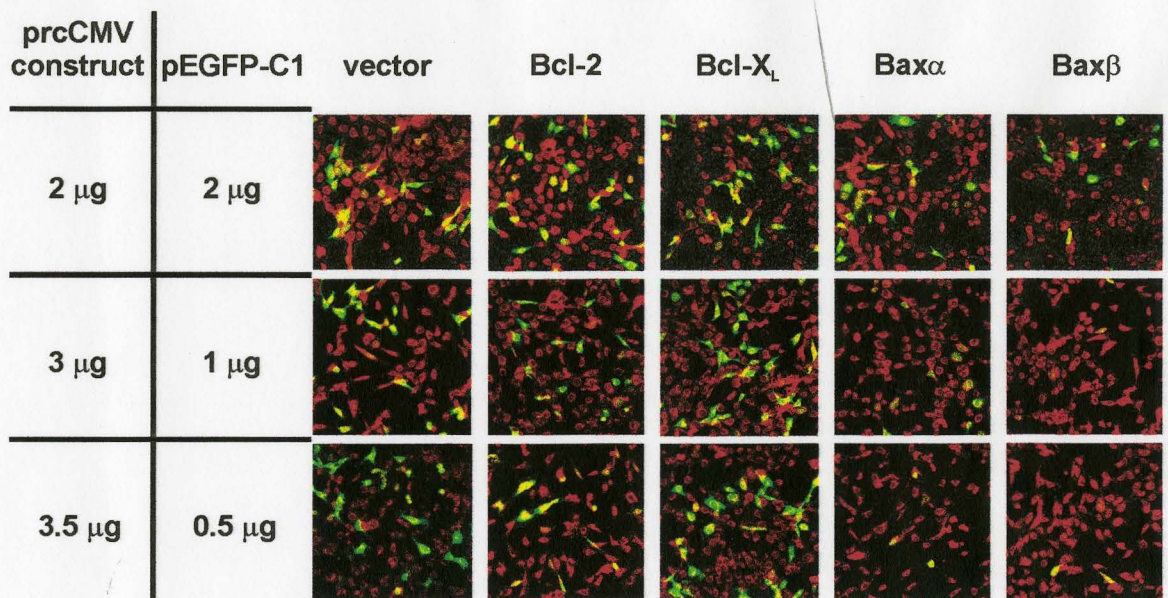


**Figure 13:** NIH 3T3 cells transiently transfected with varying amounts of prcCMV vector construct and pEGFP-C1.

Confocal microscopy images were taken of NIH 3T3 cells expressing EGFP (green) and stained with SYTO 63 (red).

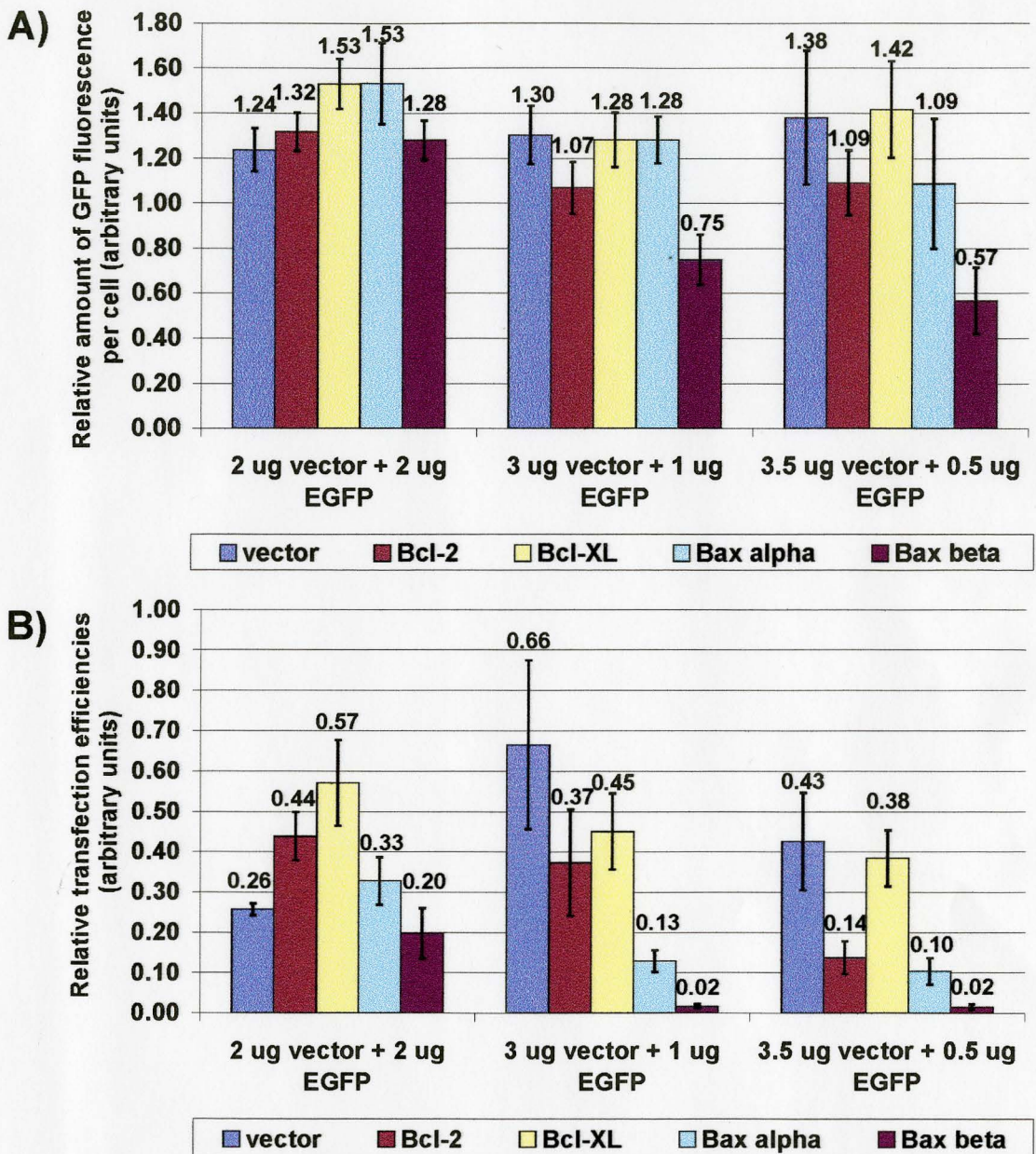


**Figure 14:** The relative amount of EGFP fluorescence per cell (A) and the relative transfection efficiencies (B) of NIH 3T3 cells transiently transfected with varying amounts of prcCMV vector construct and pEGFP-C1.

Varying amounts of different Bcl-2 family genes in the prcCMV vector were co-transfected with the pEGFP-C1 vector into NIH 3T3 cells. The relative amount of EGFP fluorescence per cell and the relative transfection efficiency for each sample were calculated. A minimum of three samples were analyzed for each point, and the error expressed is the standard error of the mean.

insertion sequence demonstrated that this effect is probably due to non-specific toxicity of overexpressed protein at mitochondria (Wang *et al.*, 2001).

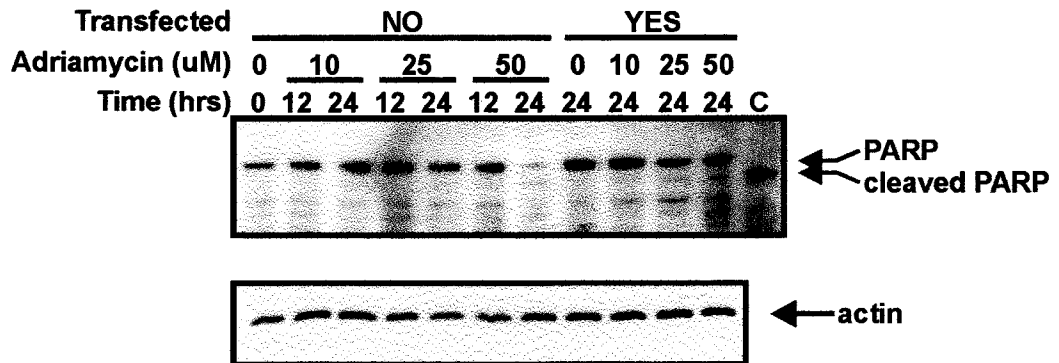
Transfection of *bcl-X<sub>L</sub>* is not toxic (Figures 13, 14B), possibly because only a fraction of Bcl-X<sub>L</sub> targets to mitochondria (Wang *et al.*, 2001, Hsu *et al.*, 1997).

Bax $\alpha$  exhibited a pro-apoptotic phenotype when the amount of transfected *bax $\alpha$ -prcCMV* was 3  $\mu$ g or more. At these higher doses of Bax $\alpha$ , the amount of protein was high enough to cause cell death. These results agree with the known apoptotic functions of these proteins. Thus, under appropriate conditions, this assay can be used to measure the pro-apoptotic effect of a transfected protein.

Bax $\beta$  had a strong cytotoxic phenotype, shown by a very low transfection efficiency and reduced levels of EGFP fluorescence (Figures 13, 14). This suggests that Bax $\beta$  is more toxic than Bax $\alpha$ . Comparison of this data with that obtained with the pBabe MN IRES GFP transfections (Figure 9) suggests that Bax $\beta$  is less lethal than Bax $\alpha$ - $\Delta$ S184.

To confirm that the changes in EGFP transfection efficiencies were due to effects of the co-transfected genes on apoptosis, a separate assay was used. Transfected cells were treated with drugs to induce cell death. A variety of agents were screened to determine which would effectively induce apoptosis in NIH 3T3 cells, using cleavage of the caspase substrate PARP as an indicator. Treatment with 1  $\mu$ M staurosporine did not result in any significant PARP cleavage (Figure 15). Serum starvation for 48 hours was also ineffective (data

A)



B)

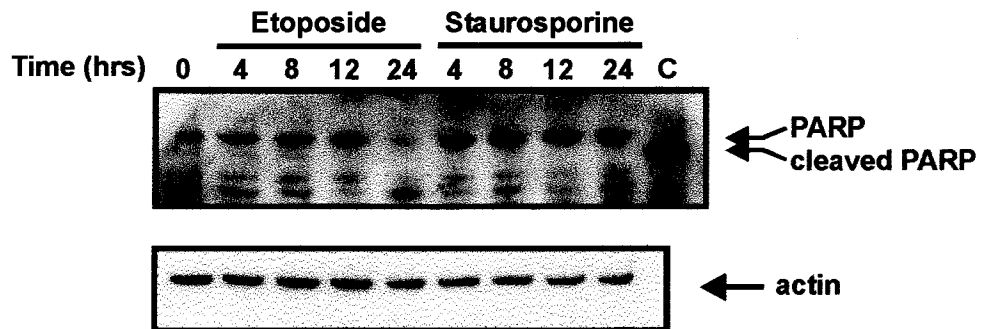


**Figure 15:** Cleavage of the caspase substrate PARP in NIH 3T3 cells treated with Adriamycin, etoposide and staurosporine.

- A) Immunoblots of 5  $\mu$ g of protein from SDS lysates of untransfected NIH 3T3 cells and NIH 3T3 cells transfected with 3  $\mu$ g of prcCMV and 1  $\mu$ g of pEGFP-C1 were done with  $\alpha$ PARP antibody. The cells were treated with 0 to 50  $\mu$ M of Adriamycin for 0 to 24 hours. The migrations of full-length and cleaved PARP proteins are indicated (arrows). Actin was run as a control demonstrating that equal equal amounts of protein were loaded in each lane. The control (C) is NP-40 lysate from MCF-7 breast cancer cell line treated with 10  $\mu$ M Adriamycin for 24 hours, a condition known to result in cleavage of PARP.
- B) Immunoblots of 5  $\mu$ g of protin from SDS lysates of untransfected NIH 3T3 cells were done with  $\alpha$ PARP antibody. The cells were treated with 100  $\mu$ M etoposide or 1  $\mu$ M staurosporine for 0 to 24 hours. The migrations of full-length and cleaved PARP proteins are indicated (arrows). Actin was run as a control demonstrating that equal amounts of protein were loaded in each lane. The control (C) is NP-40 lysate from MCF-7 breast cancer cell line treated with 10  $\mu$ M Adriamycin for 24 hours, a condition known to result in

not shown). Incubation with 100  $\mu\text{M}$  etoposide for 24 hours did result in some PARP cleavage, and this was also seen with 50  $\mu\text{M}$  Adriamycin for 24 hours (Figure 15). Adriamycin treatment also induced changes in cell morphology consistent with apoptosis, whereas this effect was less pronounced with etoposide (data not shown). Transfection of NIH 3T3 cells with 3  $\mu\text{g}$  prcCMV and 1  $\mu\text{g}$  pEGFP-C1 had no effect on the susceptibility to Adriamycin-induced apoptosis. This allowed the use of Adriamycin with cells transfected with our Bcl-2 family constructs.

Eighteen hours post-transfection with 3  $\mu\text{g}$  of prcCMV construct and 1  $\mu\text{g}$  of pEGFP-C1, the cells were treated with various doses of Adriamycin for 24 hours. Only the treated cells were cultured for the additional 24 hours. This did not affect the measurements for relative transfection efficiency, as Adriamycin inhibited cell division (data not shown). Adriamycin exposure did not alter EGFP fluorescence per cell, except upon transfection of *bax $\beta$*  (Figures 16, 17A). The amount of GFP fluorescence per cell in the *bax $\beta$* -transfected population was much lower than the other transfections at elevated doses of 50  $\mu\text{M}$  Adriamycin (Figure 17A). The number of surviving transfected cells was significantly affected upon expression of the different Bcl-2 family proteins (Figures 16, 17B). Adriamycin killed vector transfected cells in a dose dependent fashion, as shown by a decreasing number of EGFP positive cells with higher doses of drug (Figures 16, 17B). Bcl-X<sub>L</sub> was strongly protective against Adriamycin at all doses (Figures 16, 17B). The effect of Bcl-2 on Adriamycin-induced cell death was a

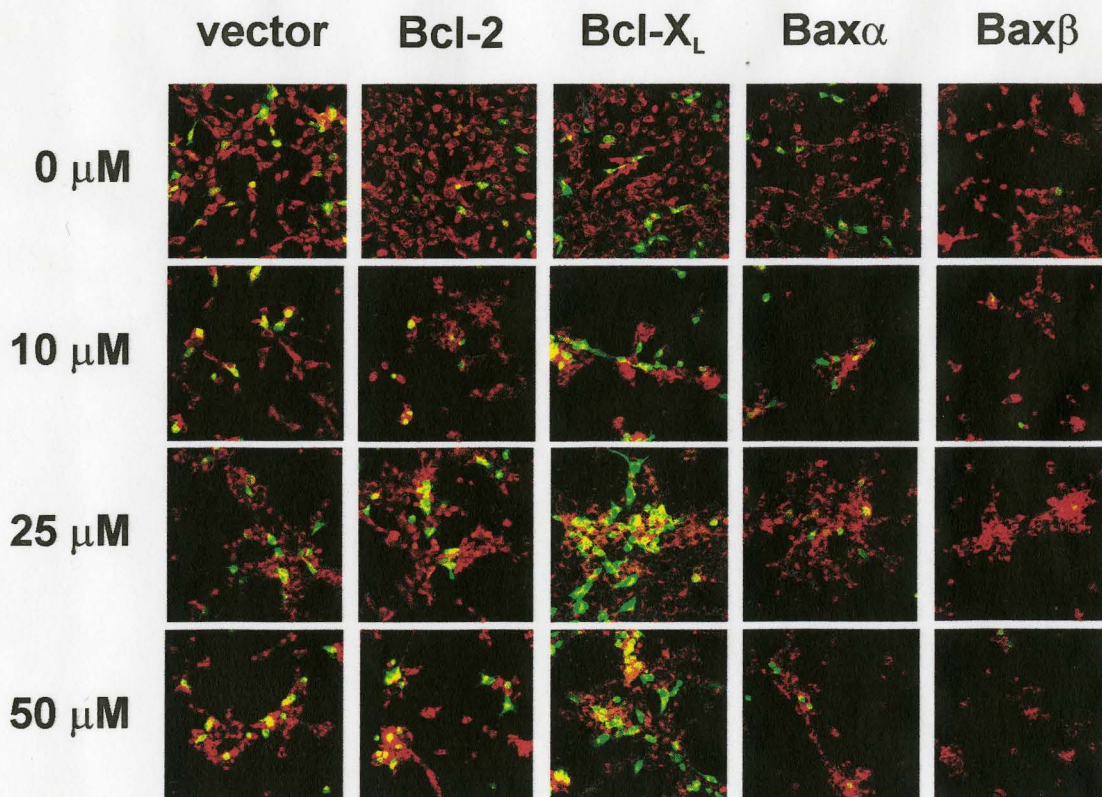


**Figure 16:** NIH 3T3 cells transiently transfected with 3  $\mu$ g prcCMV constructs and 1  $\mu$ g pEGFP-C1 treated with 0 to 50  $\mu$ M Adriamycin for 24 hours.

Confocal microscopy images were taken of NIH 3T3 cells expressing EGFP (green) and stained with SYTO 63 (red).

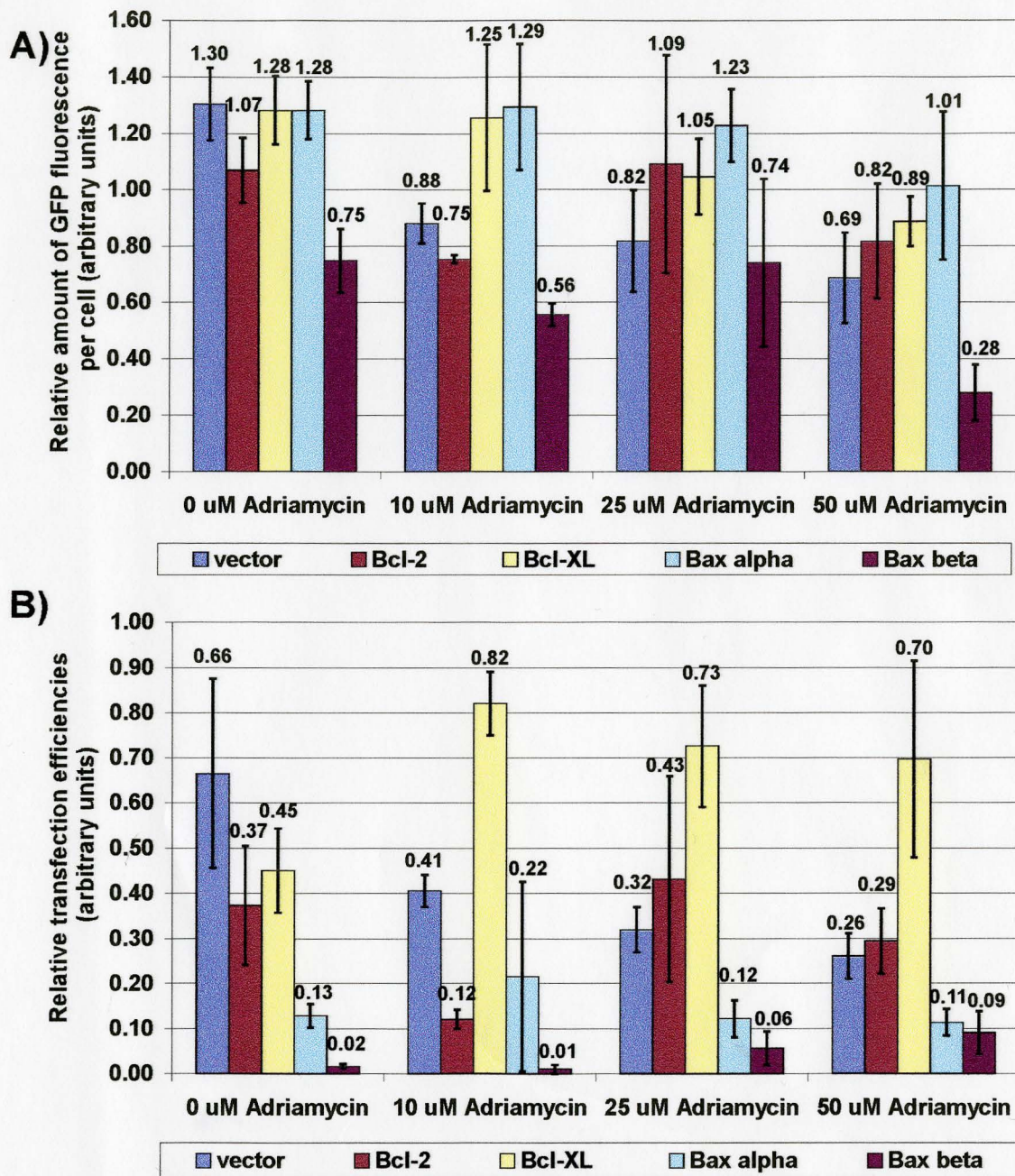


**Figure 17:** The relative amount of EGFP fluorescence per cell (A) and the relative transfection efficiencies (B) of transiently transfected NIH 3T3 cells treated with 0 to 50  $\mu$ M Adriamycin for 24 hours.

NIH 3T3 cells were transfected with 3  $\mu$ g prcCMV vector construct and 1  $\mu$ g pEGFP-C1. Eighteen hours post-transfection, they were treated with 0 to 50  $\mu$ M Adriamycin for 24 hours. The relative amount of EGFP fluorescence per cell and the relative transfection efficiency for each sample were calculated. A minimum of three samples were analyzed for each point, and the error expressed is the standard error of the mean.

complex function of drug dose. At lower concentrations of drug, the toxicity due to Bcl-2 overexpression was observed, while at higher doses the cells that maintained Bcl-2 expression were delayed from undergoing apoptosis. The combination of the toxicity of overexpression of Bcl-2 and its anti-apoptotic effect resulted in numbers of surviving cells similar to that of the vector transfected cells (Figures 16, 17B). The presence of Bax $\alpha$  caused cell death, irrespective of the presence of Adriamycin (Figures 16, 17B). Very few cells survived in the *bax $\beta$* -transfected population. The toxicity of Bax $\beta$  was so high that an increase in cell death due to Adriamycin could not be seen. Thus unlike the previous assays, enhancement of Adriamycin-induced apoptosis as measured by persistence of EGFP fluorescence clearly demonstrated the anti-apoptotic function of Bcl-X<sub>L</sub>, the pro-apoptotic function of Bax $\alpha$ , and the even more lethal function of Bax $\beta$ . The dual effect of Bcl-2 is likely due to toxicity of mitochondrial targeted proteins in transient assays, as discussed previously.

Therefore, Bax $\beta$  is highly toxic in transiently transfected NIH 3T3 cells, with very few cells surviving and those cells that do survive having lower amounts of EGFP fluorescence per cell. This induction of cell death is greater than that shown by Bax $\alpha$ , but still less than that of Bax $\alpha$ - $\Delta$ S184.

### **3.2.3 Conformation of the Bax $\beta$ Amino-Terminus**

Bax $\alpha$  undergoes a functionally significant conformational change at its amino-terminus that is associated with activation and integration into the

mitochondrial membrane (Hsu and Youle, 1997, Goping *et al.*, 1998, Nechushtan *et al.*, 1999, Soucie *et al.*, 2001). As the carboxyl-terminus of Bax $\beta$  differs from Bax $\alpha$ , we determined whether Bax $\beta$  exhibited this amino-terminal conformational change associated with Bax $\alpha$  activation.

The conformation of the amino-termini of  $^{35}\text{S}$  methionine labeled *bax $\alpha$* , *bax $\beta$* , and *bax $\alpha$ - $\Delta$ S184* in solution were investigated with the 6A7 antibody that detects the activated amino-terminal conformation of Bax $\alpha$ . Two different detergents were used: the non-ionic detergent Triton X-100 that induces the conformational change, and the zwitterionic detergent CHAPS that does not (Hsu and Youle, 1998). The supernatants from these immunoprecipitations were re-immunoprecipitated with 2D2, an antibody that recognizes both conformations of the Bax protein, as a control and to determine how much protein remained. After quantification of the immunoprecipitates through phosphorimager analyses, the amounts of Bax protein immunoprecipitated in each experimental condition were examined relative to that immunoprecipitated in Triton X-100 detergent with the 6A7 antibody.

Similar to the results of Hsu and Youle (1998), Bax $\alpha$  showed minimal 6A7 reactivity compared to 2D2 reactivity in the CHAPS buffer (Figure 18). Bax $\alpha$  $\Delta$ S184 also had reduced 6A7 reactivity compared to 2D2 reactivity in the CHAPS buffer, although not quite as low as Bax $\alpha$  as small amounts of Bax $\alpha$  $\Delta$ S184 were reproducibly immunoprecipitated (Figure 18). In contrast, Bax $\beta$  showed strong 6A7 reactivity in both of these conditions (Figure 18).

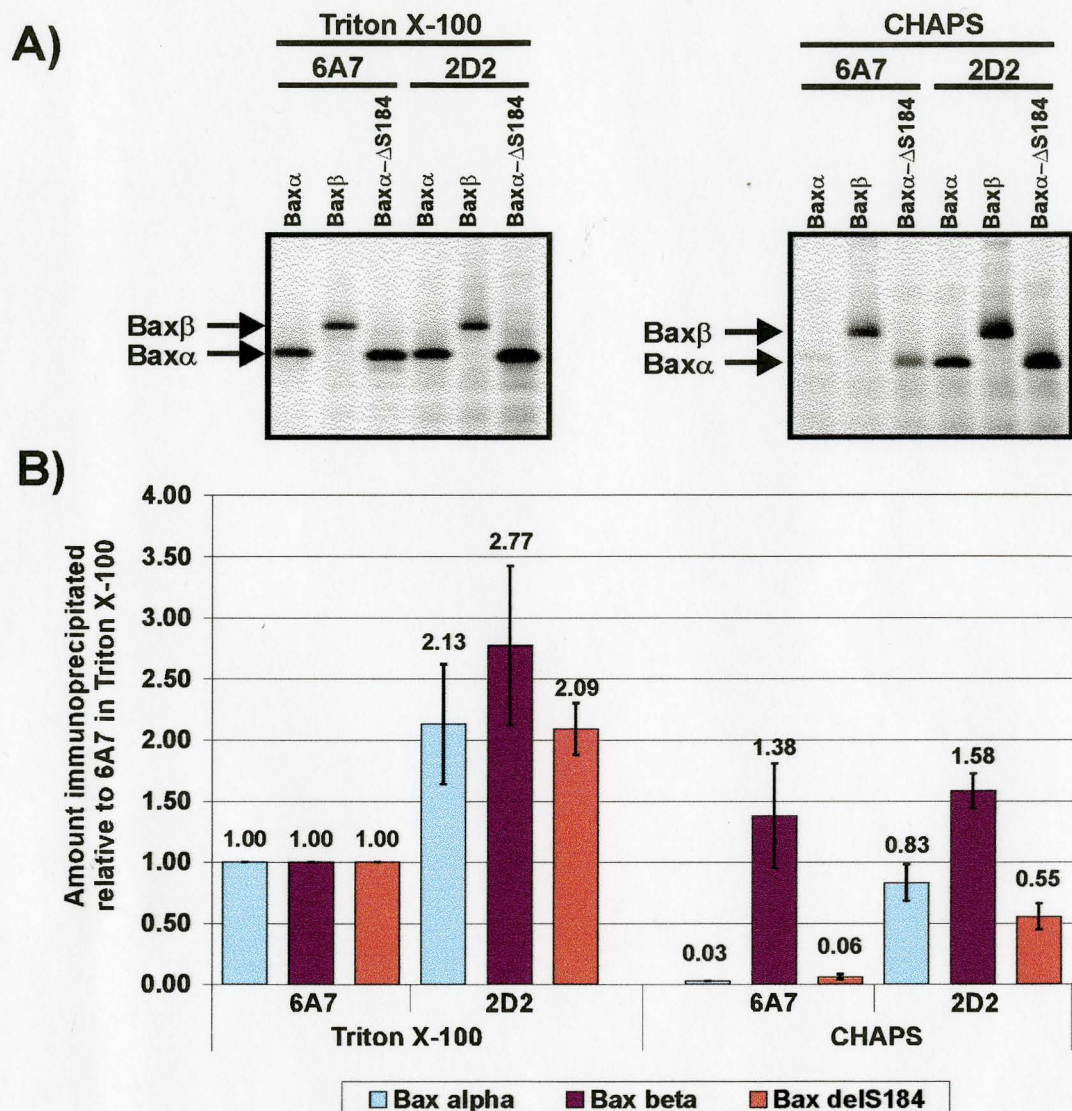


**Figure 18:** Immunoprecipitations of Bax $\alpha$ , Bax $\beta$ , and Bax $\alpha$ - $\Delta$ S184 with the 6A7 and 2D2 antibodies at pH 7.5.

A)  $^{35}$ S methionine labeled Bax $\alpha$ , Bax $\beta$ , and Bax $\alpha$ - $\Delta$ S184 that had been expressed *in vitro* were immunoprecipitated using the amino-terminal conformation-specific 6A7 monoclonal antibody in buffers of either 0.2% Triton X-100 or 0.2% CHAPS at pH 7.5. The supernatant was subsequently re-immunoprecipitated with the monoclonal 2D2 antibody that recognizes all conformations of the Bax amino-terminus. The immunoprecipitated proteins were analyzed by SDS-PAGE and autoradiography. The data shown here is a representative of six independent replicates.

B) Quantification of the immunoprecipitations relative to the amount of protein immunoprecipitated with the 6A7 antibody in Triton X-100 buffer, as determined by phosphorimaging. The error expressed is the standard error of the mean for six independent experiments.

These same immunoprecipitations were carried out at pH 6.9 and 8.1 to investigate the pH-dependent changes in conformation reported by Khaled *et al.* (1999). No pH dependent change in 6A7 reactivity was observed for any of the proteins (Figures 19, 20).

The observation that Bax $\beta$  is constitutively in the activated 6A7-positive conformation could explain its cell death inducing activity: it is possible that the carboxyl-terminus and BH3 domain are accessible for protein-protein interactions. An immunoprecipitation assay, which previously demonstrated interactions among Bcl-2 family members, was used to determine if Bax $\alpha$  and Bax $\beta$  associated in solution. No such interactions were found (Appendix 6.1). The 6A7-positive conformation was not affected by changes in pH, which agrees with the results of Suzuki *et al.*, (2000). The pre-disposition of Bax $\alpha$ - $\Delta$ S184 for 6A7 epitope exposure (Figure 18) could be indicative of a decreased threshold for activation of Bax $\alpha$ - $\Delta$ S184 in apoptosis which would correlate with its greater cytotoxicity compared to Bax $\alpha$  (Nechushtan *et al.*, 1999).

### **3.3 Significance of the Bax $\beta$ Carboxyl-Terminus**

Investigations to determine the significance of the unique Bax $\beta$  carboxyl-terminus did not provide insight into the mechanism of its cell death inducing function. The reduced levels of exogenous Bax $\beta$  expression in cells suggests that Bax $\beta$  could be of short half-life, and perhaps the carboxyl-terminus is

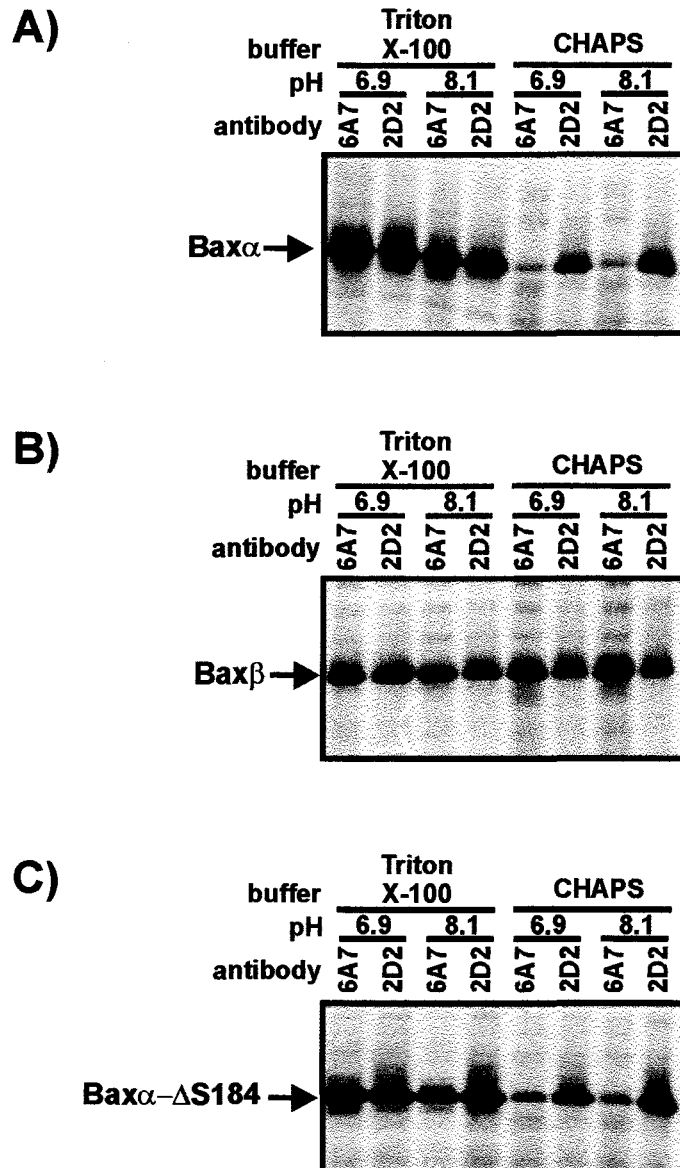


**Figure 19:** Immunoprecipitations of Bax $\alpha$  (A), Bax $\beta$ (B), and Bax $\alpha$ - $\Delta$ S184 (C) with the 6A7 and 2D2 antibodies at pH 6.9 and 8.1.

<sup>35</sup>S methionine labeled Bax $\alpha$ , Bax $\beta$ , and Bax $\alpha$ - $\Delta$ S184 that had been expressed *in vitro* were immunoprecipitated using the amino-terminal conformation-specific 6A7 monoclonal antibody in buffers of either 0.2% Triton X-100 (TX-100) or 0.2% CHAPS at a pH of either 6.9 or 8.1. The supernatant was subsequently re-immunoprecipitated with the monoclonal 2D2 antibody that recognizes all conformations of the Bax amino-terminus. The immunoprecipitated proteins samples were analyzed by SDS-PAGE and autoradiography. The data shown here is a representative of three independent replicates.

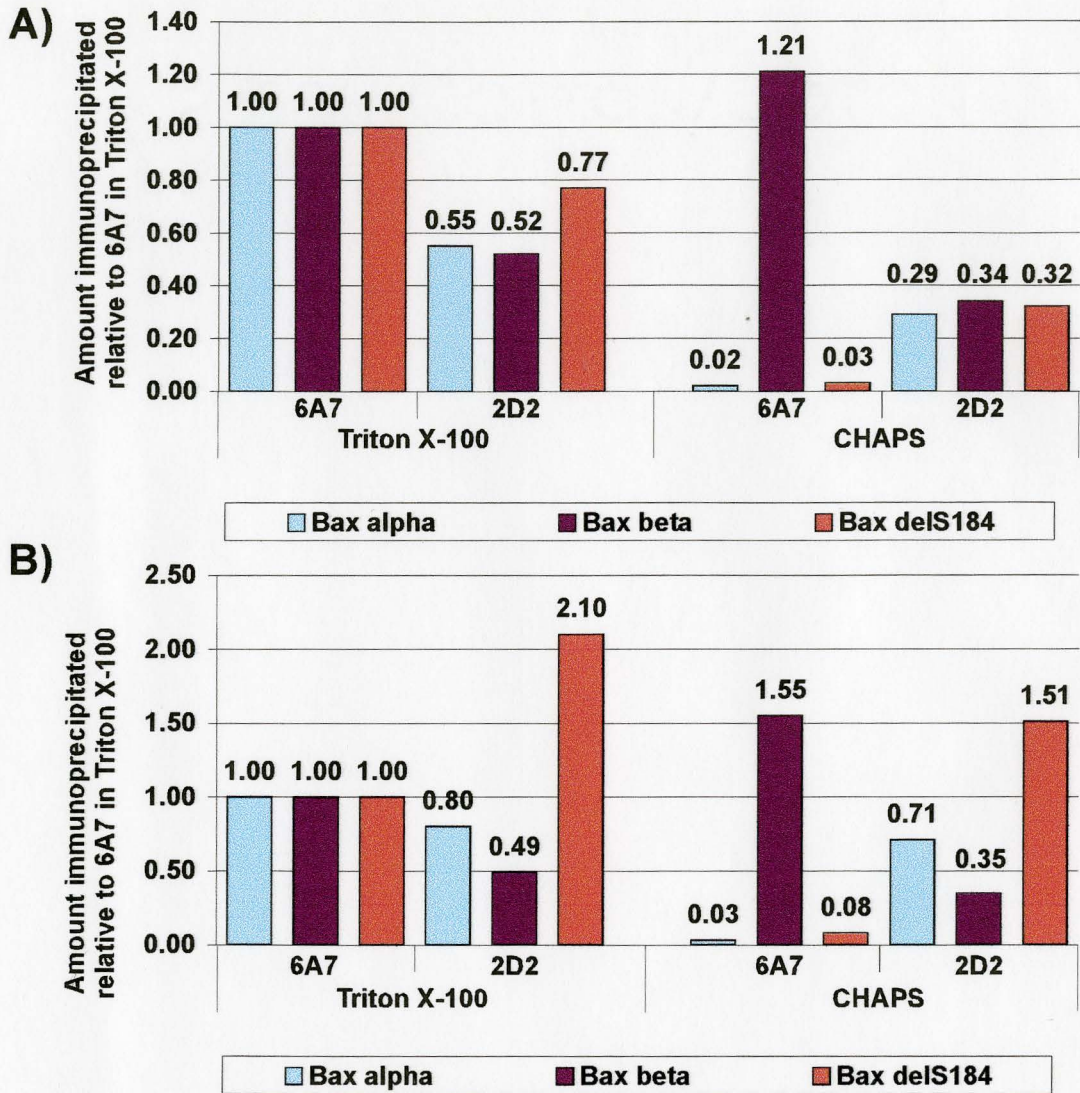


**Figure 20:** Quantification of immunoprecipitations of Bax $\alpha$ , Bax $\beta$ , and Bax $\alpha$ - $\Delta$ S184 with the 6A7 and 2D2 antibodies at pH 6.9 (A) and 8.1 (B).

<sup>35</sup>S methionine labeled Bax $\alpha$ , Bax $\beta$ , and Bax $\alpha$ - $\Delta$ S184 that had been expressed *in vitro* were immunoprecipitated using the amino-terminal conformation-specific 6A7 monoclonal antibody in buffers of either 0.2% Triton X-100 or 0.2% CHAPS at a pH of either 6.9 or 8.1. The supernatant was subsequently re-immunoprecipitated with the monoclonal 2D2 antibody that recognizes all conformations of the Bax amino-terminus. The samples were analysed by SDS-PAGE and quantified by phosphorimaging. The amount of protein immunoprecipitated with the 6A7 antibody in Triton X-100 buffer was set to 1.0, and the other amounts of immunoprecipitated protein are expressed as an amount relative to this value. The data shown is a representative of three independent experiments.

mediating rapid degradation of the protein. Determination of the half-life of Bax $\beta$  was attempted in these studies, however the protein was not labeled with <sup>35</sup>S methionine, and consequently no half-life could be ascertained (Appendix 6.2). c-Src and Bif-1 were found to not be authentic SH3 domain binding partners of Bax $\beta$ , and no suitable assay was found to screen many different SH3 domains for Bax $\beta$  binding activity. Thus, whether the carboxyl-terminal tail of Bax $\beta$  has SH3 binding capabilities was not resolved (Appendix 6.3).

#### 4. DISCUSSION

In this study Bax $\beta$  was found to induce cell death to a greater extent than Bax $\alpha$  upon transient transfection of NIH 3T3 cells. This correlated with it being in an activated conformation, as seen by exposure of the 6A7 antibody epitope, and with low levels of protein expression compared to Bax $\alpha$ .

Previous assays used to compare the death inducing function of proteins in adherent cells have used FACS analyses to determine the number of transfected cells in the population (Inohara *et al.*, 1997, Gross *et al.*, 1998, Shi *et al.*, 1999, Wang *et al.*, 2001). This is not appropriate for the study of adherent cells, as a loss of cell adhesion induces apoptosis, which confounds the results by increasing the apparent toxic effect of the protein (Gilmore *et al.*, 2000). A transient transfection assay to study the effect of a protein on apoptosis in adherent cells was designed to determine the function of Bax $\beta$ . It enabled the study of overexpression of the protein of interest alone, or with the application of apoptotic stimuli. This assay is able to be used with any type of adherent cells that can be transfected with reasonably high efficiency. One important discovery was that the reporter gene, GFP in this study, could not be under the control of an IRES element when studying apoptosis. If IRES elements were used, no differences were seen in either the amount of green fluorescence per cell or in the transfection efficiencies among the different Bcl-2 family members (Figure

11). As IRES controlled genes are constitutively expressed during the apoptotic process, only large apoptotic effects that caused the cells to detach from the adherent cell population could be detected. This occurred with the Bax $\alpha$ - $\Delta$ S184 expressing cells (Figure 11). Expression of the reporter gene such that it underwent cap-dependent translation remedied this problem. Co-transfection of *bcl-X<sub>L</sub>* with *egfp* produced high transfection efficiencies (Figures 13, 14B), and its anti-apoptotic activity was evident in the presence of Adriamycin (Figures 16, 17B). Transient expression of Bcl-2 resulted in a pro-apoptotic effect of reduced transfection efficiencies (Figures 13, 14B) likely due to overexpression of this molecule causing non-specific toxicity at mitochondria (Wang *et al.*, 2001). The anti-apoptotic function of Bcl-2 was observed during Adriamycin-induced apoptosis as EGFP expressing cells were protected from cell death (Figures 16, 17B). Bax $\alpha$  exhibited a pro-apoptotic phenotype irrespective of the presence of Adriamycin (Figures 13, 14B, 16, 17B), which is consistent with overexpression of this molecule causing apoptosis (Oltvai *et al.*, 1993). Thus, this assay proved a valid means to determine the apoptotic function of a protein in adherent cells, relative to the function of other pro- and anti-apoptotic proteins.

Bax $\beta$  had a lethal effect on the transiently transfected cells, as indicated by a reduced intensity of EGFP (Figures 13, 14A, 16, 17A) as well as a dramatically reduced transfection efficiency with or without Adriamycin (Figures 13, 14B, 16, 17B). This toxic activity was greater than that of Bax $\alpha$ , and less than that of Bax $\alpha$ - $\Delta$ S184. While it is clear that Bax $\beta$  induces cell death, the

mechanism of this death is not yet known. Supplementary assays to explore the mechanism of Bax $\beta$  induced cell death include determination of caspase activity by inhibition of these molecules with the caspase inhibitor zVAD-fmk.

Examination of the transfected cells for morphological characteristics of apoptosis such as DNA fragmentation by TUNEL assay and phosphatidylserine exposure by Annexin V staining would also indicate whether Bax $\beta$  is inducing apoptosis. Transfection of *bax $\beta$*  into Bcl-2 or Bcl-X<sub>L</sub> expressing cell lines would indicate if the toxic effects of Bax $\beta$  could be prevented by these anti-apoptotic Bcl-2 family members. Additionally, examination of the effect of Bax $\beta$  on cell death in *bax $\alpha$*  knockout cells would show if Bax $\alpha$  is required for Bax $\beta$  to induce cell death.

PARP cleavage was examined in pooled Rat-1 *myc* ERTM cells, however Bax $\beta$  had no observable effect on the susceptibility of the cells to apoptosis triggered by etoposide, serum starvation, or Adriamycin. As these cells had very low levels of Bax $\beta$  expression the magnitude of the effect of Bax $\beta$  could have been too low to detect. As well, the cells were passaged to create the pooled cell lines, which could have selected for cells that were resistant to Bax $\beta$ .

Endogenous Bax $\beta$  was not found expressed in any of the cells or tissues probed (Figures 5, 6). Also, exogenous Bax $\beta$  was expressed to only low levels compared to Bax $\alpha$ , when transfected into different cell types using different vectors (Figures 7, 9, 12). If Bax $\beta$  was only expressed to these levels *in vivo*, it

would be practically undetectable above background using the available molecular techniques and could be why it was not found in these experiments. The reduced levels of exogenous Bax $\beta$  in the cell suggest that Bax $\beta$  could be of short half-life and the presence of a putative PEST sequence in the Bax $\beta$  carboxyl-tail (Figure 3) supports this idea. It is possible however, that Bax $\beta$  would be expressed at higher levels or its expression stabilized in the appropriate cell type in some circumstances. However, testing all of the possible cell types in all apoptotic stages is unfeasible. The low levels of expression observed in this study agree with Bax $\beta$  as cytotoxic, as high levels of a pro-apoptotic protein can induce cell death (Oltvai *et al.*, 1993).

Oltvai *et al.* (1993) and Krajewski *et al.* (1994) previously identified 24 kDa proteins as Bax $\beta$  in RL-7 cells and mouse pancreatic and intestinal tissues. It is possible that the 24 kDa proteins they identified as Bax $\beta$  were in fact Bax $\omega$  or Bax $\kappa$ , as all three are 24 kDa and share the amino-terminal sequence recognized by the Bax antibodies. In this study, mouse tissues were unsuccessfully probed due to secondary antibody cross-reactivity on the immunoblots with immunoglobulin protein present in the tissue samples. I probed the RL-7 cell line but did not detect a 24 kDa protein. The cells examined here were potentially in different conditions than those used in the studies by Oltvai *et al.* (1993), which could have facilitated production or stabilization of the 24 kDa protein.

The activation of Bax $\alpha$  is associated with an amino-terminal conformational change that exposes the 6A7 antibody epitope. Bax $\beta$  was found

to be constitutively in the 6A7 positive conformation (Figure 18), independent of pH (Figures 19, 20). In Bax $\alpha$ , 6A7 epitope exposure correlates with exposure of the BH3 domain (Nechushtan *et al.*, 1999, Goping *et al.*, 1998). As Bax $\beta$  is identical to Bax $\alpha$  other than at the carboxyl-terminus, 6A7 epitope exposure in Bax $\beta$  could be indicative of availability of its BH3 domain for protein-protein interactions. The 6A7-reactive conformation of Bax $\beta$  is a possible explanation for the cell death inducing activity of Bax $\beta$ , as 6A7 reactivity is only found in activated Bax $\alpha$ . (Nechushtan *et al.*, 1999, Goping *et al.*, 1998).

Bax $\beta$  displayed cell death inducing activity that is greater than that of Bax $\alpha$  when transiently expressed in NIH 3T3 cells. One possible explanation for this function is that Bax $\beta$  is constitutively in the activated conformation of Bax that involves 6A7 epitope exposure. The expression levels of Bax $\beta$  were always much reduced compared to Bax $\alpha$ , which agrees with its cell death inducing function, as overexpression of a toxic protein can have lethal effects. These observed differences are due to the unique carboxyl-terminal sequence of Bax $\beta$ . While the mechanism of action remains elusive, this study has identified Bax $\beta$  as a Bax isoform of greater toxicity than Bax $\alpha$ .

## 5. REFERENCES

- Adams, J. M., and S. Cory. 1998. The Bcl-2 protein family: arbiters of cell survival. *Science*. 281: 1322-1326.
- Annis, M., N. Zamzami, W. Zhu, L. Z. Penn, G. Kroemer, B. Leber, and D. W. Andrews. 2001. Endoplasmic reticulum localized Bcl-2 prevents apoptosis when redistribution of cytochrome *c* is a late event. *Oncogene*. 20: 1939-1952.
- Antonsson, B., F. Conti, A. Ciavatta, S. Montessuit, S. Lewis, I. Martinou, L. Bernasconi, A. Bernard, J. Mermoud, G. Mazzei, K. Maundrell, F. Gambale, R. Sadoul, and J. Martinou. 1997. Inhibition of Bax channel-forming activity by Bcl-2. *Science*. 277: 370-372.
- Antonsson, B., S. Monessuit, S. Lauper, R. Eskes, and J. C. Martinou. 2000. Bax oligomerization is required for channel-forming activity in liposomes and to trigger cytochrome *c* release from mitochondria. *Biochemical Journal*. 345: 271-278.
- Antonsson, B., S. Montessuit, B. Sanchez, and J. C. Martinou. 2001. Bax is present as a high molecular weight oligomer/complex in the mitochondrial membrane of apoptotic cells. *Journal of Biological Chemistry*. 276:11615-11623.
- Apte, S. S., M. Mattei, and B. R. Olsen. 1995. Mapping of the human Bax gene to chromosome 19q13.3-q13.4 and isolation of a novel alternatively spliced transcript, Bax $\delta$ . *Genomics*. 26: 592-594.
- Basanez, G., A. Nechushtan, O. Dorzhinin, A. Chanturiya, E. Choe, S. Tutt, K. A. Wood, Y. Hsu, J. Zimmerberg, and R. J. Youle. 1999. Bax, but not Bcl-X<sub>L</sub>, decreases the lifetime of planar phospholipid bilayer membranes at subnanomolar concentrations. *Proceedings of the National Academy of Sciences*. 96: 5492-5497.
- Boise. L. H., M. Gonzalez-Garcia, C. E. Postems, L. Ding, T. Lindglen, L. A., Turka, X. Mao, G. Nunez, and G. B. Thompson. 1993. Bcl-X<sub>L</sub>, a Bcl-2-related gene that functions as a dominant regulator of apoptotic cell death. *Cell*. 74: 597-608.

- Boyd, J. M., G. J. Gallo, B. Elangovan, A. B. Houghton, S. Malstrom, B. J. Avery, R. G. Ebb, T. Subramanian, T. Chittenden, R. J. Lutz, and G. Chinnadurai. 1995. Bik, a novel death-inducing protein shares a distinct sequence motif with Bcl-2 family proteins and interacts with viral and cellular survival-promoting proteins. *Oncogene*. 11: 1921-1928.
- Chittenden, T., E. A. Harrington, R. O'Connor, C. Flemington, R. J. Lutz, G. I. Evan, and B. C. Gould. 1995. Induction of apoptosis by the Bcl-2 homologue Bak. *Nature*. 374: 733-736.
- Chou, J. J., H. Li, G. S. Salvesen, J. Yuan, and G. Wagner. 1999. Solution structure of BID; an intracellular amplifier of apoptotic signaling. *Cell*. 96: 615-624.
- Clemens, M. J., M. Bushell, I. W. Jeffrey, V. M. Pain, and S. J. Morley. 2000. Translation initiation factor modifications and the regulation of protein synthesis in apoptotic cells. *Cell Death and Differentiation*. 7: 603-615
- Coldwell, M. J., S. A. Mitchell, M. Stoneley, M. MacFarlane, and A. E. Willis. 2000. Initiation of Apaf-1 translation by internal ribosome entry. *Oncogene*. 19: 899-905.
- Cuddeback, S. M., H. Yamaguchi, K. Komatsu, T. Miyashita, M. Yamada, C. Wu, S. Singh, and H.-G. Wang. 2001. Molecular cloning and characterization of Bif-1: a novel SH3 domain-containing protein that associates with Bax. *Journal of Biological Chemistry*. 276: 20559-20565.
- Eskes, R., S. Desagher, B. Antonsson, and J. C. Martinou. 2000. Bid induces oligomerization and insertion of Bax into the outer mitochondrial membrane. *Molecular and Cellular Biology*. 20: 929-935.
- Gibson, L. S. P. Holmgren, D. C. S. Huang, O. Bernard, N. G. Copeland, N. A. Jenkins, G. R. Sutherland, E. Baker, J. M. Adams, and S. Cory. 1996. *bcl-w*, a novel member of the *bcl-2* family, promotes cell survival. *Oncogene*. 13: 665-675.
- Gilmore, A. P., A. D. Metcalfe, L. H. Romer, and C. H. Streuli. 2000. Integrin-mediated survival signals regulate the apoptotic function of Bax through its conformation and subcellular localization. *The Journal of Cell Biology*. 149: 431-445.
- Goping, I. S., A. Gross, J. N. Lavoie, M. Nguyen, R. Jemmerson, K. Roth, S. J. Korsmeyer, and G. C. Shore. 1998. Regulated targeting of Bax to mitochondria. *Journal of Cell Biology*. 143: 207-215.

- Gross, A., J. Jockel, M. C. Wei, and S. J. Korsmeyer. 1998. Enforced dimerization of Bax results in its translocation, mitochondrial dysfunction, and apoptosis. *EMBO*. 17: 3878-3885.
- Gross, A., J. M. McDonnell, and S. J. Korsmeyer. 1999. Bcl-2 family members and the mitochondria in apoptosis. *Genes and Development*. 13: 1899-1911.
- Gygi, S. P., Y. Rochon, B. R. Franzy, and R. Aebersold. 1999. Correlation between protein and mRNA abundance in yeast. *Molecular and Cellular Biology*. 19: 1720-1730.
- Holcik, M., N. Sonenberg, and R. G. Korneluk. 2000a. Internal ribosome initiation of translation and the control of cell death. *Trends in Genetics*. 16: 469-473.
- Holcik, M., C. Yeh, R. G. Korneluk, and T. Chow. 2000b. Translational upregulation of X-linked inhibitor of apoptosis (XIAP) increases resistance to radiation induced cell death. *Oncogene*. 19: 4174-4177.
- Hsu, Y., and R. J. Youle. 1997. Nonionic detergents induce dimerization among members of the Bcl-2 family. *Journal of Biological Chemistry*. 272: 13829-13834.
- Hsu, Y., K. G. Wolter, and R. J. Youle. 1997. Cytosol-to-membrane redistribution of Bax and Bcl-X<sub>L</sub> during apoptosis. *Proceedings of the National Academy of Sciences*. 94: 3668-3672.
- Hsu, Y., and R. J. Youle. 1998. Bax in murine thymocytes is a soluble monomeric protein that displays differential detergent-induced conformations. *Journal of Biological Chemistry*. 273: 10777-10783.
- Ideker, T., Y. Thorsson, J. A. Ranish, R. Christmas, J. Buhler, J. K. Eng, R. Bumgarner, D. R. Goodlett, R. Aebersold, and L. Hood. 2001. Integrated genomic and proteomic analyses of a systematically perturbed metabolic network. *Science*. 292: 929-934.
- Inohara, N., L. Ding, S. Chen, and G. Nunez. 1997. *harakiri*, a novel regulator of cell death, encodes a protein that activates apoptosis and interacts selectively with survival-promoting proteins Bcl-2 and Bcl-X<sub>L</sub>. *EMBO*. 16: 1686-1694.

- Jin, K. L., S. H. Graham, X. O. Mao, X. He, T. Nagayama, R. P. Simon, and D. A. Greenberg. 2001. Bax $\kappa$ , a novel Bax splice variant from ischemic rat brain lacking an ART domain, promotes neuronal cell death. *Journal of Neurochemistry*. 77: 1508-1519.
- Jurgensmeier, J. M., Z. Xie, Q. Deveraux, L. Ellerby, D. Bredesen, and J. C. Reed. 1998. Bax directly induces release of cytochrome c from isolated mitochondria. *Proceedings of the National Academy of Sciences*. 95: 4997-5002.
- Khaled, A. R., K. Kim, R. Hofmeister, K. Muegge, and S. K. Durum. 1999. Withdrawal of IL-7 induced Bax translocation from cytosol to mitochondria through a rise in intracellular pH. *Proceedings of the National Academy of Sciences*. 96: 14476-14481.
- Kharbanda, S., Z. Yuan, R. Weichelbaum, and D. Kufe. 1997. Functional role for the c-Abl protein tyrosine kinase in the cellular response to genotoxic stress. *Biochimica et Biophysica Acta*. 1333: O1-O7.
- Knudson, C. M., K. S. K. Tung, W. G. Tourtellotte, G. A. J. Brown, and S. J. Korsmeyer. 1995. Bax-deficient mice with lymphoid hyperplasia and male germ cell death. *Science*. 270: 96-99.
- Kozopas, K. M., T. Yang, H. L. Buchan, P. Zhou, and R. W. Craig. 1993. MCL-1, a gene expressed in programmed myeloid cell differentiation, has sequence similarity to BCL-2. *Proceedings of the National Academy of Sciences*. 90: 3516-3520.
- Krajewski, S., M. Krajewska, A. Shabai, T. Miyashita, H. G. Wang, and J. C. Reed. 1994. Immunohistochemical determination of *in vivo* distribution of Bax, a dominant inhibitor of Bcl-2. *American Journal of Pathology*. 145: 1323-1336.
- Li, P., D. Nijhawan, I. Budihardjo, S. M. Srinivasula, M. Ahmad, E. S. Alnemri, and X. Wang. 1997. Cytochrome c and dATP-dependent formation of Apaf-1/Caspase-9 complex initiates an apoptotic protease cascade. *Cell*. 91: 479-489.
- Lin, E. Y., A. Orlofsky, M. S. Berger, and M. B. Prytowsky. 1993. Characterization of A1, a novel hemopoietic-specific early-response gene with sequence similarity to *bcl-2*. *Journal of Immunology*. 151: 1979-1988.

- Lindsten, T., A. J. Ross, A. King, W.-X. Zong, J. C. Rathwell, H. A. Shiels, E. Ulrich, K. G. Waymire, P. Mahar, K. Frauwirth, Y. Chen, M. Wei, V. M. Eng, D. M. Adelman, M. C. Simon, A. Ma, J. A. Golden, G. Evan, S. J. Korsmeyer, G. R. MacGregor, and C. B. Thompson. 2000. The combined functions of pro-apoptotic Bcl-2 family members Bak and Bax are essential for normal development of multiple tissues. *Molecular Cell*. 6: 1389-1399.
- Lipford, E., J. J. Wright, W. Urba, J. Whang-Peng, I. R. Kirsch, M. Raffeld, J. Cossman, D. L. Longo, A. Bakhshi, and S. J. Korsmeyer. 1987. Refinement of lymphoma cytogenetics by the chromosome major breakpoint region. *Blood*. 70: 1816-1823.
- Liu, H. S., M. S. Jan, C. K. Chou, P. H. Chen, and N. J. Ke. 1999. Is green fluorescent protein toxic to the living cells? *Biochemical and Biophysical Research Communications*. 260: 712-717.
- Martinez-Senac, M., S. Corbalan-Garcia, and J. C. Gomez-Fernandez. 2001. Conformation of the C-terminal domain of the pro-apoptotic protein Bax and mutants and its interaction with membranes. *Biochemistry*. 40: 9983-9992.
- Marzo, I., C. Brenner, N. Zamzami, J. M. Jurgensmeier, S. A. Susin, H. L. A. Vieira, M. Prevost, Z. Xie, S. Matsuyama, J. C. Reed, and G. Kroemer. 1998. Bax and adenine nucleotide translocator cooperate in the mitochondrial control of apoptosis. *Science*. 281: 2027-2031.
- Mikhailov, V., M. Mikhailove, D. J. Pulkrabek, Z. Dong, M. A. Venkatachalam, and P. Saikumar. 2001. Bcl-2 prevents Bax oligomerization in the mitochondrial outer membrane. *Journal of Biological Chemistry*. 276: 18361-74.
- Mongioli, A. M., P. R. Romano, S. Panni, M. Mendoza, W. T. Wong, A. Musacchio, G. Cesareni, and P. P. Di Fiore. 1999. A novel peptide – SH3 interaction. *EMBO*. 18: 5300-5309.
- Muchmore, S. W., M. Sattler, H. Liang, R. P. Meadows, J. E. Harlan, H. S. Yoon, D. Nettlesheim, B. S. Chong, C. B. Thompson, S. L. Wong, S. L. Ng, and S. W. Fesik. 1996. X-ray and NMR structure of human Bcl<sub>xL</sub>, an inhibitor of programmed cell death. *Nature*. 381: 335-341.

- Narita, M., S. Shimizu, T. Ito, T. Chittenden, R. J. Lutz, H. Matsuda, Y. Tsujimoto. 1998. Bax interacts with the permeability transition pore to induce permeability transition and cytochrome c release in isolated mitochondria. *PNAS*. 95: 14681-14686.
- Naumovski, L., and M. L. Cleary. 1996. The p53-binding protein 53BP2 also interacts with Bcl-2 and impedes cell cycle progression at G2/M. *Molecular and Cellular Biology*. 16: 3884-3892.
- Nechushtan, A., C. L. Smith, Y. Hsu, and R. J. Youle. 1999. Conformation of the Bax C-terminus regulates subcellular location and cell death. *EMBO*. 18: 2330-2341.
- Nechushtan, A., C. L. Smith, I. Lamensdorf, S.-H. Yoon, and R. J. Youle. 2001. Bax and Bak coalesce into novel mitochondria-associated clusters during apoptosis. *Journal of Cell Biology*. 6: 1265-1276.
- Oltvai, Z. N., C. L. Milliman, and S. J. Korsmeyer. 1993. Bcl-2 Heterodimerizes in vivo with a conserved homolog, Bax, that accelerates programmed cell death. *Cell*. 74: 609-619.
- Pawson, T. 1995. Protein modules and signaling networks. *Nature*. 373: 573-580.
- Rogers, S., R. Wells, and M. Rechsteiner. 1986. Amino acid sequences common to rapidly degraded proteins: the PEST hypothesis. *Science*. 234: 364-368.
- Rosse, T., R. Olivier, L. Monney, M. Rager, S. Conus, I. Fellay, B. Jansen, and C. Borner. 1998. Bcl-2 prolongs cell survival after Bax-induced release of cytochrome c. *Nature*. 391: 496-499.
- Ruffolo, S. C., D. G. Breckenridge, M. Nguyen, I. S. Goping, A. Gross, S. J. Korsmeyer, H. Li, J. Yuan, and G. C. Shore. 2000. Bid-dependent and Bid-independent pathways for Bax insertion into mitochondria. *Cell Death and Differentiation*. 7: 1101-1108.
- Saito, M., S. J. Korsmeyer, and P. H. Schlesinger. 2000. Bax-dependent transport of cytochrome c reconstituted in pure liposomes. *Nature Cell Biology*. 2: 553-555.

- Schlesinger, P. H., A. Gross, X. Yin, K. Yamamoto, M. Saito, G. Waksman, and S. J. Korsmeyer. 1997. Comparison of the ion channel characteristics of proapoptotic BAX and antiapoptotic BCL-2. *Proceedings of the National Academy of Sciences*. 94: 11357-11362.
- Schmitt, E., C. Paquet, M. Beauchemin, J. Derver-Bertrand, and R. Bertrand. 2000. Characterization of bax- $\nu$ sigma, a death inducing isoform of Bax. *Biochemical and Biophysical Research Communications*. 270: 868-79.
- Sedlak, T. W., Z. N. Oltvai, E. Yang, K. Wang, L. H. Boise, C. B. Thompson, and S. J. Korsmeyer. 1995. Multiple Bcl-2 family members demonstrate selective dimerizations with Bax. *Proceedings of the National Academy of Sciences*. 92: 7834-7838.
- Shi, B., D. Triebe, S. Kajiji, K. K. Iwata, A. Bruskin, and J. Mahajna. 1999. Identification and characterization of bax $\epsilon$ , a novel bax variant missing the BH2 and the transmembrane domains. *Biochemical and Biophysical Research Communications*. 254: 779-85.
- Shimizu, S., T. Ide, T. Yanagida, and Y. Tsujimoto. 2000. Electrophysiological study of a novel large pore formed by Bax and the voltage-dependent anion channel that is permeable to cytochrome c. *Journal of Biological Chemistry*. 275: 12321-12325.
- Shinoura, N., Y. Yoshida, M. Nishimura, Y. Muramatsu, A. Assai, T. Kirino, and H. Hamada. 1999. Expression level of Bcl-2 determines anti- or proapoptotic function. *Cancer Research*. 59: 4119-4128.
- Simonian, P. L., D. A. Grillot, D. W. Andrews, B. Leber, and G. Nunez. 1996a. Bax homodimerization is not required for Bax to accelerate chemotherapy-induced cell death. *Journal of Biological Chemistry*. 271: 32073-32077.
- Simonian, P. L., D. A. M Grillot, R. Merino, and G. Nunez. 1996b. Bax can antagonize Bcl-X<sub>L</sub> during etoposide and cisplatin-induced cell death independently of its heterodimerization with Bcl-X<sub>L</sub>. *Journal of Biological Chemistry*. 271: 22764-22772.
- Soucie, E. L., M. G. Annis, J. Sedivy, J. Filmus, B. Leber, D. W. Andrews, and L. Z. Penn. 2001. Myc potentiates apoptosis by stimulating Bax activity at the mitochondria. *Molecular and Cellular Biology*. 21: 4725-4736.
- Sparks, A. B., N. B. Adey, L. A. Quilliam, J. M. Thorn, and B. K. Kay. 1995. Screening phage-displayed random peptide libraries for SH3 ligands. *Methods in Enzymology*. 255: 498-509.

- Sparks, A. B., J. E. Rider, N. G. Hoffman, D. M. Fowlkes, L. A. Quilliam, and B. K. Kay. 1996. Distinct ligand preferences of Src homology 3 domains from Src, Yes, Abl, Cortactin, p53BP2, PLC $\gamma$ , Crk, and Grb2. *Proceedings of the National Academy of Sciences*. 93: 1640-1544.
- Suzuki, M., R. J. Youle, and N. Tjandra. 2000. Structure of Bax: coregulation of dimer formation and intracellular localization. *Cell*. 103: 645-654.
- Uhlmann, E. J., T. Subramanian, C. A. Vater, R. Lutz, and G. Chinnadurai. 1998. A potent cell death activity associated with transient high level expression of Bcl-2. *Journal of Biological Chemistry*. 273: 17926-17932.
- Wang, K., X. Yin, D. T. Chao, C. L. Milliman, and S. J. Korsmeyer. 1996. BID: a novel BH3 domain-only death agonist. *Genes and Development*. 10: 2859-2869.
- Wang, K., A. Gross, G. Waksman, and S. J. Korsmeyer. 1998. Mutagenesis of the BH3 domain of Bax identifies residues critical for dimerization and killing. *Molecular and Cellular Biology*. 18: 6083-6089.
- Wang, N. S., M. T. Unkila, E. Z. Reineks, and C. W. Distelhorst. 2001. Transient expression of wild-type or mitochondrially-targeted Bcl-2 induces apoptosis while transient expression of ER-targeted Bcl-2 is protective against Bax induced cell death. *Journal of Biological Chemistry*. 276: 44117-44128.
- Wei, M. C., W.-X. Zong, E. H.-Y. Cheng, T. Lindsten, V. Panoutsakopoulou, A. J. Ross, K. A. Roth, G. R. MacGregor, C. B. Thompson, and S. J. Korsmeyer. 2001. Pro-apoptotic Bax and Bak: a requisite gateway to mitochondrial dysfunction and death. *Science*. 292: 727-730.
- Welsh, S., and S. A. Kay. 1997. Reporter gene expression for monitoring gene transfer. *Current Opinion in Biotechnology*. 8: 617-22.
- Wolter, K. G., Y. Hsu, C. L. Smith, A. Nechushtan, X. Xi, and R. J. Youle. 1997. Movement of Bax from the cytosol to mitochondria during apoptosis. *Journal of Cell Biology*. 139: 1281-1292.
- Wood, K. V. 1995. Marker proteins for gene expression. *Current Opinion in Biotechnology*. 6: 50-58.

- Yamabhai, M., and B. K. Kay. 1997. Examining the specificity of Src-homology 3 domain – ligand interactions with alkaline phosphatase fusion proteins. *Analytical Biochemistry*. 247: 143-151.
- Yang, E., J. Zha, J. Jockel, L. H. Boise, C. B. Thompson, and S. J. Korsmeyer. 1995. Bad, a heterodimeric partner of Bcl-X<sub>L</sub> and Bcl-2, displaces Bax and promotes cell death. *Cell*. 80: 285-291.
- Zamzami, N., and G. Kroemer. 2001. The mitochondrion in apoptosis: how Pandora's box opens. *Nature Reviews Molecular and Cellular Biology*. 2: 67-71.
- Zha, H., C. Aime-Sempe, T. Sato, and J. C. Reed. 1996a. Proapoptotic protein Bax heterodimerizes with Bcl-2 and homodimerizes with Bax via a novel domain (BH3) distinct from BH1 and BH2. *Journal of Biological Chemistry*. 271: 7440-7444.
- Zha, H., H. A. Fisk, M. P. Yaffe, N. Mahajan, B. Herman, and J. C. Reed. 1996b. Structure-function comparisons of the proapoptotic protein Bax in yeast and mammalian cells. *Molecular and Cellular Biology*. 16: 6494-6508.
- Zhou, M., S. D. Demo, T. N. McClure, R. Crea, and C. M. Bitler. 1998. A novel splice variant of the cell death-promoting protein Bax. *Journal of Biological Chemistry*. 273: 11930-11936.
- Zhu, W., A. Cowie, G. W. Wasfy, L. Z. Penn, B. Leber, D. W. Andrews. 1996. Bcl-2 mutants with restricted subcellular location reveal spatially distinct pathways for apoptosis in different cell types. *EMBO Journal*. 15: 4130-4141.
- Zou, H., W. J. Henzel, X. Liu, A. Lutschg, and X. Wang. 1997. Apaf-1, a human protein homologous to *C. elegans* CED-4, participates in cytochrome c-dependent activation of Caspase-3. *Cell*. 90: 405-413.

## 6. APPENDICES

### 6.1 Binding Among Bax Molecules

The BH3 domain of Bax $\alpha$  enables it to bind to other Bax molecules and Bcl-2 family members (Zha *et al.*, 1996a, Wang *et al.*, 1998, Simonian *et al.*, 1996a), and Bax $\alpha$  forms oligomers of large size in membranes of apoptotic cells (Gross *et al.*, 1998, Mikhailov *et al.*, 2001). Bax $\beta$  could function by enhancing the ability of Bax $\alpha$  to kill cells by increasing the probability of oligomer formation.

Binding between Bax $\beta$  and Bax $\alpha$  or Bax $\alpha$ - $\Delta$ S184 was examined through co-immunoprecipitations with an antibody specific to the unique Bax $\beta$  carboxyl-terminus. This antibody had to be used as any other available Bax antibodies, which recognize epitopes in the amino-terminal region of the protein, immunoprecipitate all of the Bax molecules. <sup>35</sup>S methionine labeled proteins were immunoprecipitated in buffers of either Triton X-100 or CHAPS to determine if the conformational change associated with exposure of the 6A7 epitope is required for binding.

Neither Bax $\alpha$  nor Bax $\alpha$ - $\Delta$ S814 co-immunoprecipitated with Bax $\beta$  in the Triton X-100 and CHAPS buffers (Figure 21). Thus these proteins do not interact *in vitro* regardless of amino-terminal conformation. If the unique Bax $\beta$  epitope was hidden, it is possible that the  $\alpha$ Bax $\beta$  antibody may not recognize the hetero-oligomer. While the Bax $\beta$  carboxyl-terminus could block the BH3 region,

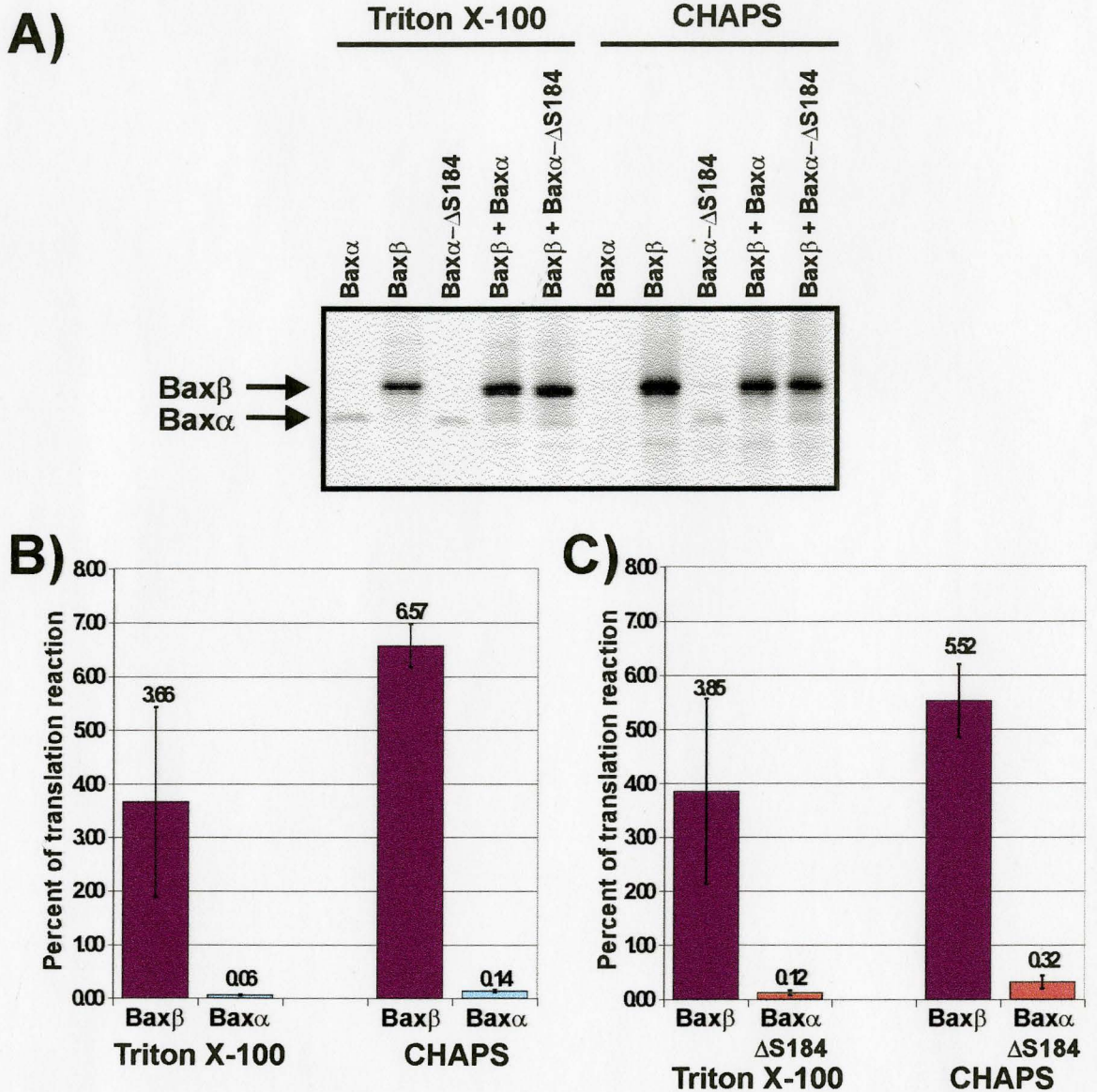


**Figure 21:** Co-immunoprecipitations of Bax $\beta$  and Bax $\alpha$ , and Bax $\beta$  and Bax $\alpha$ - $\Delta$ S184 with the  $\alpha$ Bax $\beta$  antibody at pH 7.5.

<sup>35</sup>S methionine labeled Bax $\beta$  and Bax $\alpha$  or Bax $\alpha$ - $\Delta$ S184 proteins that had been expressed *in vitro* were mixed in equal volumes and immunoprecipitated using the  $\alpha$ Bax $\beta$  antibody in buffer containing either 0.2% Triton X-100 or 0.2% CHAPS at pH 7.5. The immunoprecipitated proteins were run on a SDS-PAGE gel and the associated proteins visualized by autoradiography (A) and quantified by phosphorimaging (B and C). The error expressed is the standard error of the mean for three independent experiments.

its amino acid composition is very different from the Bax $\alpha$  carboxyl  $\alpha$ -helix, and therefore it is unlikely that they would share a similar function. Therefore Bax $\beta$  does not bind Bax $\alpha$  molecules, unless another protein binding partner or membrane, present *in vivo* but not included in this assay, is required.

## 6.2 PEST Sequence

The reduced levels of Bax $\beta$  protein expression observed in the pooled cell lines (Figure 7), and transient transfections (Figures 9, 12), raised the possibility that Bax $\beta$  has a short half-life. The carboxyl-terminus of Bax $\beta$  is the only region of the protein different from Bax $\alpha$  and thus it would be responsible for any differences in half-life between the two isoforms. One possibility is that this region of Bax $\beta$  contains a PEST sequence. These sequences are regions rich in proline (P), glutamic acid (E), serine (S), and threonine (T) and are often flanked by positive amino acids (Rogers *et al.*, 1986). PEST sequences are found in proteins that exhibit short half-lives, usually of less than two hours (Rogers *et al.*, 1986). The unique carboxyl-terminal sequence of Bax $\beta$  was compared to twelve known PEST sequences (Figure 22). While no definitive conclusions could be made due to the lack of well-defined consensus sequences for PEST regions, the Bax $\beta$  tail does contain a high number of proline, serine, and threonine residues and very few positively charged amino acids. Thus it is feasible that this carboxyl-terminal sequence causes a rapid degradation of Bax $\beta$ .

|                                |   |
|--------------------------------|---|
| <b>Bax<math>\beta</math></b>   | .+..+PP+P+++..OO.P.PPO.PP.OP.P...O.O-P.P+OO.....O.+ |
| <b>E1A</b>                     | +...PPO-----.-...-O.-+                              |
| <b>c-myc</b>                   | +O...PO-PP-..O-OOO.+                                |
| <b>p53</b>                     | +O...PO-PP-..O-OOO.+                                |
| <b>c-fos</b>                   | +...OP----+   |
| <b>ODC</b>                     | +-.P.O-----O.-.O..OO..-.O.O.....O-+                 |
| <b>PHYT</b>                    | +....-...O..O.....-.-.....-O-.P....+                |
| <b>v-myb</b>                   | +...-...P.-OO+                                      |
| <b>HSP70</b>                   | +OOPOO...O-O-+                                      |
| <b>HMG CoA</b>                 | +..OO.---P..O.-+                                    |
| <b>TAT</b>                     | +..P-.-.-.-O-+                                      |
| <b><math>\alpha</math>-CAS</b> | +...-O.OOO--..P.O..-+                               |
| <b><math>\beta</math>-CAS</b>  | +...-...P.-.-O.OOO--O.O+                            |

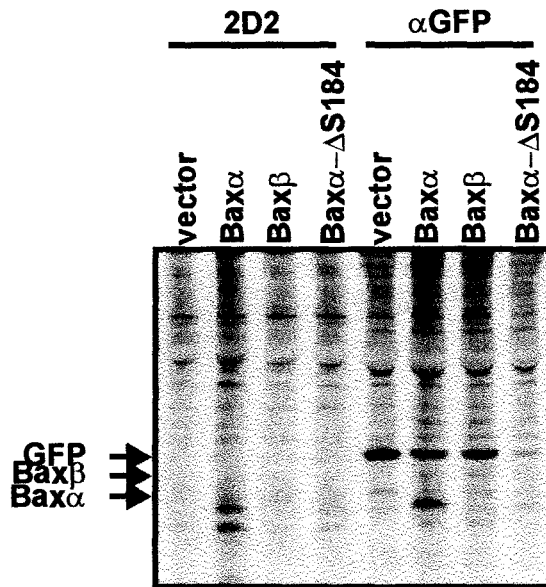
**Figure 22:** Schematic representation of PEST sequences.

Several PEST sequences are presented in schematic form, including the entire Bax $\beta$  unique carboxyl terminus. + indicates Arg, Lys, or His, - indicates Glu or Asp, O indicates Ser or Thr, P indicates proline, and all other amino acids are indicated by a dot. The region of the Bax $\beta$  carboxyl terminus that resembles the PEST sequences the most is highlighted in yellow.

(Modified from Rogers et. al., 1986).

Pulse labeling of Bax-expressing transiently transfected NIH 3T3 cells and of Rat-1 *myc* ERTM pooled cell lines with  $^{35}\text{S}$  methionine was done to elucidate the half-life of Bax $\beta$ . The GFP present in the cells as an internal control was successfully labeled in a four hour pulse of  $^{35}\text{S}$  methionine, and was immunoprecipitated from NP-40 lysates of the cells (Figure 23). However, no labeled Bax isoforms were immunoprecipitated from any of the cell lines (Figure 23). Shorter pulses of 10, 30, and 60 minutes of  $^{35}\text{S}$  methionine were done to determine if the four-hour pulse was too long, however, no labeled Bax $\alpha$  was immunoprecipitated with either the 2D2 or the Max5 antibody, even from MCF-7 cells which have high endogenous Bax $\alpha$  (Figure 24). NP-40 lysates release the Bax protein from all these cell types, and Bax $\alpha$  is immunoprecipitated with the antibodies (Figures 5, 7, 9, 12). Thus, the problem lies with the ability to label Bax $\alpha$  and Bax $\beta$  with  $^{35}\text{S}$  methionine. These proteins have eight and seven methionine residues, respectively, so labeled Bax would have been easily visualized. The reason why Bax $\alpha$  and Bax $\beta$  would not label with  $^{35}\text{S}$  methionine is unclear. Consequently, the half-life of the Bax $\beta$  molecule was not deduced from these experiments. A further experiment, outside the scope of this study, would be to tag a protein of known half-life with the Bax $\beta$  carboxyl-terminal region, and follow its expression in a pulse-chase experiment. Western blots to determine the amount of Bax $\beta$  remaining in the cell at various times after treatment with cycloheximide would also indicate if it is being degraded. This assay has previously revealed the function of PEST sequences.

**A) NIH 3T3**



**B) Rat-1 myc ERTM**

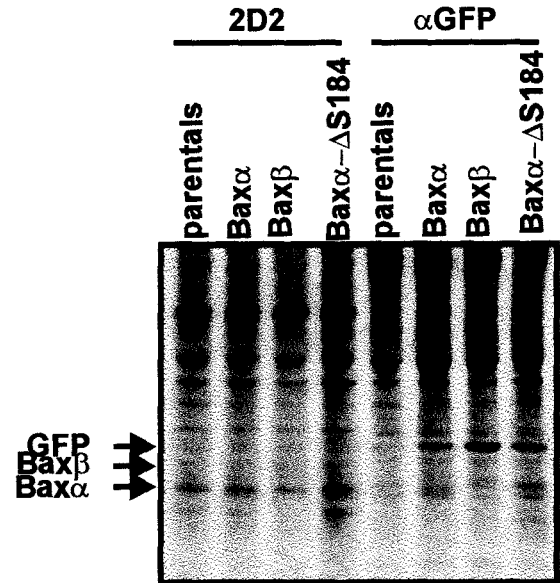


**Figure 23:** Pulse labeling of transfected NIH 3T3 cells and of Rat-1 *myc* ERTM pooled cell lines for Bax $\alpha$ , Bax $\beta$ , Bax $\alpha$ - $\Delta$ S184, and GFP.

- A) Immunoprecipitates of NP-40 lysates of 80  $\mu$ g of NIH 3T3 cells transiently transfected with the parent pBabe MN IRES GFP vector, or *bax $\alpha$* , *bax $\beta$* , *bax $\alpha$ - $\Delta$ S184* in the pBabe MN IRES GFP vector labeled with  $^{35}$ S methionine for four hours were done with the 2D2 and  $\alpha$ GFP antibodies. The positions of Bax $\alpha$ , Bax $\beta$  and GFP migration are indicated (arrows).
- B) Immunoprecipitates of NP-40 lysates of 140  $\mu$ g of the Rat-1 *myc* ERTM parental cell line and pooled cell lines made with the *bax $\alpha$* , *bax $\beta$* , *bax $\alpha$ - $\Delta$ S184* in the pBabe MN IRES GFP vectors labeled with  $^{35}$ S methionine for four hours were done with the 2D2 and  $\alpha$ GFP antibodies. The positions of Bax $\alpha$ , Bax $\beta$  and GFP migration are indicated (arrows).

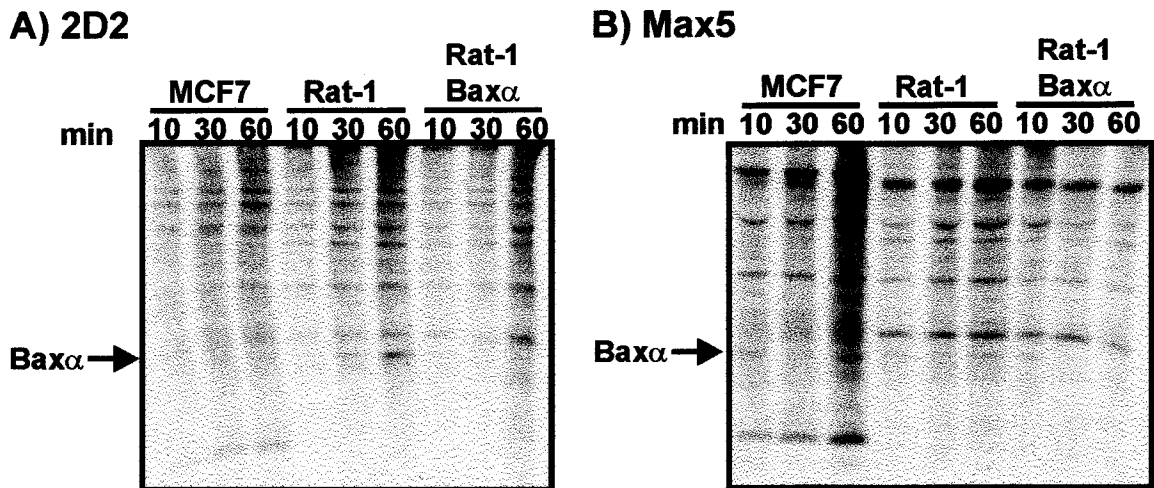


**Figure 24:** Pulse labeling of MCF-7 cells, of Rat-1 *myc* ERTM parental cells, and of Rat-1 *myc* ERTM *bax $\alpha$*  pBabe MN IRES GFP cells for Bax $\alpha$ .

- A) Immunoprecipitates of 80  $\mu$ g of NP-40 lysates of MCF-7 cells, Rat-1 *myc* ERTM parental cells, and of Rat-1 *myc* ERTM *bax $\alpha$*  pBabe MN IRES GFP cell lines labeled with  $^{35}$ S methionine for 10, 30, and 60 minutes were done with the 2D2 antibody. The position of Bax $\alpha$  migration is indicated (arrow).
- B) Immunoprecipitates of 80  $\mu$ g NP-40 lysates of MCF-7 cells, Rat-1 *myc* ERTM parental cells, and of Rat-1 *myc* ERTM *Bax $\alpha$*  pBabe MN IRES GFP cell lines labeled with  $^{35}$ S methionine for 10, 30, and 60 minutes were done with the MaxV antibody. The position of Bax $\alpha$  migration is indicated (arrow).

Other potential mechanisms which were not investigated in this study could have lead to the disappearance of Bax $\beta$ : Bax $\beta$  might interact through its carboxyl-terminus with other cellular proteins that then target it for degradation, or the carboxyl-terminal of Bax $\beta$  could be a target for ubiquitination that would lead to degradation of Bax $\beta$  at the proteasome.

### **6.3 Interactions with SH3 Domains**

The Bax $\beta$  carboxyl-terminal tail contains proline-enriched regions that are potential SH3 binding sites that would mediate protein-protein interactions (Figure 3). Many SH3 domain proteins are oncogenic, and have interactions in the cell death pathway (Kharbanda *et al.*, 1997, Naumovski and Cleary, 1996). The core ligand of an SH3 domain contains the consensus XPpXP motif, where X tends to be an aliphatic side chain. The 2 conserved prolines (P) are crucial for high affinity binding, and an intervening scaffold residue also tends to be proline (p) (Pawson, 1995). The Bax $\beta$  tail contains three of these motifs (APAPPS, PPSLPP and LPPATP), and a fourth motif that contains prolines, but positively charged instead of aliphatic amino acids (KPPHPH) (Figure 3). Mongiovi *et al.* (1999) determined the consensus sequence of ligands for the SH3 domain of the Eps8 protein conform to the sequence PXXDY, with the aspartic acid (D) and tyrosine (Y) residues indispensable for ligand binding. Thus, the XPpXP SH3 binding motif might not be absolutely required.

GST fusions of the SH3 domains of a variety of proteins were received from Dr. Brian K. Kay from the University of Wisconsin-Madison and used to examine the binding properties of Bax $\beta$ . These included the SH3 domains from c-Abl, PLC $\gamma$ , p53BP2, and c-Src. Upon overexpression, the GST-SH3 domain proteins were the most abundant proteins in the cell lysates, and passage of these lysates over a glutathione column resulted in GST-SH3 proteins of enhanced purity (Figure 25).

Dr. Kay has developed an enzyme-linked immunosorbent assay (ELISA) based method for detecting SH3 domain – ligand interactions (Sparks *et al.*, 1996, Yamabhai and Kay, 1997). The purified GST-SH3 domain proteins are bound to microtitre plates and probed with the potential binding proteins. The latter proteins were fused to alkaline phosphatase, the enzymatic activity of which was used to indicate binding (Yamabhai and Kay, 1997, Sparks *et al.*, 1995). This assay was attempted following the methods of Dr. Kay's research group using purified GST-c-Abl SH3, GST-p53BP2 SH3 and GST-Src SH3 domains and probing with a Src-ligand-BAP fusion protein, a peptide that specifically recognizes the Src SH3 domain fused to alkaline phosphatase (Yamabhai and Kay, 1997). The GST-SH3 domain fusions were bound to high-binding microtitre plate wells, unbound surfaces were blocked, and the wells washed. Src-ligand-BAP was induced in *E. coli* cells, and the alkaline phosphatase moiety of the fusion protein caused it to be secreted from the bacterium into the culture supernatant, enabling the protein to be used without

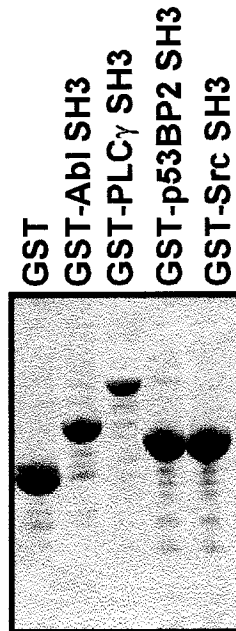


**Figure 25:** GST-SH3 domain fusion protein samples.

The eluted fractions of Glutathione Sepharose columns that were used to purify the GST and GST-SH3 domain fusion proteins of c-Abl, PLC $\gamma$ , p53BP2, and c-Src were run on a SDS-PAGE gel and stained with Coomassie blue. The induced GST-SH3 domain fusions are the predominant proteins in each of the samples.

further purification (Yamabhai and Kay, 1997). The Src-ligand-BAP containing supernatant was added to the microtitre plate wells and left to incubate. After washing, a *p*-nitrophenol phosphate (*p*NPP) substrate was added. A yellow colour change, detectable at 405 nm, occurred if the alkaline phosphatase moiety was present due to binding of the ligand protein. When the *p*NPP substrate was mixed with the Src-ligand-BAP fusion protein-containing supernatant, a yellow colour change did occur, indicative of functional alkaline phosphatase and *p*NPP substrate (data not shown). Yet none of the GST-SH3 samples bound to the microtitre wells reacted with the Src-ligand, even the GST-Src SH3 fusion, an interaction which has been optimized by Dr. Kay's group (Yamabhai and Kay, 1997). Increasing the amounts of the GST-SH3 domain fusions ten-fold yielded no positive results nor did incubation of the Src-ligand BAP on the plate prior to blocking the wells (data not shown). Thus, it appeared that the GST-SH3 domain fusion proteins were not adhering to the microtitre wells for the duration of the assay. Consultation with Dr. Kay determined that the correct methodologies were being followed. On account of the difficulties experienced with this assay, alternative experiments were explored.

Slot blots of purified GST-Abl SH3, GST-p53BP2 SH3 and GST-Src SH3 proteins were probed with potential binding proteins. Dilutions of the GST-SH3 domain proteins were slot blotted onto nitrocellulose, and the membranes were blocked and washed. The blots were probed with equal amounts of <sup>35</sup>S methionine labeled Bax $\alpha$ , Bax $\beta$ , Src-ligand-BAP as a positive control, and Pre-

prolactin as a negative control that were made *in vitro* and salt exchanged over G25 Sephadex to remove unincorporated <sup>35</sup>S methionine. The pre-prolactin negative control bound to all of the GST-SH3 domain samples, even as low as 0.001 mg of GST-SH3 protein (data not shown). Numerous buffers were tested to try and increase the stringency of the assay. However neither increasing the amount of detergent from 0.1% to 1% Triton X-100, or using 1% Triton X-100 with 0.1% SDS, nor changing the concentration of salt in the wash buffers from 25 mM to 100 mM NaCl reduced the levels of background binding (data not shown). Buffer with 1M NaCl reduced the Pre-prolactin binding, however Bax $\alpha$ , Bax $\beta$ , and Src-ligand-BAP were also unable to bind in these conditions (data not shown). Due to these obstacles encountered in finding optimal conditions for the assay, a third approach was tried.

Each GST-SH3 domain cell lysate was mixed with equivalent amounts of either Bax $\alpha$ , Bax $\beta$ , or Src-ligand BAP that were labeled with <sup>35</sup>S methionine, immunoprecipitated with  $\alpha$ GST antibody or glutathione beads, and the associated radio-labeled proteins visualized by autoradiography. Various buffer conditions and amounts of GST-SH3 proteins were tried to find a condition in which Src-ligand-BAP would bind to the SH3 domain proteins but not to GST alone. It was likely that Src-ligand-BAP would bind to all SH3 domains tested due to the relatively low stringency of this assay. The best condition found was incubating the GST-SH3 domain proteins with the <sup>35</sup>S methionine labeled proteins in phosphate buffered saline (PBS) and adding TBS-T buffer that

contains 0.1% Tween-20 prior to adding the antibody. However, this resulted in Bax $\alpha$ , Bax $\beta$ , and Src-ligand-BAP binding to all of the GST-SH3 fusions (data not shown). Performing all steps of the immunoprecipitations in the TBS-T buffer resulted in too stringent a condition in which no binding occurred (data not shown). Thus, appropriate conditions to determine if Bax $\beta$  bound SH3 domains using this assay were never found. In light of all of the information gathered in the other avenues of this study regarding the very low expression levels and indeterminate half-life of Bax $\beta$ , these SH3 binding studies were discontinued.

Co-immunoprecipitations of higher stringency with <sup>35</sup>S methionine labeled Bax $\alpha$  or Bax $\beta$  and c-Src were performed with antibodies to both Bax and c-Src in the stringent TXSWB buffer. Bax $\beta$  did not interact with c-Src above background levels (Figure 26). Thus c-Src is not the SH3 domain containing protein with which Bax $\beta$  interacts.

Bif-1, a widely expressed SH3 domain protein, binds the amino-terminus of Bax $\alpha$ , and the association between these two molecules increases upon the induction of apoptosis (Cuddeback *et al.*, 2001). Additionally, overexpression of Bif-1 in apoptotic cells promoted the activation of Bax $\alpha$  (Cuddeback *et al.*, 2001). However, the SH3 domain of Bif-1 does not mediate its interaction with Bax $\alpha$ . An intriguing possibility was that the poly-proline regions in the Bax $\beta$  carboxyl-terminal tail might bind to the SH3 domain of Bif-1, in addition to interactions like Bax $\alpha$ . Dr. Hong-Gang Wang's laboratory at the Lee Moffitt

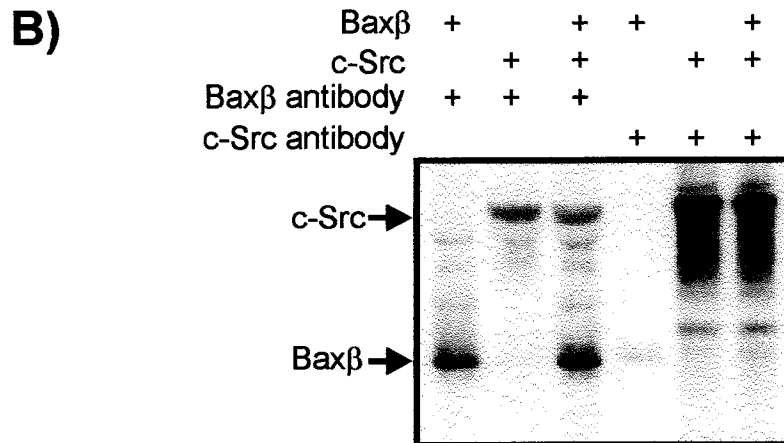
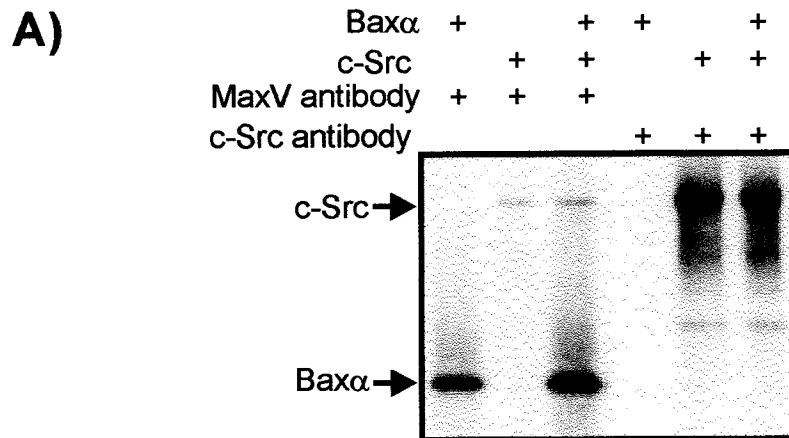


**Figure 26:** Immunoprecipitations of  $^{35}\text{S}$  methionine labeled Bax $\alpha$  and c-Src and Bax $\beta$  and c-Src.

- A) Equal amounts of  $^{35}\text{S}$  methionine labeled Bax $\alpha$  and c-Src protein that had been expressed *in vitro* were incubated with Protein A beads, Max5 antibody, or  $\alpha$ c-Src antibody. The immunoprecipitated proteins were visualized by autoradiography. The migration positions of the Bax $\alpha$  and c-Src proteins are indicated (arrows).
- B) Equal amounts of  $^{35}\text{S}$  methionine labeled Bax $\beta$  and c-Src protein that had been expressed *in vitro* were incubated with Protein G beads,  $\alpha$ Bax $\beta$  antibody, or  $\alpha$ c-Src antibody. The immunoprecipitated proteins were visualized by autoradiography. The migration positions of the Bax $\beta$  and c-Src proteins are indicated (arrows).

Cancer Center and Research Institute performed these studies with Bax $\beta$ . They found that the SH3 domain of Bif-1 was not required for the interaction of Bax $\beta$  with Bif-1, and Bax $\beta$  interacted with the Bif-1 molecule in the same manner as Bax $\alpha$  (Dr. H.-G. Wang, personal communication). Therefore, Bif-1 is also not an SH3 domain containing protein with which Bax $\beta$  interacts.

It was determined that neither c-Src nor Bif-1 is an authentic SH3 domain binding partner of Bax $\beta$ . However, no suitable assay was found to screen many different SH3 domains for Bax $\beta$  binding activity. Thus, it is inconclusive whether the carboxyl-terminal tail of Bax $\beta$  has SH3 binding capabilities.